

The effect of hypoxia on epithelial-to-mesenchymal transition and microbiome composition in the invertebrate model organism *Daphnia magna*

Emile CLAPPAERT

Promotor: Prof. Dr. E. Decaestecker
Aquatic Biology - KU Leuven KULAK

Co-promotor: Prof. Dr. C. Verslype
Hepatology – KU Leuven

Mentor: Dr. E. Beert
Aquatic Biology – KU Leuven KULAK

Thesis presented in
fulfillment of the requirements
for the degree of Master of Science
in Biology

Academic year 2016-2017

© Copyright by KU Leuven

Without written permission of the promotors and the authors it is forbidden to reproduce or adapt in any form or by any means any part of this publication. Requests for obtaining the right to reproduce or utilize parts of this publication should be addressed to KU Leuven, Faculteit Wetenschappen, Geel Huis, Kasteelpark Arenberg 11 bus 2100, 3001 Leuven (Heverlee), Telephone +32 16 32 14 01.

A written permission of the promotor is also required to use the methods, products, schematics and programs described in this work for industrial or commercial use, and for submitting this publication in scientific contests.

Dankwoord

Mijn masterthesis is een sluitstuk waar ik al vroeg in mijn opleiding met grote verwachtingen naartoe werkte. Een mooi afgewerkte en uitgebreide studie van een interessant onderwerp is voor mij één van de belangrijkste opdrachten als wetenschapper. Ik heb er dan ook al vanaf dag één mijn tanden in gezet. Het verzorgen van presentaties over mijn onderzoeksdomein deed ik dan ook met veel plezier. Mensen warm maken voor mijn onderzoek zie ik dan ook als een belangrijke taak als onderzoeker. Ik vind het dan ook leuk om de verwonderde blikken op de gezichten te zien wanneer ik vertel over de toekomstige rol van de voor velen onbekende watervlo in kankeronderzoek.

Allereerst wil ik mijn promotor, professor Ellen Decaestecker, bedanken voor de vele kansen en de steun die ze me gaf doorheen het hele jaar. Een eerste introductie in het academische leven van een onderzoeker, het schrijven van beursaanvragen en het indienen van abstracts voor conferentiezingen gaven een extra dimensie aan mijn laatste jaar als masterstudent. Daarnaast werd mij aangeboden om de begeleiding op mij te nemen van twee bachelor studenten uit de KULAK voor hun bachelorproef en drie scholieren uit Lier voor hun eindproject van het middelbaar. Ik vond het een heel toffe ervaring om uit eerste hand mijn kennis over een onderwerp te kunnen doorgeven en hen in die weken te laten kennis maken met het leven en werken in een onderzoekslabo. Ook een excursie naar het GhenToxLab in Gent deed ik met veel plezier. Ik kijk er dan ook naar uit om in de toekomst verder jonge mensen te kunnen inspireren om wetenschappelijk onderzoek te gaan uitvoeren.

Daarnaast wil ik natuurlijk ook mijn mentor dr. Eline Beert bedanken voor het aanleren van moleculair labowerk, het verstrekken van de protocols en de vele behulpzame tips bij het geduldig nalezen van mijn teksten. Mijn dank gaat ook uit naar de labo medewerkers van Aquatic Biology alsook het Trombose lab die altijd klaar stonden om mijn vragen omtrent het gebruik van apparaten of het vervangen van gasflessen te beantwoorden. In het bijzonder wil ik dr. Emilie Macke, dr. Martijn Callens en Isabel Vanoverberghe bedanken voor de vele hulp bij het voorbereiden van de sequencing en data-analyse.

Ten slotte wil ik ook de mensen uit mijn persoonlijke kring bedanken voor hun raad en niet-aflatende steun.

Summary

Epithelial-to-mesenchymal transition (EMT) is a conserved reversible process in which non-motile epithelial cells become mobile mesenchymal cells under the influence of stress, e.g. hypoxia and toxins. EMT plays a substantial role in embryonic development, but also in tumor metastasis. As no reliable *in vivo* EMT model is available yet, the eco-toxicological model *Daphnia magna* was here introduced to study EMT when exposed to hypoxia and the toxic cyanobacterium *Microcystis aeruginosa*.

In whole and gut samples of the *Daphnia magna* F clone, the gene expression of hypoxia-inducible factor α (*HIF α*) and EMT marker genes SNAIL (*SNAI1*), TWIST (*TWIST*), E-cadherin (*ECAD*) and N-cadherin (*NCAD*) was measured via qPCR over different hypoxia and *Microcystis aeruginosa* exposure periods.

The *HIF α* and EMT marker gene expression levels in both the gut as the whole *Daphnia magna* exposed to hypoxia were contradictory to what is expected during EMT. Also in the *Microcystis aeruginosa* exposure no clear evidence was found indicating the activation of EMT. This indicates the possible existence of a protection mechanism that counteracts EMT. However, these results are still preliminary and need confirmation via further experiments with more replicates exposed to the stressors and more standardization in the qPCR analyses.

Additionally, through 16S rRNA gene sequencing, the change of the gut microbiome composition in *Daphnia magna* exposed to hypoxia was investigated. The gut microbiome composition shifted under hypoxia from a β -Proteobacteria-rich community to a Sphingobacteria-rich community. However, further research and optimization of the experimental set-up is needed to obtain significant results.

Samenvatting

De epitheliale-naar-mesenchymale transitie (EMT) is een geconserveerd omkeerbaar proces waarbij onbeweeglijke epitheliale cellen worden omgezet in beweeglijke mesenchymale cellen, onder invloed van o.a. hypoxie en toxinen. EMT speelt een belangrijke rol tijdens de embryonale ontwikkeling, maar ook in tumor metastase. Aangezien een betrouwbaar *in vivo* EMT model organisme nog niet beschikbaar is, werd hier het ecotoxicologische model *Daphnia magna* geïntroduceerd om EMT te bestuderen, geïnduceerd onder invloed van hypoxie en de toxische cyanobacterie *Microcystis aeruginosa*.

In volledige individuen en in de darm van *Daphnia* werd via qPCR de expressie gemeten van hypoxia-inducible factor α (*HIF α*) en de EMT merkgenen SNAIL (*SNAI1*), TWIST (*TWIST*), E-cadherine (*ECAD*) en N-cadherine (*NCAD*) gedurende verschillende perioden van blootstelling aan hypoxie en *Microcystis aeruginosa*.

De genexpressie van *HIF α* en EMT merkgenen in zowel de darm als de volledige *Daphnia magna* blootgesteld aan hypoxie was tegengesteld aan wat verwacht wordt tijdens EMT. Ook in de *Microcystis aeruginosa* blootstelling werd geen duidelijke aanwijzing voor de activatie van EMT gevonden. Deze resultaten zijn echter preliminair en bevestiging is vereist door middel van verder onderzoek met meer replica blootgesteld aan de stressors en meer standaardisatie in de qPCR analyses.

Via het sequencen van het 16S rRNA gen werd de verandering in de samenstelling van het darm microbioom bestudeerd in *Daphnia magna* blootgesteld aan hypoxie. De darm microbioom samenstelling veranderde onder hypoxie van een β -Proteobacteria-rijke samenstelling naar een Sphingobacteria-rijke samenstelling. Desalniettemin is er meer onderzoek en optimalisatie van de experimentele opzet vereist om significante resultaten te verkrijgen.

Table of Contents

Dankwoord	i
Summary	ii
Samenvatting	iii
Table of Contents	iv
List of Abbreviations	vi

PART I

Literature review	1
Chapter 1: Epithelial-to-Mesenchymal Transition (EMT)	1
1.1. What is EMT?	1
1.2. Seven hallmarks of EMT in humans	2
1.2.1. Hallmark 1: Loss of cell junctions and apico-basal polarity	2
1.2.2. Hallmark 2: Cytoskeletal rearrangements	4
1.2.3. Hallmark 3: Gain of motility	4
1.2.4. Hallmark 4: Degradation and remodeling of ECM	4
1.2.5. Hallmark 5: Arrest of cell cycle	4
1.2.6. Hallmark 6: Resistance to apoptosis	5
1.2.7. Hallmark 7: Acquirement of stem-cell like properties	5
1.3. EMT regulators	7
1.4. Three different types of EMT throughout the animal kingdom	9
1.4.1. First type: EMT in development	10
1.4.2. Second type: EMT during wound healing	10
1.4.3. Third type: EMT in cancer	11
1.4.3.1. Hypoxia-induced metastasis	13
1.4.3.2. In vivo models for hypoxia-induced EMT?	15
1.5. <i>Microcystis sp.</i> as EMT inducer?	16
Chapter 2: Microbiome, EMT and cancer	18
2.1. The microbiome	18
2.2. Roles of microbiota in EMT and carcinogenesis	18
Chapter 3: <i>Daphnia magna</i>	21
3.1. Biology of <i>Daphnia magna</i>	21
3.2. <i>Daphnia magna</i> as a model organism	23
3.3. <i>Daphnia magna</i> and hypoxia	24
3.4. <i>Daphnia magna</i> and <i>Microcystis sp.</i>	24
3.5. <i>Daphnia magna</i> and EMT	25
3.6. <i>Daphnia magna</i> and its microbiota	25
Objectives	26

PART II	
Material and Methods	27
1. <i>Daphnia magna</i> clones	27
2. Effect of hypoxia and <i>Microcystis aeruginosa</i> on the expression of <i>HIFα</i> and EMT marker genes in <i>Daphnia magna</i> : experimental set-up	28
2.1. Hypoxia experiment	28
2.1.1. Short-term hypoxia exposure (STH) effects on the expression of <i>HIFα</i>	28
2.1.2. Long-term hypoxia exposure (LTH) effects on the expression of <i>HIFα</i> and EMT marker genes	29
2.2. Short-term <i>Microcystis aeruginosa</i> exposure (STM) effects on the expression of <i>HIFα</i> and EMT marker genes	29
3. <i>Daphnia magna</i> sampling	29
4. Total RNA extraction and single strand cDNA synthesis	30
4.1. Total RNA extraction	30
4.2. Single strand cDNA synthesis	32
5. qPCR	32
5.1. qPCR primer optimization	32
5.2. Standards	33
5.3. Relative qPCR	35
5.4. Analysis of qPCR data	35
6. Gut microbiome composition	36
6.1. Experimental set-up	36
6.2. DNA isolation	37
6.3. Library preparation and Illumina Sequencing	37
6.4. Analysis	38
PART III	
Results	39
1. qPCR primer optimization: <i>ECAD</i> , <i>NCAD</i> , <i>SNAI1</i> and <i>TWIST</i>	39
2. Real-time expression level of <i>HIFα</i> and EMT marker genes <i>SNAI1</i> , <i>TWIST</i> , <i>NCAD</i> and <i>ECAD</i> via qPCR	40
3. Gut microbiota composition in <i>Daphnia magna</i> after exposure to hypoxia	46
PART IV	
Discussion	48
1. Effect of hypoxia and <i>Microcystis aeruginosa</i> on the expression level of <i>HIFα</i> and EMT marker genes in <i>Daphnia magna</i>	48
2. Effect of hypoxia on the microbiota composition in <i>Daphnia magna</i>	55
Conclusion and future perspectives	57
References	58
Addendum	
A. Risk Analysis	A1
B. Supplementary Tables	A2
C. Supplementary Figure	A4

List of Abbreviations

ADaM	Aachener Daphnien medium
ARNT	Aryl hydrocarbon receptor nuclear translocator
bHLH	Basic helix-loop-helix
CDH1	Cadherin 1/E-cadherin/epithelial cadherin
CyanoHAB	Cyanobacterial harmful algal bloom
Cp	Crossing point
CSL	Recombination signal binding protein for immunoglobulin kappa J region
CtBP	C-terminal binding protein
CTC	Circulating tumor cell
ECAD	E-cadherin
ECM	Extracellular matrix
EDTA	Ethylene-diamine-tetra-acetic acid
EM	Intermediate epithelial/mesenchymal cell
EMT	Epithelial-to-mesenchymal transition
EndoMT	Endothelial-to-mesenchymal transition
FGF (-R)	Fibroblast growth factor (-receptor)
GSK3 β	Glycogen synthase kinase β
HIF (-1 α)	Hypoxia-inducible factor (-1 α)
HRE	Hypoxia-responsive elements
Hb	Hemoglobin
IDs	Inhibitors of differentiation
LTH	Long-Term Hypoxia Exposure
MC (-LR)	Microcystin (-leucine arginine)
MET	Mesenchymal-to-epithelial transition
MMP	Matrix metalloprotease
NCAD	Neural-cadherin/N-cadherin
OATP	Organic anion transporting peptides
PAA	Peracetic acid
PHD	Prolyl hydroxylase
PP2A	Protein phosphatase 2A
RE1	Repressor Element 1
REST	Repressor Element 1-Silencing Transcription Factor
RPL32	Ribosomal protein L32
RT	Room temperature
SCFA	Short-chain fatty acid
STH	Short-Term Hypoxia Exposure

STM	Short-Term <i>Microcystis aeruginosa</i> exposure
TAM	Tumor associated macrophages
TGFβ	Transforming Growth Factor β
VHL	von Hippel-Lindau
ZEB	Zinc-finger E-box binding

PART I: Literature Review

Chapter 1

Epithelial-to-mesenchymal transition (EMT)

1.1. What is EMT?

In multicellular organisms, the presence of cell junctions is crucial for cell-cell and cell-matrix interactions laying at the base of further organization into tissues. In these organized systems, there are two basic tissue types: epithelium and mesenchyme. The epithelium comprises highly organized epithelial cells that know an apical-basal polarity, with a lumen at the apical site and the basal lamina at the basal site. This basal lamina keeps the epithelial layer separate from the mesenchymal cells (Warzecha & Carstens, 2012). The mesenchymal cells are characterized by a minimum of cell junctions, lack of polarity, spindle shape morphology and are surrounded by extracellular matrix (ECM).

Epithelial-to-mesenchymal transition or EMT can be defined as a conserved biological process whereby epithelial cells lose their typical epithelial features and become individual, mobile, mesenchymal cells (Figure 1) (Nieto *et al.*, 2016). EMT is crucial for the development of organisms into a wide range of different body plans as well as in wound healing, but this process can also be abused in certain cases such as in cancer and fibrosis. The transition is activated by a vast array of growth factors, hypoxia, inflammation, starvation or toxins (Nieto *et al.*, 2016; Wang *et al.*, 2016).

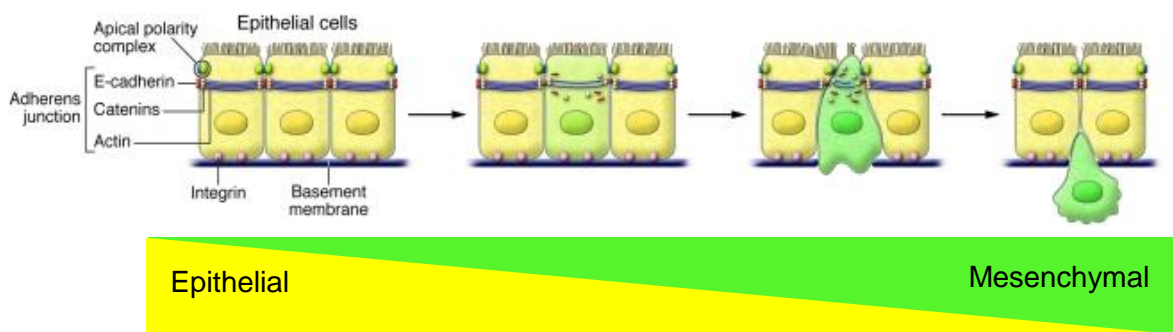


Figure 1: EMT as a transition from an epithelial to a mesenchymal phenotype. This is characterized by a gradual loss of epithelial markers such as E-cadherin, catenins and integrins making up cell junctions of epithelial cells showing an apical-basal polarity. At the same time there is a gradual gain of mesenchymal markers like N-cadherin and actin rearrangements to obtain a more spindle-like shape. Following the transition, also the basal lamina and ECM is degraded (adapted from Acloque *et al.*, 2009).

When EMT was first discovered, it was mistaken for a transformation rather than a transition. This representation as a 'transformation' was not correct since EMT knows different transition stadia. During these transition stadia, epithelial features are gradually downregulated while mesenchymal traits are gradually upregulated (Figure 1), forming different intermediate stages displaying both epithelial and mesenchymal characteristics (Nieto *et al.*, 2016). The exact opposite event occurs during mesenchymal-to-epithelial transition or MET (Kalluri & Weinberg, 2009). This is important in recreating a consistent tissue of epithelial cells when migrating mesenchymal cells arrive via chemotaxis at their destination and makes EMT a reversible process (Chaffer *et al.*, 2007).

1.2. Seven hallmarks of EMT in humans

When EMT is induced, a gene switch in the nucleus, mediated by specific EMT transcription regulators, leads to the activation of seven EMT hallmarks. These hallmarks comprise: (1) Loss of cell junctions and apical-basal polarity, (2) Cytoskeletal rearrangements, (3) Gain of motility, (4) Degradation and remodeling of the ECM, (5) Cell cycle arrest, (6) Resistance to apoptosis and (7) Acquisition of stem cell-like properties. In Figure 2, the four phenotypically visible hallmarks are depicted.

1.2.1. **Hallmark 1:** Loss of cell junctions and apical-basal polarity

(a) Loss of cell junctions

Epithelial cells are firmly bound to each other, forming an epithelial barrier separating lumen from interstitial space. Four different types of membrane protein complexes cooperate in this tight sealing: tight junctions, adherens junctions, desmosomes and gap junctions (Lamouille *et al.*, 2014). Tight junctions bring the membranes of the two cells in close contact with each other and are the main protein complexes responsible for the creation of a barrier (Komarova *et al.*, 2007). Adherens junctions and desmosomes are important to attach cells to each other, however not as strict as tight junctions and without barrier formation. This is achieved through interactions of the complexes with the cytoskeleton of both cells. Gap junctions provide a cytoplasmic connection in order to exchange cytosol and signaling molecules and in this way link cells to each other (Figure 2).

When EMT is induced, cell junctions will be degraded or relocalized in the cell (Figure 1; Figure 2). An important universal marker for EMT is the disappearance of the cell surface protein epithelial cadherin/E-cadherin (ECAD) or Cadherin 1 (CDH1) through transcriptional repression and active cleavage (Kume *et al.*, 2013). E-cadherin is attached to the cytoskeleton by intracellular catenins (Figure 1). The extracellular part of E-cadherin binds to the E-cadherin of a neighboring cell leading to the formation of adherens junctions (Harris & Tepass, 2010). E-cadherin also possesses transcription factor properties and intracellular

signaling properties (Du *et al.*, 2014). Additionally, it plays an important role in the entry of viruses (Li *et al.*, 2016) and fungi (Wächtler *et al.*, 2012).

When the cell becomes mesenchymal, an alternative surface molecule is expressed: neural cadherin (N-cadherin). This type of cadherin is attached to the cytoskeleton but allows cell migration (Rogers *et al.*, 2013). Qian *et al.* (2014) depicted N-cadherin as an oncogene, as the overexpression, mediated through the upregulation of fibroblast growth factor receptors (FGF-R), leads to a higher level of EMT in cancer. In biomedical research, this switch from E-cadherin to N-cadherin is often used as an indicator for EMT (Kume *et al.*, 2013).

Other characteristic changes in surface molecules are the disappearance of the tight junction molecules occludin and claudin, and a lowered quantity of connexin of which desmosomes are built of (Lamouille *et al.*, 2014). In the mesenchymal phenotype there is also the occurrence of vimentin (cytoskeletal protein) and fibronectin (ECM compound), which are, like N-cadherin, valuable markers to prove that cells underwent EMT (Qian *et al.*, 2014).

(b) Loss of polarity

The extracellular parts of the junction protein complexes interact with each other to ensure intercellular interactions. The intracellular part of the junction protein complexes ensures an important characteristic of the epithelial cell: the apical-basal polarity. The tight junction complexes Par & Crumbs are typically associated with the apical part of the cell and adherens junction complex Scribble is associated with the basolateral part of the cell (Johnston & Ahringer, 2010). In the gut, the apical part is orientated towards the lumen and the basolateral part rests at the basal lamina. It is the interaction with the basal lamina that indicates where the basal-lateral part of the cell is situated. During EMT the protein complexes are degraded, resulting in a switch from an apical-basal polarity to a front-rear polarity, characteristic for the more motile, unicellular mesenchymal phenotype (Figure 2).

1.2.2. **Hallmark 2:** Cytoskeletal rearrangements

Epithelial cells are phenotypically characterized by a columnar shape without any cellular extensions. When EMT is switched on, the cortical actin cytoskeleton is reorganized leading to a more spindle-like shaped cell (Figure 1; Figure 2). Cellular extensions like lamellipodia, filopodia and invadopodia increase the cell motility, degrade ECM and play a role in the cells sensory system to gain mostly mechanical information about the environment (Ridley, 2011).

1.2.3. **Hallmark 3:** Gain of motility

Epithelial cells are immobile and firmly anchored in the epithelium, in contrast to the more motile mesenchymal cells. In the mesenchymal cells, the changed gene expression during EMT leads to the transcription of e.g. actin stress fibers and Rho-GTPases (Narumiya *et al.*, 2009). Actin stress fibers are associated with a higher cell contraction and movement. This is accomplished through the formation and arrangement of these fibers by Rho-GTPases like RhoA, Rho-associated protein kinase and Dia1. Rho-associated protein kinase will also phosphorylate the myosin light chains, leading to contraction and movement of the cell, similar to smooth muscles (Narumiya *et al.*, 2009). These changes together with the sensory action of lamellipodia, filopodia and invadopodia will enable a directional migration of the mesenchymal cell (Figure 2).

1.2.4. **Hallmark 4:** Degradation and remodeling of the ECM

When mesenchymal cells escape the epithelial layer, the basal membrane and ECM have to be degraded. Therefore, the EMT transcription factor SNAIL upregulates the expression of for instance matrix metalloproteases like MMP4, providing the mesenchymal cell a clear escape route out of the protein mass (Figure 2) (Nistico *et al.*, 2012). Some proteases, like MMP3 and MMP13 are also known to induce EMT via a positive feedback loop through indirect increase of intracellular Reactive Oxygen Species. Thus, MMPs are not only a result of EMT but are also able to induce EMT indirectly (Said & Williams, 2011). During EMT, the ECM will also be remodeled to a matrix that is more competent to the motile cell by upregulating collagen, integrins and fibronectin (Lamouille *et al.*, 2014).

1.2.5. **Hallmark 5:** Arrest of cell cycle

The cytoskeletal changes in the cell occurring during EMT make it impossible to be in a highly proliferative state, as both processes require a lot of energy (Vega *et al.*, 2004). As such, the amount of energy that the cell needs to accomplish a high motility will not be available for proliferation, leading to cell cycle arrest. This is accomplished through SNAIL-mediated repression of Cyclin D expression by binding of SNAIL to E-boxes in the Cyclin D promotor. In addition, SNAIL upregulates the transcription of p21 (Pilli *et al.*, 2015), retaining the nuclear cell cycle machinery setting on the S-phase. In this way, DNA replication does not occur. Overall, both mechanisms explain the low proliferation rate in invasive tumor cells that underwent EMT. However, when the tumor cell arrives at its new niche, the cell cycle that supports the original high proliferation rate is restored after the tumor underwent MET (Vega *et al.*, 2004).

1.2.6. **Hallmark 6:** Resistance to apoptosis

Resistance to apoptosis is a necessary trait for mesenchymal cells and circulating tumor cells to survive an environment without the growth factors present in their original niche (Vega *et al.*, 2004). Depletion of these growth factors leads to cellular stress and causes the onset of the apoptotic program via intracellular sensors. Mesenchymal cells counteract apoptosis via the activation of the PI3-K/Akt and MEK/ERK pathway, both promoting cell survival, like through the upregulation of the Bcl-2 family members (Vega *et al.*, 2004).

1.2.7. **Hallmark 7:** Acquisition of stem cell-like properties

During wound healing, differentiated adult cells become mesenchymal via EMT initiated by growth factors. In this scenario, there is a regain of the stem cell properties. Likewise, invasive tumor cells that express mesenchymal markers, have an increase of stemness (Mani *et al.*, 2009). The emergence of this stemness is attributable to the EMT transcription factors (SNAIL and TWIST) as they regulate the transcription of genes that are associated with stemness (Nieto *et al.*, 2016). For instance, SNAIL induces gain of stemness through the activation of miR-146a expression, leading to a switch from asymmetric to symmetric cell division (Hwang *et al.*, 2014). Likewise, the hypoxic situation in the tumor microenvironment leads to the activation of hypoxia-inducible factor (HIF), not only leading to expression of mesenchymal genes but also of genes implicated in stemness. HIF can be seen as a 'master regulator of stemness' as it sets on pluripotency genes (Mimeault & Batra, 2013). And, as the activated PI3-K/Akt pathway leads to higher survival (see 1.2.6.), this also contributes to the EMT-induced stemness (Vega *et al.*, 2004). There are still questions rising on EMT-induced cancer stem cells as these cells may also originate from cancer cells that were originally stem cells instead of originating from somatic tumor cells (Thiery *et al.*, 2009). Nieto *et al.* (2016) even suppose an uncoupling of the tumor stemness and EMT based on recent research.

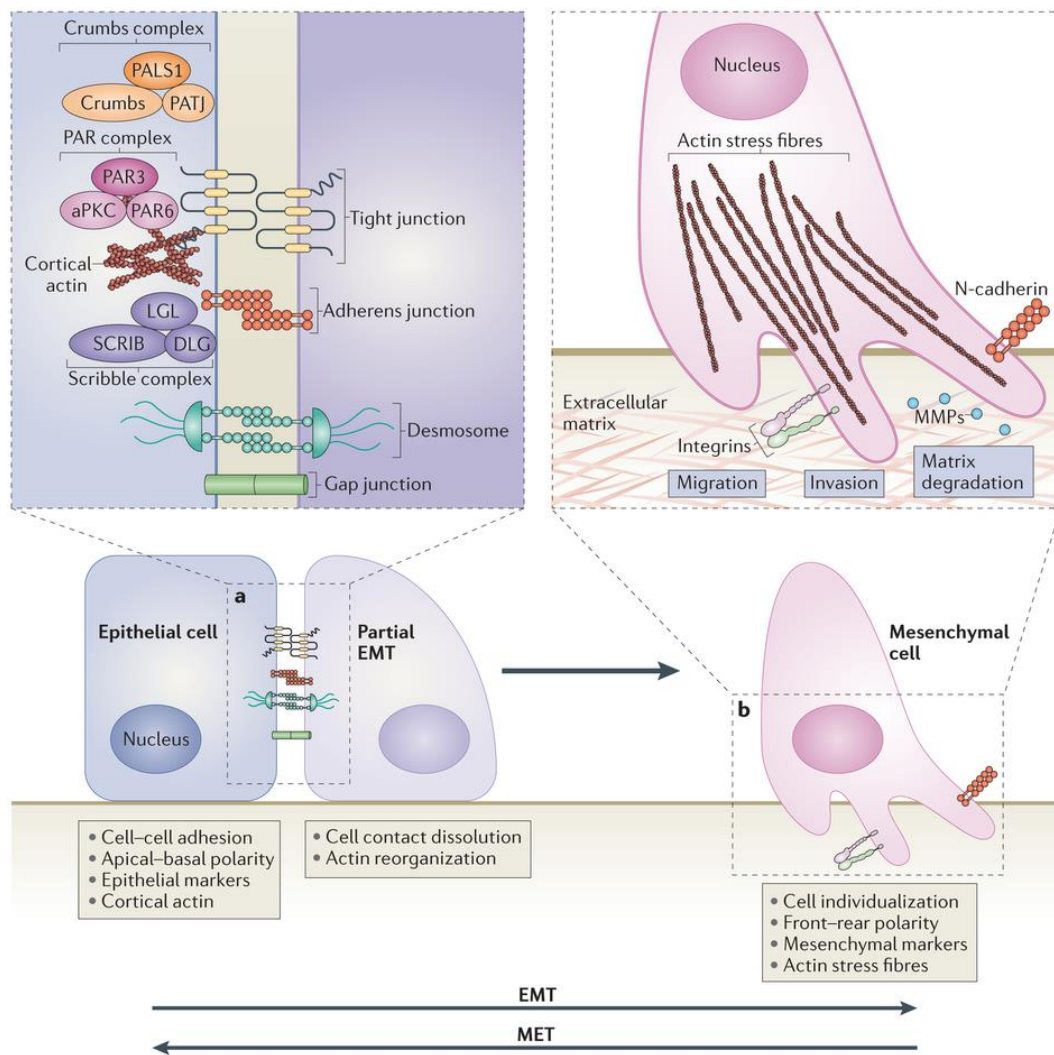


Figure 2: Representation of four clearly visible phenotypical hallmarks: (1) Loss of apical-basal polarity and cell junctions, (2) cytoskeleton rearrangements, (3) higher motility and (4) degradation and remodeling of the ECM. In the first hallmark of EMT tight junctions, adherens junctions, desmosomes and gap junctions are degraded when cells become mesenchymal. Cells undergoing partial EMT can still express some of these junctions but in fully mesenchymal cells, there is expression of N-cadherin as alternative cadherin. The loss of junctions will also lead to the loss of polarity. The second hallmark is the rearrangement of the cytoskeleton, leading to the formation of cellular extensions like filopodia. The cytoskeleton also plays a role in the enhancement of the motility of mesenchymal cells, which will promote the migration, being the third hallmark. The final visible phenotypical hallmark in the figure is the degradation of the ECM through the production of matrix-degrading enzymes such as MMPs. The opposite direction of the events (MET) is also possible (Lamouille *et al.*, 2014).

1.3. EMT regulators

After extracellular signals/inducers are recognized, downstream pathways are switched on leading to the transcription and activation of typical EMT regulators. At the moment, the involvement is assumed of six different regulating pathways during EMT, namely (i) transcription factors (Lamouille *et al.*, 2014), (ii) miRNAs (Diaz-Lopez *et al.*, 2014), (iii) epigenetic alterations (Tam & Weinberg, 2013), (iv) non-coding RNAs (Crea *et al.*, 2014), (v) subcellular localization (Zhang *et al.*, 2012) and (vi) alternative splicing (Warzecha & Carstens, 2012). In this thesis, only transcription factors present in invertebrates are of special interest.

Transcription factors play a prominent role in activating and maintaining the EMT program. Therefore, they are often used as markers to prove the occurrence of EMT. Most important EMT transcription factors are SNAIL and TWIST (vertebrates and invertebrates) and Zinc-finger E-box Binding transcription factor (ZEB) (only vertebrates) (Lamouille *et al.*, 2014). They bind to specific boxes in different promoters to repress or activate expression of genes essential to EMT, discussed in 1.2.

SNAIL, a zinc-finger transcription factor, is one of the most important EMT regulators, having a vast array of functions in development and disease (Lamouille *et al.*, 2014). It also maintains the mesenchymal state by inhibiting apoptosis and inducing stem cell properties (Cobaleda, *et al.*, 2007). SNAIL was first described in 1987 in *Drosophila* (Boulay *et al.*, 1987) and is now part of the SNAIL superfamily which comprises two major branches, namely the SNAIL family and the Scratch family. As the SNAIL family has a role in EMT, Scratch transcription factors have a role in neuronal development (Manzanares *et al.*, 2001). In vertebrates, three SNAIL proteins are present which have a common protein organization with four to six zinc fingers and a SNAG domain: SNAI1 (SNAIL), SNAI2 (SLUG) and SNAI3 (SMUC) (Figure 3). These SNAIL proteins not only function in embryological development and wound healing, but also in adult tissue, for instance during spermatogenesis (Cobaleda *et al.*, 2007). In invertebrates only one SNAIL protein can be found. Because of the high relatedness, SNAIL genes in vertebrates still show a high rate of homology with the invertebrate SNAIL genes (Barallo-Gimeno & Nieto, 2005).

The major role of SNAIL during EMT is the transcriptional repression of genes associated with epithelial junctions, like E-cadherin (Kume *et al.*, 2013). SNAIL zinc-fingers bind to E-boxes (CAGGTG) in promoters of target genes (Figure 4) and repress transcription via the SNAG domain or together with co-repressors such as C-terminal binding protein (CtBP), which recruits Histone Deacetylase, leading to epigenetic changes (Cobaleda *et al.*, 2007; Lamouille *et al.*, 2014). Furthermore, SNAIL can downregulate gene transcription indirectly through promoting alternative splicing of tight junctions genes (Ohkubo & Ozawa, 2004).

When the EMT program is not turned on, SNAIL activity is kept low in vertebrates through the inhibitory role of glycogen synthase kinase β (GSK3 β) that actively phosphorylates SNAIL leading to its ubiquitination and degradation (Figure 4). Also p53, as tumor suppressor protein can inhibit the action of SNAIL. When the EMT program is activated, the MAPK, Wnt and PI3-K/Akt pathway inhibit GSK3 β , leading to the accumulation and activation of SNAIL (Zhou *et al.*, 2004).

Basic helix-loop-helix (bHLH) transcription factors are proteins characterized by their ability to repress transcription through binding to an E-box sequence in a promotor (Xu *et al.*, 2009; Ozdemir *et al.*, 2011). These bHLHs have two parallel α -helices linked by a loop and act as a dimer. bHLHs are divided into seven classes, based on their interaction with DNA (Xu *et al.*, 2009). Only three of these classes are involved in EMT: class I (E12 and E47), class II (TWIST1 and TWIST2) and class V (inhibitors of differentiation or IDs) (Xu *et al.*, 2009). In accordance to SNAIL, these transcription factors repress genes associated with the epithelial phenotype (Figure 4). TWIST can therefore serve as a valid marker for the occurrence of EMT in research using vertebrates and invertebrates (Wang *et al.*, 2006; Xu *et al.*, 2009).

Other important transcription factors in vertebrates are the ZEB transcription factors. The repression of epithelial genes by ZEB1 and ZEB2 can occur after recruitment of CtBP but there are also cases where this recruitment is not necessary (Lamouille *et al.*, 2014). In *Drosophila*, a ZEB homologue, Zfh-1, was found. However, it does not appear to have a role in EMT but rather in stem cell migration (Broihier *et al.*, 1998) and in maintaining the somatic progenitor cell fate in the gonads (Leatherman & DiNardo, 2008). As ZEB only has a clear role in EMT in vertebrates, this transcription factors is not of special interest in this thesis.

HIF as an EMT regulating transcription factor is discussed in 1.4.3.1.

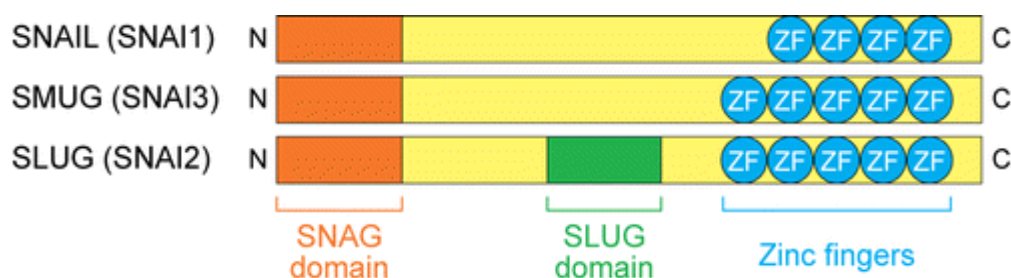


Figure 3: Representation of the three vertebrate SNAIL proteins. The three vertebrate SNAIL proteins have a common protein organization that comprises a C-terminal region with four to six zinc-fingers that interact with DNA and a repressive N-terminal SNAG domain. SNAI2 has a specific SLUG domain playing a repressive role on transcription through the binding to E-boxes in the promoters of the target genes (adapted from Cobaleda *et al.*, 2007).

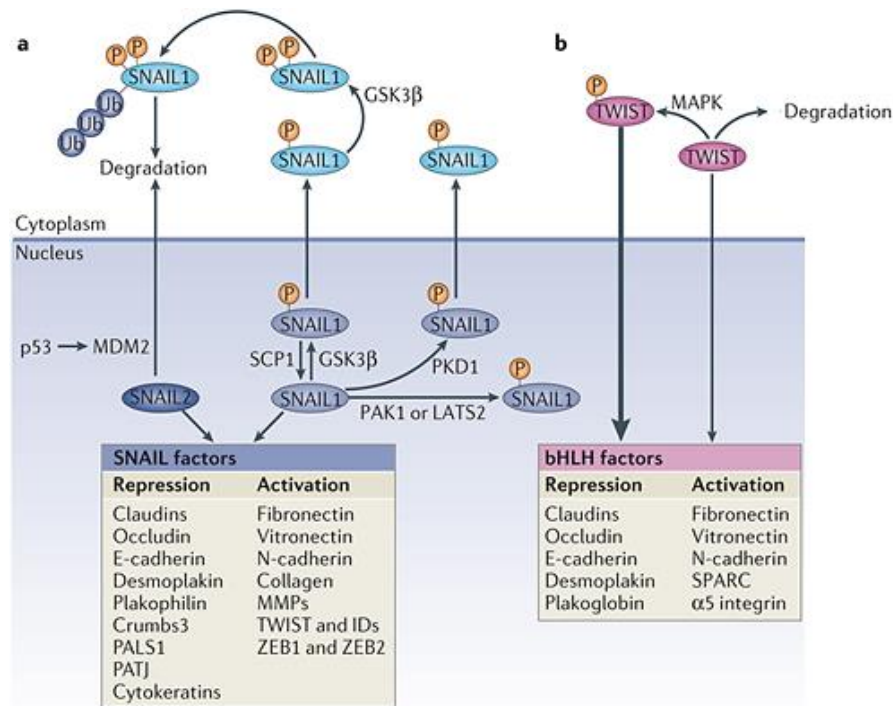


Figure 4: Mode of action of the zinc-finger transcription factors SNAIL and the bHLH transcription factor TWIST. Clearly presented are the genes that are actively repressed or expressed. In the pathway of SNAIL the activity of p53 is necessary as a protective transcription factor against EMT as it leads to the degradation of SNAIL2. SNAIL1 is actively degraded after phosphorylation by GSK3β or transported out of the nucleus after phosphorylation by PAK1 or PKD1. Claudin, Occludin, E-cadherin, Desmoplakin, Plakophilin, Crumbs3, PALS1 and PATJ are involved in cell-cell junctions. Fibronectin, vitronectin, integrin and collagen on the other hand are involved in the interaction with the ECM. The expression of these ECM proteins, while there is also expression of ECM degrading enzymes is contradictory at first view, however implicates that mesenchymal cells remodel the ECM into a matrix with a different composition, more competent to the motile cell (Lamouille *et al.*, 2014).

1.4. Three different types of EMT throughout the animal kingdom

As cell junctions ensure proper function of an organ, and even the organism as a whole, in some processes cells have to step out of their highly organized epithelial frame to fulfill a role at other sites in the organism. According to their functional role in the body, three different types of EMT can be distinguished. Each type has its typical inducers to activate EMT at the appropriate time and place. The loss of cell junctions will for instance appear in embryonic development in which cells have to migrate in order to give rise to the different organs at their appropriate sites in the embryo (Thiery *et al.*, 2009). Beside this function in the embryological development, the loosening of cells will also play a role in the healing process to restore the epithelial layer. In cancer, tumor cells can abuse this mechanism to escape from the primary tumor site in order to colonize another site where the environmental factors are more favorable, called metastasis (Hanahan & Weinberg, 2011).

1.4.1. **First type:** EMT in development

The first type of EMT occurs during embryogenesis and can be divided into primary, secondary and tertiary EMT, according to the moment of the transition (Thiery *et al.*, 2009). These subtypes of developmental EMT are mainly applied on vertebrate embryogenesis. In mammals, primary EMT occurs at endometrial blastocyst implantation (Uchida *et al.*, 2012), placenta formation (Kokkinos *et al.*, 2010), gastrulation and neural crest cell migration (Rogers *et al.*, 2013). During gastrulation, EMT is induced by Transforming Growth Factor β (TGF β) and subsequent regulated by EMT transcription factor SNAIL. After induction of the transition, expression of SNAIL will be maintained by FGF. During neural crest cell migration, EMT is activated through interplay between FGF, Wnt, Notch, Retinoic Acid and Bone Morphogenic Protein 4 (Sauka-Spengler and Bronner-Fraser, 2008). Secondary EMT will be induced during formation of the muscles, internal organs (liver, pancreas and reproductive tracts), two cardiogenic areas around the primitive gut (Nakajima *et al.*, 2000) and the limb buds (Gros & Tabin, 2014). Tertiary EMT is also known as endothelial-to-mesenchymal transition (EndoMT) (Lin *et al.*, 2012). This is the transition from endothelial cells, defining blood vessels, to mesenchymal cells. EndoMT is located at the heart, where it will shape the heart valves (Lin *et al.*, 2012).

1.4.2. **Second type:** EMT during wound healing

During wound healing, keratinocytes surrounding the wound are activated to undergo partial EMT (Shaw & Martin, 2016). These intermediate cells will move into the reorganizing epithelial layer and undergo MET to close the epithelial barrier, a mechanism called re-epithelization (Leopold *et al.*, 2012). These partial mesenchymal cells show other characteristics than full mesenchymal cells such as the possibility of moving in cell aggregates rather than as individual cells. As with many biological processes, this mechanism can be abused in various pathological contexts. Reconsidering wound healing, the formation of an inflammatory environment in the wound can induce excessive formation of scar tissue by an accumulation of myofibroblasts secreting collagen, impairing proper organ function e.g. in liver cirrhosis (Rowe *et al.*, 2011).

1.4.3. **Third type:** EMT in cancer

Metastasis, first described by Recamier (1829), is the exit of tumor cells from the primary tumor in order to establish a secondary tumor in a new niche in the organism. It is a highly investigated process and one of the ten cancer hallmarks (Figure 5) (Hanahan & Weinberg, 2011). The presence of metastasis is generally associated with a poor survival rate (Gilkes & Semenza, 2013). Of the carcinomas, 90% is epithelial and can therefore undergo EMT. The other 10% of the carcinomas comprise e.g. types of leukemia where tumor cells are already circulating in the body (Diepenbruck & Christofori, 2016). However, because of the complexity of metastasis, a consensus about the process is far from reached (Tarin, 2005; Nieto *et al.*, 2016; Hanahan & Weinberg, 2011). It has even been proposed that EMT does not have a significant role during metastasis and that also epithelial tumor cells can invade other niches. In this case, EMT contributes to chemoresistance (Fischer *et al.*, 2015).

Under the influence of different factors, EMT will be initiated in epithelial tumor cells located in the so-called invasive front, the outer ridge of the tumor. Marcucci *et al.* (2014) recently gave five main classes of factors from the tumor micro-environment directly inducing EMT: (i) hypoxia (Carmeliet & Jain, 2011) and low pH (Estrella *et al.*, 2013), (ii) innate and adaptive immune responses through inflammation induced by tumor associated macrophages (TAMs) (Fabbri *et al.*, 2012), (iii) mechanical stress because of the high amount of cells (Gjorevski *et al.*, 2012), (iv) a stiffer ECM, which alters cell-cell interactions, cell-matrix interactions and the cytoskeleton (Imamichi & Menke, 2007) and (v) treatment with antitumor drugs (Ebos *et al.*, 2009).

The activation of the EMT process during metastasis is often seen as a survival mechanism to escape the hostile primary niche depleted of oxygen and nutrients (Tiwari *et al.*, 2012). After EMT, the intermediate (EM) or fully mesenchymal tumor cells leave the primary tumor and intravasate the blood vessels. In tumors, these vessels are often leaky and not well formed, promoting intravasation (Carmeliet & Jain, 2011). Subsequently the circulating tumor cells (CTCs) will have to endure hostile environments, such as several kinds of immune cells and a low concentration of growth factors (Sethi & Kang, 2011). When the amount of EMT inducing factors decreases, CTCs will extravasate the blood vessel and colonize a new niche. This colonization is only successful if the environment allows the tumor cells to reside there and/or if the tumor cell adapts to the new niche. These CTCs will regain their epithelial characteristics through MET in their secondary niche. After MET, they often get into a dormant state, influenced by the diminished supply of several factors, local suppression by the invaded tissue or even by systemic suppressors released by the primary tumor. The latter implies that when the primary tumor is surgically removed, the dormant tumor cells can revive (Hanahan & Weinberg, 2011). The sequence of events during metastasis is often

depicted as a cascade (Figure 5) (Talmadge & Fidler, 2010). However, this cascade does not always count for every tumor. For instance, when the cells from a secondary tumor regain their migration characteristics, secondary circulating tumor cells can recolonize the primary tumor. It has even been proposed that metastasis is set on at a much earlier time point, when the primary tumor is still small (Sethi & Kang, 2011).

In many cases, this EMT is not fully carried out, leading to circulating cancer cells that are partially mesenchymal and partially epithelial (Figure 5) (Lundgren *et al.*, 2009). Even circulating tumor cell aggregates can invade the blood vessel as a whole, being coated by blood platelets to protect them and travelling through the organism as a clump of cells. SNAIL2 and FGF-R play a principal role in this cluster formation and movement. This clump of cells can then successfully invade new niches and turn into a secondary tumor (Figure 5) (Au *et al.*, 2016). Another mode of invasion is proposed in Hanahan & Weinberg (2011), where not a motile, ECM degrading, mesenchymal cell is formed but a more amoeboid cell that moves through already existing holes in the ECM.

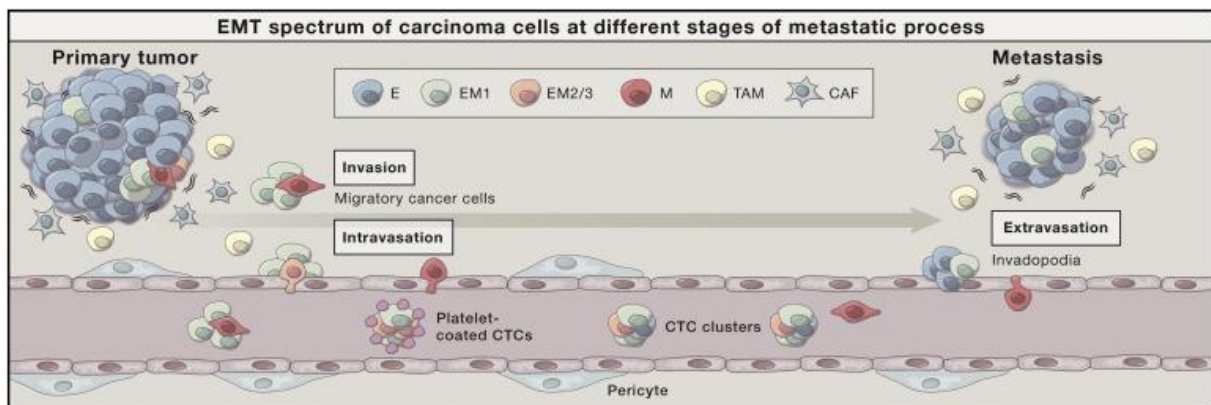


Figure 5: The metastatic cascade. In the tumor micro-environment, EMT can be induced by several factors, such as: (i) hypoxia and low pH, (ii) immune responses (inflammation) through tumor associated macrophages (TAMs) and adaptive immune cells, (iii) mechanical stress, (iv) a stiffer ECM and (v) antitumor drugs. After undergoing complete or partial EMT, single mesenchymal (M) cells, single intermediate mesenchymal cells (EM1/EM2/3) or cell clumps containing both types become CTCs, invade the tissue surrounding the tumor and intravasate the blood vessel. The CTCs then migrate through the hostile blood vessels, where they might be protected by blood platelets. When EMT inducing signals decrease, the CTCs extravasate the blood vessel and form a secondary tumor through MET. In time, tumor cells of the secondary tumor can also undergo EMT and colonize other niches or recolonize the primary tumor site (Nieto *et al.*, 2016).

1.4.3.1. Hypoxia-induced EMT

Hypoxia, or low oxygen level, is a known inducer of EMT (Nieto *et al.*, 2016). The reason is found 1600 million years ago during the Great Oxidation Event (Kump *et al.*, 2011). The atmosphere was filled with the toxic compound molecular oxygen as a waste product of cyanobacteria. Anaerobic cells died and only a few oxygen tolerant aerobic microbes were able to survive this new harsh environment. These aerobic bacteria are the ancestors of all metazoa. However, this new way of life implicates the complete dependence on oxygen for obligate aerobic cells. This is the reason why aerobic tumor cells do extreme efforts to ensure oxygen supply by activating angiogenesis upon hypoxia (Figure 6) (Carmeliet & Jain, 2011). However, when this fails, the transition from a vast cell mass to an 'each for itself'-strategy is made during EMT, whereby separate cells that ceased the alliance with other cells, leave the tissue and search an aerobic environment where the needs of the cell are satisfied (Figure 7) (Imai *et al.*, 2003). The way how the transport, namely via chemotaxis, and the transition to individual cells occurs might still be part of an ancient mechanism present from the time when individual cells or cell aggregates had to search for aerobic environments. This might explain why the expression of factors that regulate hypoxia-induced EMT as well as EMT itself are so well conserved in the animal kingdom from invertebrates up to humans.

In the cell, oxygen levels are sensed by the prolyl hydroxylases (PHD). These enzymes hydroxylate hypoxia-inducible factor - 1 α (HIF-1 α) at normal cellular oxygen levels (Aragonés *et al.*, 2008). This hydroxylation is followed by the ubiquitination of HIF-1 α by the von Hippel-Lindau (VHL) E3 ubiquitin ligase complex and its subsequent degradation by the proteasome (Figure 6) (Jiang *et al.*, 2011). In hypoxic conditions, however, HIF-1 α is stabilized as a result of low PHD-activity, which is depleted of the oxygen needed to hydroxylate HIF-1 α (Prabhakar & Semenza, 2012). Subsequently, active HIF is formed out of the stabilized HIF-1 α and HIF-1 β (aryl hydrocarbon receptor nuclear translocator (ARNT)) from the cytosol (Figure 7) (Jiang *et al.*, 2011). The active HIF is then transported to the nucleus where it binds together with TIC and p300 to hypoxia-responsive elements (HREs) located in the promoters of genes affected by the low oxygen level. These genes comprise for instance the EMT genes (for instance SNAIL and TWIST) but also hemoglobin or inducers of angiogenesis (Imai *et al.*, 2003; Yang *et al.*, 2008; Gorr *et al.*, 2004).

The activity of HIF is closely regulated in hypoxic cells as prolonged activity can have several side effects like an increase of transcription of oncogenes leading to hyper proliferation and cancer. Therefore, in prolonged hypoxia, the activity of HIF is again downregulated by HIF-mediated upregulation of its own repressor PHD, creating a negative feedback loop (Cavadas *et al.*, 2015). As the protein level of HIF-1 α transiently increases during acute hypoxia, the opposite occurs at the mRNA level, which is downregulated as soon as hypoxia

occurs. This downregulation on transcriptional level is mediated through hypoxia-induced silencing of the HIF-1 α gene by Repressor Element 1-Silencing Transcription Factor (REST). This is a zinc-finger transcription factor that binds to the 21bp Repressor Element 1 (RE1) in the HIF-1 α promotor (Cavadas *et al.* 2015). In this way, REST can be seen as a tumor suppressor gene protecting the cell from the devastating side-effects from HIF overexpression. Other negative feedback mechanisms also exist like antisense RNAs (Rossignol *et al.*, 2002) or miRNAs (Bruning *et al.* 2011). In malignant cells, these mechanisms might be downregulated, resulting in the chronic stabilization of HIF (Cavadas *et al.* 2015). However, HIF itself can also play a protective role, increasing the barrier function when activated (Furuta *et al.*, 2001; Kelly *et al.*, 2015).

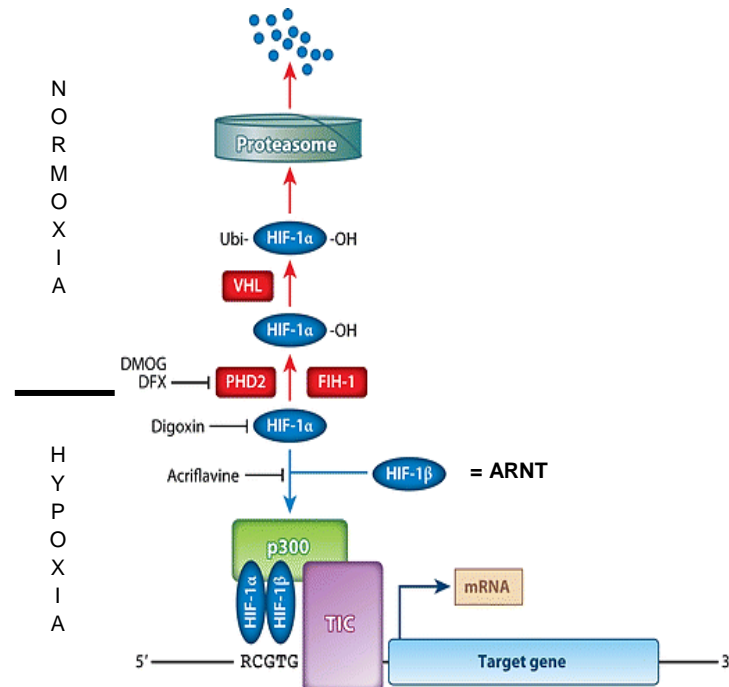


Figure 6: Function of HIF in cells under normoxic and hypoxic conditions. In cells suffering from hypoxia HIF-1 α interacts with HIF-1 β (ARNT) to form a complex together with p300 and TIC that will bind to HREs in the promoters from responsive genes. These responsive genes comprise not only angiogenesis activating factors but also EMT-inducing genes, metabolic reprogramming, immortalization and cell survival (Gilkes & Semenza, 2013). In cancer cells it can also lead to resistance to chemotherapy and invasion (Gilkes & Semenza, 2013). In cells in normoxic conditions PHD2 senses the oxygen (Aragonés *et al.*, 2008) and will hydroxylate HIF-1 α which will subsequently be degraded through the von Hippel-Lindau E3 ubiquitin ligase complex (Sahlgren *et al.*, 2008). Several inhibitors of the HIF function, digoxin and acriflavine, and from the PHD function are also given in the figure (Adapted from Semenza, 2014).

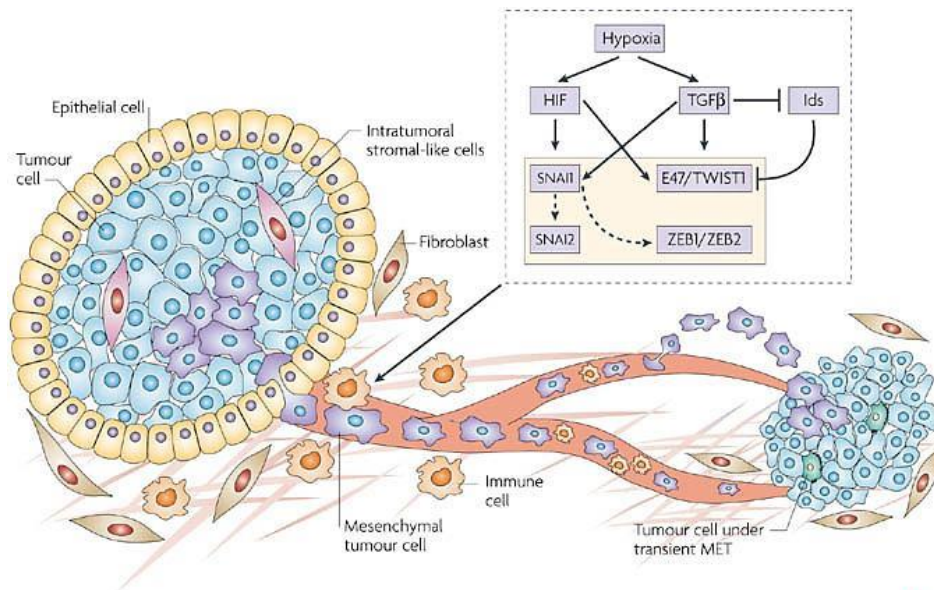


Figure 7: Representation of the hypoxic environment at the primary tumor site. This leads to EMT of tumor cells through HIF but also through TGF β signaling to escape this hostile environment and the settlement of these CTCs at a secondary site where they undergo MET to form a secondary tumor (Peinado *et al.*, 2007).

1.4.3.2. *In vivo* models for hypoxia-induced EMT

Molecular mechanisms of EMT are mostly deciphered in *in vitro* cell culture, where hypoxia, stress and toxic compounds are often used to initiate the transition (Dekervel *et al.*, 2017). However, the extrapolation to *in vivo* models has to be made to uncover regulation in a living organism. Especially the interaction with the immune system is hard to prove in *in vitro* systems. In cancer research, vertebrates are already established model organisms (Nieto *et al.*, 2016). However, the use of these animals is expensive and bound to strict ethical constraints. There is a strong need for high-throughput, easy-to-use, cheap, invertebrate model organisms, especially if one wants to study conserved responses such as EMT. In hypoxia-induced EMT research, a good *in vivo* invertebrate model is still lacking (Steinestel *et al.*, 2014). In *Drosophila melanogaster*, functional assays and genomic studies are done at such rate that it made itself a valuable organism to investigate malignant traits that also arise in mammals (Gonzalez, 2013). In metastasis research as well as in development-associated EMT, *D. melanogaster* is rising (Stefanatos & Vidal, 2011; Smallhorn *et al.*, 2004) and shows to be hypoxia-tolerant (Gorr, 2004). *Caenorhabditis elegans* is becoming a valuable model organism in cancer research to investigate several cancer hallmarks such as cell cycle regulation, apoptosis and metastasis (Kirienko *et al.*, 2010). However, tissue specific investigation of genetic alterations is more difficult to perform because of the small size of the organism.

1.5. *Microcystis sp.* as EMT inducer?

Cyanobacteria or 'blue-green algae' are bacteria that show both characteristics of algae and bacteria. They are adapted to survive in a vast array of environments around the world (Cheung *et al.*, 2013), obtain their energy through photosynthesis, fixate nitrogen (Herrero *et al.*, 2001) and are characterized by the presence of intracellular gas vesicles allowing them to move vertically in the water column (Porat *et al.*, 2001). Most species occur in colonies that can form cyanobacterial harmful algal blooms (CyanoHABs) due to dense populations upon the exposure of excessive nutrients and warmth (Cheung *et al.*, 2013). These CyanoHABs are potentially dangerous through the production of cyanotoxins (hepatotoxins, neurotoxins and dermatotoxins) as they affect wildlife and public health when occurring in ponds and drinking water reservoirs (Hudnell, 2010).

One of the most studied cyanotoxins is the hepatotoxic microcystin (MC) from *Microcystis sp.*, a cyclic peptide containing 7 amino acids (Campos & Vasconcelos, 2015). The most toxic and abundant is microcystin-leucine arginine (MC-LR). After being transported into the cell through organic anion transporting peptides (OATP), MC-LR is a potent serine/threonine phosphatase inhibitor resulting in the hyperphosphorylation of proteins (Figure 8, Wang *et al.*, 2005) leading to apoptosis (Wei *et al.*, 2014) and the inhibition of embryonic development through the loss of cell junctions (E-cadherin) (Wang *et al.*, 2005). In some scenarios, MC-LR may also be detoxified through Glutathion S Transferase (GST) and transported out of the cell (Gehring *et al.*, 2004). The loss of E-cadherin is one of the hallmarks of EMT and proven to be induced by MC-LR in mouse lungs (Wang *et al.*, 2016) mediated through the inhibition of protein phosphatase 2A (PP2A). This phosphatase has a vast array of functions in cells, like monitoring the PI3-K/Akt and MEK/ERK pathways that also play essential roles in inducing EMT (Figure 9, Wang *et al.*, 2016). The relation between PP2A and SNAIL, the repressor of E-cadherin, is not yet proven but there is a certain correlation between PP2A and E-cadherin in breast carcinomas (Suzuki & Takahashi, 2006). So, besides damage to the liver, kidneys, lungs and reproductive organs and a diminished immune function, MC-LR also knows cancer-inducing properties and leads to invasion and migration of cells (Wang *et al.*, 2016). This was also proven by Ren *et al.* (2017), where colon cancer cells underwent EMT after administration of microcystin.

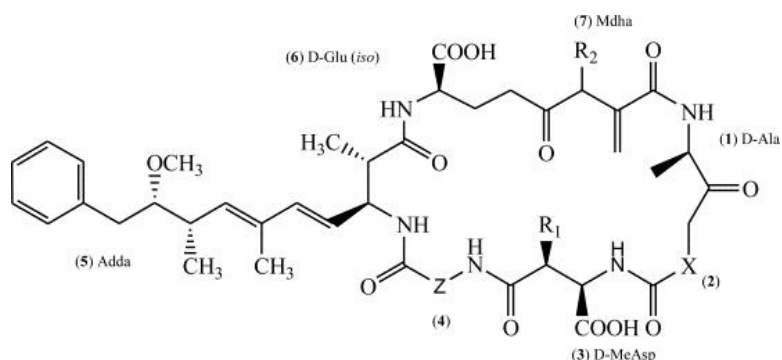


Figure 8: Microcystin (MC) with X being L-leucine, Z L-arginin and R_1 and R_2 being CH_3 in MC-LR (Campos & Vasconcelos, 2010).

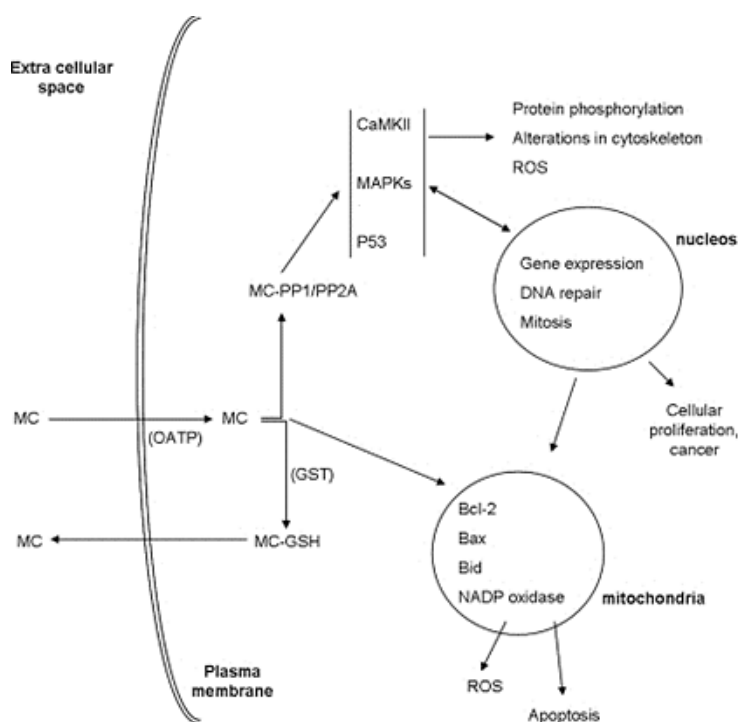


Figure 9: The entry and function of MC in the cell. The intracellular effect of MC is believed to be an increase in apoptosis but also an induction of EMT by the repression of PP1/PP2A, which are potent inhibitors of the PI3-K/Akt pathway. This pathway has a known effect on the regulation of SNAIL. Additionally, through the inhibition of PP1/PP2A, the Bcl-2 is degraded which will cause the induction of the apoptotic pathway. Also, a significant amount of Reactive Oxygen Species will enter the cytosol which will cause intracellular stress (adapted from Campos & Vasconcelos, 2010)

Chapter 2

Microbiome, EMT and Cancer

2.1. The microbiome

A multicellular organism rarely stands on its own but is accompanied by trillions of bacteria helping to fulfil different needs of the organism. These accompanying micro-organisms or microbiota, already colonize the host at birth and live in and all over the organism during its entire life. The genetic information of all the microbiota even form a second genome in the host, called the microbiome. The interaction between the host and the microbiota can be either parasitic, commensalistic or mutualistic. The parasitic interaction depicts itself as an infection and is often successfully eradicated by the immune system. During the commensalistic interaction the micro-organisms benefit from the interaction without harming the host. Mutualism will be positive for both microbiota and host, for example in food supply (Nicholson *et al.*, 2012), development (Diaz Heijtz *et al.*, 2011), immunity (Dillon *et al.*, 2005;), growth and reproduction (Sison-Mangus *et al.*, 2014) and even toxin degradation (Kohl *et al.*, 2014). In order to maintain a healthy microbiome, prebiotics are good treatments and can even boost the microbiota present in the gut.

However, the composition of this collection of microbes is not static but changes throughout the life of the host depending on different environmental effects and signals from the host itself (Tasiemski, *et al.*, 2015). This implicates co-evolution between micro-organisms and their host throughout history. As hypoxia is the major research point in this master thesis, the effect of a hypoxic environment will be tested on the composition of the microbiome. In mice with sleep apnoea, a condition that implies the appearance of short periods of hypoxia (5%), Moreno-Indias *et al.* (2015) prove that the fecal microbiota changed under influence of a low oxygen level. In European sea bass, Gatesoupe *et al.* (2016) show that their natural resistance to hypoxia is correlated with the microbiota composition.

2.2. Roles of microbiota in EMT and carcinogenesis

Recently, the importance of the microbiome is getting more and more established in the clinical world, for example its important role, protective or evocative, in cancer. However, the role of microbiota in the induction or progression of cancer is still not understood and at the moment subject of intensive investigation. Only few bacteria such as *Helicobacter pylori* and viruses like Hepatitis B and C are known to induce cancer (de Martel *et al.*, 2012; Li *et al.*, 2016).

According to Garrett (2015) there are three categories in which the microbiota can contribute to carcinogenesis: (i) altering the balance between proliferation and cell death in the host cell, (ii) guiding the immune system and (iii) affecting the metabolism of cancer drugs, nutrients and signaling factors. Microbes that are present at the tumor site are even able to become part of the tumor micro-environment and can specifically affect the tumor growth. The positive effect of the bacteria on cancer, through the release of toxins that affect tumor promoting pathways, is often the result of years of co-evolution with other bacteria. Here they had to outcompete other bacteria through the production of toxins that induce DNA damage, occasionally resulting in cancer promoting mutations in humans (Garrett, 2015).

In the colon, carcinogenesis is already elucidated by many micro-organisms such as *Fusobacterium nucleatum* (Rubinstein *et al.*, 2013). Its virulence factor, the surface adhesion *FadA*, can activate the Wnt/ β -catenin pathway leading to an increased proliferation of the epithelial cells (Dzutsev *et al.*, 2015). Also, enterotoxigenic *Bacillus fragilis* (fragilysin-mediated c-MYC ongene activation, *Bft*-toxin mediated overproduction of DNA-damaging reactive oxygen species and cytolethal distending toxin directly damaging DNA), the enteropathogenic *Escherichia coli* (DNA-damaging colibactin), *Salmonella typhi* (*AvrA*), *Streptococcus gallolyticus* and *Enterococcus faecalis* are known to induce carcinogenesis (Figure 10) (Garrett, 2015; Irrazábal *et al.*, 2014; Dzutsev *et al.*, 2015; Arthur *et al.*, 2012). However, not only toxins are able to induce tumorigenesis but also other second bacterial metabolites such as H₂S which induces the MAPK pathway in order to modulate proliferation, apoptosis and differentiation (Deplancke & Gaskins, 2003). Also chronic inflammation, caused by bacteria, is proven to induce carcinogenesis (Castellone *et al.*, 2005). Here, an impaired balance between the host and the bacteria leads to a state of chronic inflammation. In this scenario, inflammation factors are released, promoting cancer cell growth (Castellone *et al.*, 2005). The link with EMT is harder to find, however it was proven that certain bacteria, such as *H. pylori* and *S. typhi* may upregulate the β catenin pathway, a known induction pathway of EMT (Figure 10) (Abreu & Peek, 2014; Tam & Weinberg, 2013). *H. pylori* lives in the human stomach. In normal circumstances, a balance is maintained whereby the bacteria inflict no harm. However, when the immune system is low for example during stress, the toxins *cagA* and *cagE* causes transcription of EMT regulators and leads to mobile mesenchymal cells in the stomach (Chang *et al.*, 2015). *F. nucleatum* will also upregulate this pathway but relying on E-cadherin signaling (Figure 10) (Rubinstein *et al.*, 2013). *E. coli* bacteria even showed to induce EMT through a HIF-1 α mediated way (Cane *et al.*, 2010). On the other hand, Kelly *et al.* (2015) showed that bacteria also play a protective role to avoid EMT from occurring in the gut epithelium. Here, short-chain fatty acids (SCFAs), like butyrate, produced by bacteria in hypoxic conditions, activate HIF which in this case stabilizes the barrier function.

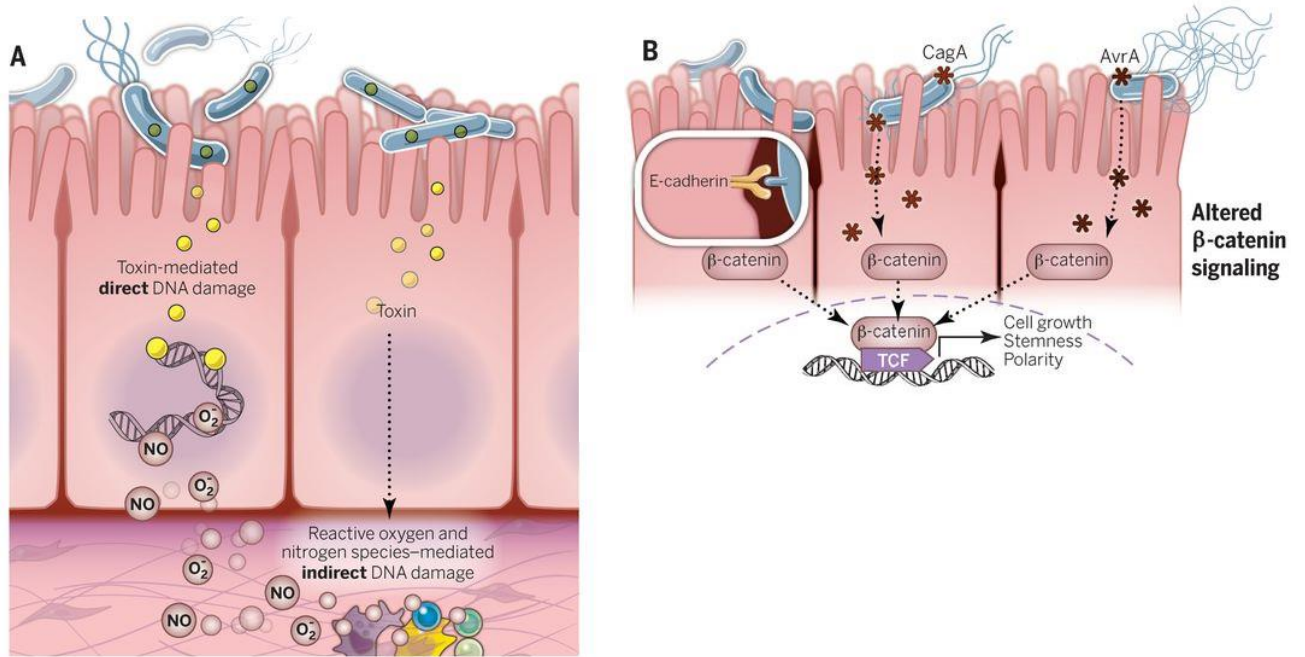


Figure 10: Interaction of cancer-inducing toxins and gut cells. (A) The production of toxins is able to directly or indirectly mediate (via ROS production) DNA damage. **(B)** Three different mechanisms to induce the β catenin pathway. The first is initiated via E-cadherin signaling (*F. nucleatum*), the second via *CagA* (*H. pylori*) and the third via *AvrA* (*S. typhi*). This β catenin pathway is also a known inducer of EMT (Tam and Weinberg, 2013) but the direct link between microbiota and EMT still needs to be elucidated (adapted from Garrett (2015)).

Chapter 3

Daphnia magna

3.1. Biology of *Daphnia magna*

Daphnia magna Straus. is a 5 mm planktonic crustacean, belonging to the class of the Branchiopoda, infraorder of the Cladocera and family of the Daphniidae (Figure 11). *Daphnia* prefers to swim in the open water (pelagic) of ponds, where they filter the water for green algae and bacteria. *Daphnia* feeding on algae will have a clear green gut as the bacteria-feeding *Daphnia* have a more transparent gut. The rate of filtering the water is maximal when food is not abundant and decreases with increasing food concentration. *Daphnia magna* shows a diel vertical migration. In night time *Daphnia* come to the surface to feed on the algae. In day time, they go to deeper regions of the pond, where they hide for predators which are active during day time (Decaestecker *et al.*, 2002).

Daphnia magna has five limbs or phylloids that generate a current towards the mouth and act as filter and respiration apparatus (Figure 11). After filtering, food is taken up via the mouth and passes through the gut via peristaltic contractions. The gut of *Daphnia magna* is divided into three parts: the esophagus, midgut and hindgut (Figure 11). The esophagus only comprises a very small part of the gut in contrary to other arthropods and is lined with a cuticle. The midgut is lined with an epithelium that is equipped with microvilli for optimal absorption. On top of the epithelium, the midgut is lined with a peritrophic membrane protecting the epithelium and preventing large food particles from landing in the ceca. These two ceca, situated at the beginning of the midgut, increase the digestion area and secrete digestive enzymes. The hindgut, again lined with cuticle, serves for water absorption and storage of feces (Ebert, 2005, Smirnov 2017).

Daphnia magna is covered by a carapax, i.e. an uncalcified exoskeleton, rich of chitin (Figure 11). This not only covers the body but also creates a cavity where the phylloids are situated and where a current is created. Inside the body itself, another current of body fluid, hemolymph, is produced by the dorsally situated heart (200 beats/min at 20°C). As *Daphnia magna* has an open circulation, no blood vessels are present. Oxygen transport can be intensified by extra hemoglobin expression, turning the animal's body red (Gorr, 2004). The nervous system comprises a cerebral ganglion ('brain') and a large compound eye (Figure 11). As in other invertebrates, mainly the innate immune system is described (Decaestecker *et al.*, 2011). Nevertheless, in *Daphnia magna*, there is a strain specific immunity described, which is passed on to the offspring by the mother. This might be seen as a possible form of acquired immunity (Little *et al.*, 2003).

Daphnia magna reproduces via cyclic parthenogenesis (Figure 12). When conditions are favorable, asexual reproduction occurs leading to the procreation of female juveniles (Miner *et al.*, 2012). The parthenogenetic eggs are stored in the dorsally situated brood chamber (Figure 11) and released after each molt (every 3-4 days). The eggs hatch the first day they enter the brood poach and develop in this poach for the next three days until the moulting of the mother. The juveniles then undergo six juvenile instars and develop their first eggs after 8-10 days, depending on environmental conditions. In unfavorable conditions the mother *Daphnia* sets on the procreation of male juveniles. These males attach to females and sexual reproduction occurs, leading to the fertilization of one or two resting eggs (Decaestecker *et al.* 2009). The resting eggs are encapsulated by an ephippium, a melanized protective shell. After shedding, the ephippia sink to the sediment and remain there for several generations (diapause) (Figure 12). At certain environmental conditions, these eggs hatch and only release female juveniles (Heckmann *et al.*, 2008).

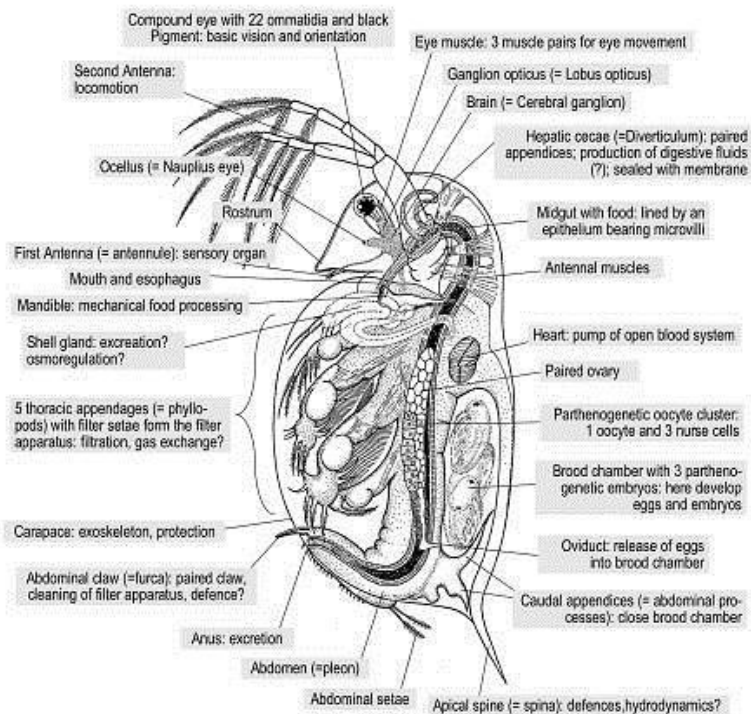


Figure 11: Representation of the *Daphnia* sp. anatomy (Ebert, 2005).

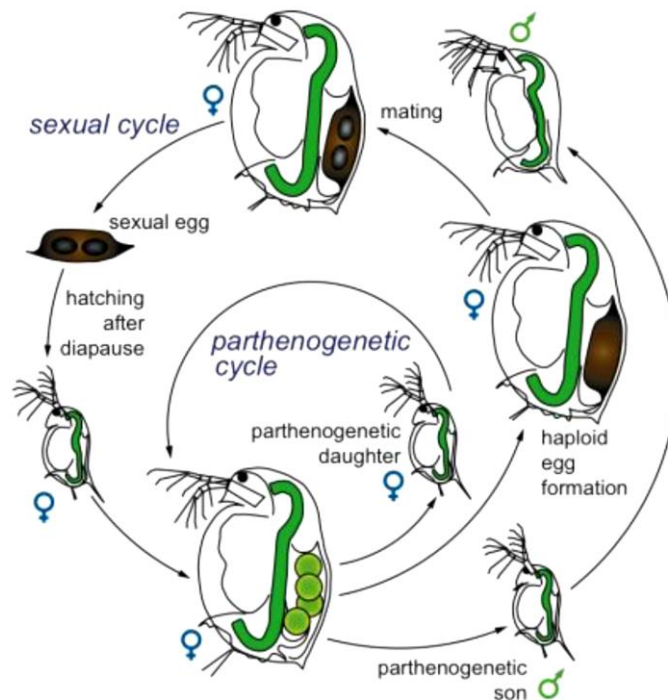


Figure 12: Cyclic parthenogenesis of *Daphnia magna*. In favorable conditions the parthenogenetic cycle is active and the sexual cycle occurs when conditions are less favorable. During the sexual cycle, the sexual eggs (1-2) are stored into a melanized ephippium. This will protect the eggs from external influences until hatching. The adult female *Daphnia magna* can carry up to 100 asexual eggs of each breed (Ebert, 2005).

3.2. *Daphnia magna* as a model organism

Daphnia magna already plays an important role as an eco-toxicological model organism (Miner *et al.*, 2012) and is a member of the list of model organisms of the National Institute of Health (<https://www.nigms.nih.gov/Research/Models/Pages/default.aspx#d>). This small crustacean has earned this title because it takes an essential place in the feeding web of aquatic ecosystems as part of the zooplankton. *Daphnia* filters the water for the present algae and as such prevents the pond from being overgrown by algae, ensuring a healthy equilibrium in the pond. *Daphnia magna* is very sensitive for external stressors and is therefore often used to study stress responses (Heckmann *et al.*, 2008). However, also in physiology *Daphnia* has a history as a model organism. In 1893 for instance, Metchnikoff already performed wound healing experiments on this crustacean. *Daphnia* has an ecoresponsive genome that shows strong adaptive expression, more in particular because it contains multiple duplicated genes (Colbourne *et al.*, 2011). The genome of *Daphnia magna* is 238 Mb in size and comprises ten chromosomes (Routtu *et al.*, 2014). Also in microbiota research, *Daphnia magna* is getting established as model (Callens *et al.*, 2016).

The choice for *Daphnia magna* as a model organism is supported by the several advantages: (1) easy breeding, (2) many offspring, (3) clonal asexual reproduction (constant genetic background), (4) small size (5) *Daphnia* genome/transcriptome is sequenced and published (wFleabase) (6) fast and strong responses to environmental stressors, (7) transparent exoskeleton and (8) no ethical concerns for use of *Daphnia magna*.

3.3. *Daphnia magna* and hypoxia

Daphnia magna well tolerates hypoxia, even up to only 2% oxygen dissolved in the water (Smirnov, 2017). As such, they can still graze ponds heavily overgrown by algae, so-called algal blooms, which lead to hypoxia in the water. A striking effect of this low oxygen level on *Daphnia* is the emergence of red hemolymph because of the transcription of hemoglobin (Hb) genes. Because of the transparent carapax of *Daphnia* this is clearly visible and the first reports on this issue already emerged in 1948 by Fox. Hemoglobin in *Daphnia* is located extracellularly and is a 454 kDa molecule with 16 subunits all possessing two heme groups (Gorr *et al.*, 2004; Lamkemeyer *et al.*, 2006). In this way *Daphnia* hemoglobin is capable of carrying up to eight times more oxygen compared to human hemoglobin. The hemoglobin synthesis occurs in the fat body through binding of active HIF to HREs in the promotor region of Hb. The transcription of six different Hb genes leads to seven Hb subunits making up the Hb macromolecule (Lamkemeyer *et al.*, 2006). Adaptations to live at low oxygen levels are mostly accompanied by a diminished growth and reproductive capacity (Homer & Waller, 1983). However, scientists have succeeded in making *Daphnia* reproducing in a hypoxic environment and saw that the adaptations to the lowered oxygen levels were passed on to the next generation (Lai *et al.*, 2016). Because of these findings the use of *Daphnia magna* as a model organism for hypoxia investigations, ecological or molecular, is supported and easily performed (Gorr, 2004).

3.4. *Daphnia magna* and *Microcystis* sp.

Microcystis sp. is present in freshwater ponds and *Daphnia magna* uses these algae as feeding source (Sarnelle *et al.*, 2010). The effect of microcystin on the fitness of *Daphnia magna* depends on the fact if the *Daphnia* are tolerant or not. Tolerant individuals are suggested to have an adapted microbiome containing bacteria that help in breaking down the toxin in non-toxic peptides (Macke *et al. in revision*). Such strains of microcystin degrading bacteria are present in the bacterioplankton (Dziga *et al.* 2013) and it is suggested that *Daphnia* is able to select these particular strains upon *Microcystis* exposure (Macke *et al. in revision*). *Daphnia* cells also undergo epigenetic changes in response to the toxin (Asselman *et al.*, 2017). The proven relationship between MC-LR and EMT gives a solid base for the investigation of *Microcystis* sp.-induced EMT in MC susceptible *Daphnia magna* in this master thesis.

3.5. *Daphnia magna* and EMT

In invertebrates, the occurrence of EMT is essential in the development of the body plan of the organism during embryogenesis. In the arthropod *Drosophila* a lot of research has already been done on EMT and MET during development (Natzle *et al.*, 2008). Different transcription factors associated with EMT have been identified such as SNAIL (Cobaleda *et al.*, 2007; Barrallo-Gimeno & Nieto, 2006) and TWIST (Ozdemir *et al.*, 2011). *Daphnia* is established as an organism that can be used for research about hypoxia (Gorr, 2004), but detailed gene expressions investigating the link of hypoxia with EMT are not available yet. The ecdysozoan *Caenorhabditis elegans* is getting more and more established in cancer research and EMT during metastasis (Kirienko *et al.*, 2010) where SNAIL (Barrallo-Gimeno & Nieto, 2006) and TWIST (Wang *et al.*, 2006) are also factors during this process. As these two organisms are closely related to *Daphnia magna* (all three are ecdysozoans), it is an incremental step to investigate the presence of these EMT regulators and effectors in this crustacean. In wFleabase the presence of E-cadherin, N-cadherin, SNAIL and TWIST in *Daphnia* is shown. As the transcription factor HIF α was characterized in *Daphnia* (Gorr, 2004) and as this is a valid inducer for EMT (Imai *et al.*, 2003; Yang *et al.*, 2008) the assumption that hypoxia-induced EMT occurs in *Daphnia magna* has been proposed by the Aquatic Biology research group @ KULAK and is tested here in this thesis. This implies the possibility of developing *Daphnia magna* as a new model organism for research on hypoxia-induced EMT and studying its role for metastasis in cancer *in vivo*.

3.6. *Daphnia magna* and its microbiota

The microbiota living in symbiosis with *Daphnia magna*, mainly consist of β -Proteobacteria and Bacteroidetes (Qi *et al.*, 2009). *Limnohabitans sp.* is designated as the most present bacteria species (Freese & Shink, 2011). The relation between *Daphnia* and its microbiota is proven to be very specific and consistent. *Daphnia* from North-America and Europe showed differences on species level but on a higher taxonomical level these showed remarkable similarities (Qi *et al.*, 2009). In 2014, Sison-Mangus *et al.* proved that *Daphnia* depleted of gut bacteria showed a significant reduction of the life span and reproduction than *Daphnia* with normal gut microbiota. Given that research on gut microbiota in *Daphnia* is already performed in the Aquatic Biology research group @ KULAK (Callens *et al.*, 2016), this model organism will be used in this thesis to investigate the effect of hypoxia on the gut microbiome. This may give rise to possibilities in the future to develop *Daphnia* as a model to study microbiota living in parts of the human gut with a lower oxygen level.

Objectives

Daphnia shares a lot of functional genes with humans, e.g. genes coding for conserved basic cellular responses or higher-level interactions of multicellular organisms, such as pathways related to animal stress responses (Colbourne *et al.*, 2011). As such, this invertebrate is a promising new model system for the investigation of hypoxia-related responses like EMT, an evolutionary conserved embryonic process (Imai *et al.*, 2003). EMT is also induced in epithelial cells when exposed to toxins, like microcystin (Wang *et al.*, 2016), a natural toxin *Daphnia* encounters during blooms of *Microcystis sp.* in freshwater systems. In this thesis project, the first aim was to study *Daphnia* upon exposure to hypoxia or a *Microcystis aeruginosa* diet to study EMT mechanisms. Whole *Daphnia* tissue and *Daphnia* guts were analyzed for alterations in gene expression of known human hypoxia and EMT marker genes.

Hypoxia marker HIF shows a dual role when activated in the case of hypoxia. This transcription factor will increase cellular survival by activating pathways like hemoglobin production (Gorr *et al.*, 2004) or increase of the cell junctions (Furuta *et al.*, 2001). On the other hand, HIF is proven to activate EMT by upregulation of EMT regulators, like SNAIL (Imai *et al.*, 2003) and TWIST (Yang *et al.*, 2008). During EMT, SNAIL and TWIST expression is upregulated leading to the subsequent downregulation of E-cadherin and upregulation of N-cadherin. Next, to study the EMT process *in se*, the second aim of this thesis was to relate the expression of HIF to the expression profile of the EMT marker genes. There are two plausible hypotheses on the outcome of the exposure: (i) increased HIF expression upon hypoxia is associated with increased activation of EMT, (ii) *Daphnia* that are naturally adapted to hypoxia will upregulate mechanisms that counteract the negative effects of HIF, more in particular downregulation of EMT, and activate other pathways beneficial for *Daphnia* fitness.

At third, I aimed to study the effect of hypoxia on the composition of the gut microbiota in *Daphnia*. These gut microbiomes were sequenced to achieve a good overview of the gut microbiome composition. Previous gut microbiome research in *Daphnia* revealed a shift when exposed to *Microcystis* (Macke *et al.*, in revision), however this was never investigated in hypoxic *Daphnia*. Here, I introduce the hypothesis that *Daphnia* will keep those bacteria that help the animal in surviving hypoxia (Kelly *et al.*, 2015).

In conclusion, I aim to realize the following goals:

- Investigate the gene expression of known EMT markers in *Daphnia* upon hypoxia and *Microcystis* exposure using quantitative PCR (qPCR) and relate them to the *HIFa* expression
- Study the changes in the gut microbiome composition of *Daphnia* exposed to hypoxia

PART II: Materials and Methods

1. *Daphnia magna* clones

Housing and Feeding of the Daphnia magna clones - In this master thesis, two *Daphnia magna* lab clones were used, bred for many generations in the IRF Life Sciences @ KULAK, Kortrijk, Belgium: KNO 15.04 (origin: Knokke, Belgium) and F clone (origin: Scotland). The F clone is a standard lab clone (obtained from the Barrata lab in Barcelona). The *Daphnia* KNO 15.04 is a clone, isolated near Knokke, Belgium and described to be a *Microcystis* resistant clone (Macke *et al.*, in revision). All clones were kept in 2L glass jars, filled with 'Aachener Daphnien medium' (ADaM) (concentration and composition according to Klüttgen, 1994). This medium was developed to obtain optimal conditions in the lab to house and breed *Daphnia*, resembling natural fresh water conditions. The ADaM stock (70 L) was aerated constantly, making it ready to use.

The medium in the 2L jars was partially refreshed every two weeks. Hereby, half of the original medium was maintained and 1L of fresh medium was added to ensure that not all of the bacteria that live in symbiosis with the *Daphnia* are washed away. The jars were kept in a constant environment with a 16h light / 8h dark cycle and a temperature of 20°C. The *Daphnia* were fed with $240 \cdot 10^6$ cells of *Chlorella vulgaris* (stored at -20°C) per 2L jar every two days. On a regular basis, pond water (3%) from a nearby pond in Kortrijk, Belgium (50°48'30"N 3°17'38"E) containing essential bacteria, that serve as food but also live in symbiosis with the *Daphnia* (Callens *et al.*, 2016), was added to boost the cultures.

Breeding of Daphnia magna - Three iso-clonal lines were set-up from each clone to reduce inter-individual variation in the reaction to the treatment to a minimal level. To set up these lines, 15 adult *Daphnia magna* were put in a 2L jar, leading to three jars per clone. The daphnids were raised for two generations. From the last generation, juveniles were isolated from the second brood to be used in the exposure experiments. The second brood is used as experience learned that the first brood shows fewer individuals and less offspring compared with the second brood. The newborn juveniles were always kept with the mother for at least one additional day before exposure. These *Daphnia magna* juveniles showed a higher survival rate compared to juveniles that were taken out immediately.

2. Effect of hypoxia and *Microcystis aeruginosa* on the expression of *HIF α* and EMT marker genes in *Daphnia magna*: experimental set-up

2.1. Hypoxia experiment

From each iso-clonal line, the second brood of the second generation since transfer of the *Daphnia magna* stock cultures (described in 1.) was taken. For each treatment different time points samples were selected (see further). Three 80 mL glass jars were filled with 30 mL of ADaM and three *Daphnia magna* juveniles (\pm 3 days old) per iso-clonal line were put into each jar, giving a total of nine juveniles for each line at each time point. For each time point, a hypoxia and control treatment was set up. In the control treatment, *Daphnia* were exposed to a normal atmospheric oxygen saturation level (9 mg/L). In the hypoxia treatment, the saturation level of 0,85 mg/L atmospheric oxygen was obtained in the Biospherix 'C-chamber sub chamber' (Figure 13) with ProOx 110 O₂ controller. The chamber was filled with N₂ gas under pressure, pushing the oxygen out of the chamber through specialized valves. This resulted in an oxygen saturation in the ADaM of 1,7 mg/L after 24h measured with the WTW Oxi 340i Dissolved Oxygen Meter. In aquatic systems, hypoxia is present in the water when an oxygen saturation level is reached lower than 2,8 mg/L (Diaz & Rosenberg, 1995). The 80mL jars were randomly put on two plates into the chamber (Figure 13). To exclude the possible effect of being placed on the top plate, the two plates were switched every time the *Daphnia* were fed. Light (16h light / 8h dark) and temperature (20°C) parameters remained stable throughout the experiment. The *Daphnia* were fed every two days with $3,6 \cdot 10^6$ cells *Chlorella vulgaris* resembling 18,36 μ g of carbon.



Figure 13: The Biospherix 'C-chamber sub chamber'. This chamber was used to create a hypoxic environment (1,7 mg/L oxygen saturation level) in the ADaM.

2.1.1. Short-term hypoxia exposure (STH) effects on *HIF α* level

For the short-term hypoxia exposure (STH), two clones were used: the F and KNO 15.04 clone. At each time point (0, 1/2, 1, 4, 7 (days)), whole *Daphnia* were sampled to investigate the effect of hypoxia on the expression level of *HIF α* via qPCR. In total, 243 *Daphnia* per

clone were used (3 iso-clonal lines x ((9 individuals x 4 STH time points) + (9 individuals x 4 control time points) + (9 individuals for time point 0))).

2.1.2. Long-term hypoxia exposure (LTH) effects on *HIF α* and EMT marker genes expression level

In the long-term exposure, only the F clone was used. Three hypoxia exposures were performed to investigate the long-term effect of hypoxia on the expression level of the EMT marker genes *ECAD*, *NCAD*, *SNAI1* and *TWIST* through follow-up of their respective mRNA level. At each time point (0, 1, 2, 7, 14, 21 days) in the first long-term hypoxia exposure experiment (1st LTH), whole *Daphnia* were sampled. In the second and third long-term hypoxia exposure experiment (2nd LTH & 3rd LTH), four whole *Daphnia* and five *Daphnia* guts were sampled per line per time point (0, 7, 14, 21, 28 days) (see 3). In the 1st LTH, a total of 297 *Daphnia magna* were used (3 iso-clonal lines x ((9 individuals x 5 STH time points) + (9 individuals x 5 control time points) + (9 individuals for time point 0))). In both the 2nd LTH and the 3rd LTH, 243 *Daphnia* were used (see 2.1.1.).

2.2. Short-term *Microcystis aeruginosa* exposure (STM) effects on *HIF α* and EMT marker genes expression level

Daphnia from the F clone were divided and subjected to two different conditions: *Microcystis aeruginosa* diet and a control *Chlorella* diet. As in 2.1., nine *Daphnia* were divided per three into 80 mL glass jars filled with 30 mL ADaM for each iso-clonal line for each time point. The *M. aeruginosa* treatment consisted of feeding the animals with 9,18 μ g carbon *M. aeruginosa* and 9,18 μ g carbon *C. vulgaris* (see 2.1.). At each time point (0, 1, 4, 7, 11, 14 days) in both the first short-term *Microcystis* exposure (1st STM) as the second short-term *M. aeruginosa* exposure (2nd STM), four whole *Daphnia* and five *Daphnia* guts were sampled (see 3.). In both experiments, a total of 297 *Daphnia* were used (3 iso-clonal lines x ((9 individuals x 5 STH time points) + (9 individuals x 5 control time points) + (9 individuals for time point 0))).

3. *Daphnia magna* sampling

Whole Daphnia magna - At each time point, *Daphnia* individuals (Figure 14(A)) were isolated and put into an Eppendorf per 4-5 as the homogenization column (4.1.) can only tolerate maximal six *Daphnia*. The *Daphnia* were washed twice with Milli-Q® water (Millipore) and subsequently submerged into 200 μ L of RNA $later$ (Qiagen). RNA $later$ protected the RNA inside the *Daphnia* until RNA extraction was performed. For the STH exposure, no RNA $later$ was used. Here the whole *Daphnia* were submerged in 200 μ L E.Z.N.A. ® RNA Lock Stabilizer Reagent (Omega Bio-tek). The *Daphnia* were stored at -20°C.

Daphnia magna gut - The *Daphnia* gut is the organ of interest where EMT might occur, given that the gut is the first line of exposure to the oxygen depleted medium and *Microcystis* sp. treatment. Therefore, to erase other tissue interference, the gut was dissected. In the 2nd LTH and 3rd LTH exposure and the 1st STM and 2nd STM exposure, five *Daphnia* for each time point were taken and dissected alive (Figure 14(B)). The guts of the three lines for each time point and each treatment were pooled (15 guts). They were submerged into 200 μ L of RNA*later*. Dissection was performed with two inox dissection needles, a stereoscope (Olympus® SZX10) and an additional external light source (Euromex Fiber Optic Light Source EK-1). The guts were stored at -20°C.

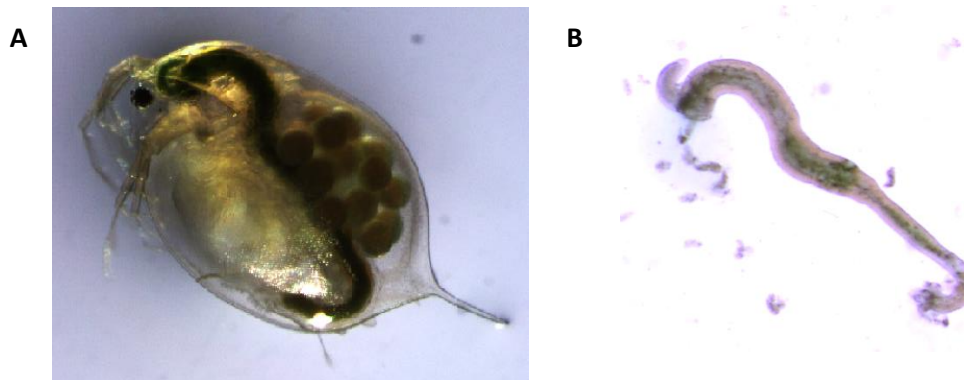


Figure 14: *Daphnia magna* samples. (A) Picture of a whole female *Daphnia magna* (Emile Clappaert). **(B)** Intact *Daphnia magna* gut, containing ceca, midgut and hindgut. The esophagus was not retrieved during dissection (Emile Clappaert).

4. Total RNA extraction and single strand cDNA synthesis

4.1. Total RNA extraction

Prior to total RNA extraction, the cells of the *Daphnia* were crushed and the content homogenized using the QIAshredder™ kit (Qiagen). From this homogenized solution, RNA was extracted using the RNeasy™ Mini Kit (Qiagen). After DNase treatment with Amplification Grade DNase I (Sigma-Aldrich ®), RNA was precipitated and used for cDNA synthesis. All steps were performed at room temperature (RT) unless mentioned otherwise.

Lysis and homogenization - In the first step, the whole *Daphnia* or *Daphnia* guts were washed twice with Milli-Q® water. Then the organisms or guts were crushed with a sterile pestle and 600 μ L of RLT lysis mixture was added. To obtain this RLT lysis mixture, 10 μ L of β -mercapto-ethanol (Sigma-Aldrich ®) was added per 1 mL of RLT lysis buffer from the RNeasy Mini Kit. The lysate was then thoroughly mixed for 1 min, subsequently transferred to a QIAshredder Spin Column and centrifuged for 2 min at 13300 rpm (MicroCL 21R,

Thermo Fisher Scientific). Next, the column was discarded and 600 μL of ethanol (70%) was added to the flow-through to activate the RNeasy™ Mini Spin Column membrane.

RNA extraction - First, the lysate was transferred to an RNeasy™ Mini Spin Column and centrifuged at 10000 rpm for 15 s. The flow-through was discarded. Secondly, 700 μL of RW1 washing buffer from the kit was added to the column and centrifuged at 10000 rpm for 15 s. The flow-through was discarded. Thirdly, 500 μL of RPE washing buffer from the kit was added to the column. The column was inverted few times prior to centrifugation for 15 s at 10000 rpm. The flow-through was discarded. The former step was repeated and centrifuged for 2 min at 10000 rpm. Fourthly, the column was placed in a new tube and centrifuged for 1 min at 13300 rpm to remove all RPE. Subsequently, the column was air-dried for 5 min. Finally, 50 μL of RNase free water from the kit was added to the column, placed into a new Eppendorf. After an incubation of 5 min, the column was centrifuged for 1 min at 10000 rpm and the final step was repeated with the flow-through (incubation 1 min). The flow-through containing the RNA was kept on ice (+4°C) until DNA degradation.

DNA degradation - First, 6,25 μL of Reaction Buffer and 6,25 μL of Amplification Grade DNase I was added to the RNA extract. This mixture was then incubated during 15 min. After addition of stop solution (6,25 μL) the samples were heated for 10 min at 70°C, which denatured the DNase and the mRNA, making it easier to use during reverse transcription. The RNA was kept on ice (+4°C) prior to precipitation.

RNA precipitation - To perform an ammonium acetate - ethanol precipitation, 35 μL of $\text{NH}_4\text{Acetate}$ (5M) and 175 μL of ice-cold ethanol (100%) was added to 70 μL of the RNA solution from the previous step. The different iso-clonal lines of the *Daphnia* sampled as a whole, were pooled prior to this step. The mixture was put in the freezer (-20°C) overnight and then centrifuged for 15 min at 13000 rpm at 4°C. Subsequently the supernatant was removed, the pellet washed in 70 μL of ice-cold ethanol (70%) and centrifuged for 5 min at 13000 rpm at 4°C. The supernatant was removed and the pellet air-dried for 30-60 min. Finally, the pellet was dissolved in 10 μL of RNase free water from the kit and kept on ice (+4°C) until concentration determination.

RNA concentration determination - The concentration of RNA was determined using the Qubit™ 2.0 Fluorometer (Thermo Fisher Scientific) and the Qubit RNA HS kit (Thermo Fisher Scientific). A working buffer was prepared, containing 200 μL of RNA HS Assay buffer and 1 μL of RNA HS Assay reagent per sample/standard. For the Qubit RNA standards I and II, 10 μL of standard was added to 190 μL of working buffer in a Qubit test tube. To measure the samples, 1 μL was added to 199 μL of working buffer. Test tubes were gently mixed for 2 s and incubated for 2 min. Subsequently, the standards were read in the Qubit™ 2.0 Fluorometer and the RNA concentration of the samples determined.

4.2. Single strand cDNA synthesis

Reverse transcription was performed using the Transcriptor First Strand cDNA Synthesis Kit (Roche Life Science). To 1 µg of RNA, 2 µL of Random Hexamer Primers (600 µM) was added. Sterile water was added to a volume of 13 µL. After an incubation of 10 min at 65°C, the cDNA synthesis Master Mix was added. This Master Mix comprised 1X Reaction buffer, RNase inhibitor (20 U), 1 mM dNTP mix and Reverse Transcriptase (10 U). Table Addendum B1(A) shows the followed PCR program in the Peltier Thermal Cycler PTC-200 (MJ Research®). Subsequently, the cDNA concentration was determined with the Qubit™ 2.0 Fluorometer (Thermo Fisher Scientific) as in 4.1.5., using the Qubit ssDNA kit (Thermo Fisher Scientific). The cDNA was stored at -20°C.

5. qPCR

5.1. qPCR primer optimization

Primers for the *Daphnia* genes of interest (*HIFα*, *ECAD*, *NCAD*, *SNAI1* and *TWIST*) and the reference gene ribosomal protein L32 (*RPL32*) were developed by dr. E. Beert and delivered by Thermo Fisher Scientific (Table 1). To optimize the use of the primers for *ECAD*, *NCAD*, *SNAI1* and *TWIST* for qPCR, several PCRs with different annealing temperatures (54°C, 56°C, 58°C, 60°C, 62°C) were run.

Polymerase chain reaction - The optimization PCRs were performed with material from two testing conditions (Normoxia and Hypoxia) of previous hypoxia exposures done by dr. E. Beert. Also a negative control (water) was included. The PCR was performed following the Platinum *Taq*®-protocol from Thermo Fisher Scientific. Platinum *Taq* DNA polymerase (5U), dNTP mix (10 mM), 10X PCR buffer and MgCl₂ (50 mM) were supplied by Thermo Fisher Scientific. For each gene a Master Mix was produced comprising 1X PCR buffer, 0,2 mM dNTP mix, 1,5 mM MgCl₂, 0,2 µM Reverse primer, 0,2 µM Forward primer, 20ng cDNA, 1 U *Taq* DNA polymerase and sterile water till 15 µL. The PCR program is given in Table Addendum B1 (B).

Gel electrophoresis - A 2% agarose gel was prepared (1g UltraPure™ Agarose (Thermo Fisher Scientific), 1X Tris-borate-ethylene-diamine-tetra-acetic acid (EDTA) buffer and 0.75X GelRed™ (Biotium)). A 6X loading dye was added to the PCR product. The mixture was then loaded (10 µL) into the gel slots. Finally, 2 µL of Small Fragments Smartladder (Eurogentec) was added to the last slot. The gel ran at 135V for 20 min in the Mupid®-One (Eurogentec) filled with 1X Tris-borate-EDTA buffer. With the BioDoc-It™ Imaging System UVP, UV images were made of the gel. The lengths of the cDNA fragments of the EMT genes are given in Table 2.

Table 1: Primer sequences for PCR and qPCR.

Gene	Forward/Reverse	Sequence (5'-3')
EMT marker genes		
<i>ECAD</i>	Forward	ggtgcgagtcagaacgaag
	Reverse	gctaccgaattctccaggac
<i>NCAD</i>	Forward	aaagttgaggatgcaaccgc
	Reverse	atacctggatgtcagctcgc
<i>TWIST</i>	Forward	catgcaacacgagaacagcc
	Reverse	caacgaattctccgatcgcc
<i>SNAI1</i>	Forward	cgcacagcatcaccaatacg
	Reverse	tggaagcggccgaataacaac
Hypoxia-related gene		
<i>HIF1A</i>	Forward	gcgcaaggagaaatcccgtg
	Reverse	ttgccaaggagagactgtgc
Reference gene		
<i>RPL32</i>	Forward	ccaactttggcataaggactg
	Reverse	gaccaaagggtattgacaacaga

Table 2: The length of the cDNA fragments of the EMT marker genes

DNA-fragment	Length
<i>ECAD</i>	129 bp
<i>NCAD</i>	124 bp
<i>RPL32</i>	67 bp
<i>SNAI1</i>	97 bp
<i>TWIST</i>	100 bp
<i>HIFα</i>	170 bp

5.2. Standards

For Advanced Analysis during a qPCR, a standard curve was necessary from samples of which the concentration of cDNA is known. Following dilution series are made: (i) 1/10 for *HIF α* , *RPL32*, and *SNAI1*, (ii) 1/5 for *ECAD* and *TWIST* and (iii) 1/2 for *NCAD*. Standards of *HIF α* , *RPL32*, *ECAD*, *NCAD* and *TWIST* were made by dr. E. Beert. Standards of *SNAI1* were produced through the cloning of a cDNA fragment of the EMT marker gene (Table 3) into a pJET1.2/Blunt vector containing an ampicillin resistance gene and the lethal gene *eco47IR* for positive selection (Thermo Fisher Scientific). All steps were performed at RT unless mentioned otherwise.

Purification of the SNAI1 PCR fragment - After a PCR (annealing temperature 58°C) and gel electrophoresis as described in 5.1., the PCR fragment was purified using the QIAquick gel extraction kit (Qiagen). A piece of agarose containing the PCR band (< 400 mg) was excised out of the gel, put into an Eppendorf tube and for each 100 mg of gel, 300 µL of QG buffer from the kit was added. During an incubation of 10 min at 50°C, the tube was vortexed every 2 or 3 min. One volume of isopropanol was added to the sample (One volume = weight of original PCR fragment, 100 mg~100µL), mixed and applied to the QIAquick column. After centrifugation (1 min at 13300 rpm) the flow-through was discarded and 750 µL of PE buffer from the kit was added. Subsequently, after 5 min of incubation, centrifugation (1 min at 13300 rpm), and discarding of the flow-through, the column was placed into a new tube. To the column, 30 µL of EB buffer from the kit was added and the sample incubated for 5 min. After centrifugation (1 min at 13300 rpm), the DNA was stored at -20°C.

Cloning of the SNAI1 PCR fragment into a pJET1.2/Blunt vector - First, the blunting reaction (Thermo Fisher Scientific) was performed on ice (+4°C). To 0,15 pmol PCR fragment, 10 µL of 2X reaction buffer and 1 µL of DNA blunting enzyme was added. Sterile water was added till 17 µL. The mixture was briefly mixed for 3-5 s and incubated for 5 min at 70°C. After cooling on ice, the ligation reaction was set up, adding 1 µL pJET1.2/blunt cloning vector (50 ng/µL) and 1 U of T4 DNA ligase. Again, this was briefly mixed and incubated for 5 min.

Transformation of competent E. coli cells - To 50 µL of competent cells, 2 µL of plasmid was added, followed by gently mixing. The cells were then incubated for 30 min on ice prior to the heat-shock for 30 s at 42°C. The cells were put on ice for 2 min, followed by the addition of 250 µL of Super Optimal broth with Catabolite repression medium. The vial was sealed with parafilm and shaken horizontally for 1 hour at 37°C. Subsequently, all of the transformed cells were spread on a Luria-Bertani Broth agar-amp (100 µg/mL) (Sigma-Aldrich®) plate, prepared by dr. E. Beert. After overnight incubation at 37°C, a colony was picked from the plate and transferred into 5 mL of liquid Luria-Bertani Broth (+ amp (100 µg/mL)) medium, prepared by dr. E. Beert. After another 16 hours at 37°C, the bacteria were transferred to a 15 mL falcon and pelleted at 5400 g for 10 min at 4°C.

Plasmid purification - Plasmid purification was performed using the NucleoSpin® Plasmid EasyPure kit (Marchery-Nagel). After removing the supernatant, the pellet was resuspended in 150 µL of A1 buffer from the kit. Next, 250 µL of buffer A2 from the kit was added, followed by inverting the tube and 2 min incubation. Subsequently, 350 µL of buffer A3 from the kit was added, followed by inverting the tube and centrifugation at 13300 rpm for 3 min. The supernatant was transferred to a NucleoSpin® column and centrifuged for 30 s at 2000 g. Flow-through was discarded and 450 µL of buffer AQ from the kit was added to the column. After centrifugation for 1 min at 13300 rpm the column was placed into a new Eppendorf tube

and 50 μL of AE buffer was added, followed by 1 min of incubation. Finally, after centrifugation of 1 min at 13300 rpm, the plasmid solution was stored at -20°C .

Subsequently, the concentration of DNA was determined with the Thermo Fisher Scientific Qubit™ dsDNA BR Assay Kit (see 4.1.). Through the knowledge of the exact amount of basepairs of the vector (2974 bp) and the insert (Table 3), the amount of copies was determined. Through a serial dilution the different standards of 10^6 copies/ μL , 10^5 copies/ μL , 10^4 copies/ μL , 10^3 copies/ μL and 10^2 copies/ μL were prepared.

5.3. Relative qPCR

QPCR was used to investigate the changes in expression during the different exposures (hypoxia or *M. aeruginosa* diet) of the hypoxia marker gene *HIF α* and EMT marker genes *ECAD*, *NCAD*, *SNAI1* and *TWIST*. As a reference gene, the housekeeping gene *RPL32* was used (Yang *et al.*, 2014). The qPCR reaction was performed in the Lightcycler® 480 Multiwell Plate 96 (Roche Life Science). The qPCR reaction comprised 5 μL of cDNA (20 ng) and 15 μL of mastermix. First the mastermix was made for each gene and comprised 1X Lightcycler® 480 SYBR Green I Master (Roche Life Science), forward primer (0.5 μM), reverse primer (0.5 μM) and water (Lightcycler® 480 SYBR Green I Master kit (Roche)) to a volume of 15 μL .

The cDNA of each used time point was diluted with sterile water until a concentration of 20 ng cDNA per 5 μL was obtained. Each time point was added in triplicate for each gene on the multiwell plate. Of each gene three no template controls (NTCs) were added, serving as a negative control, containing 5 μL of sterile water instead of cDNA. For each exposure, time point 0 was the positive calibrator. On the multiwell Plate, for each gene one Standard (see 5.2.) was included. This Standard will be placed onto the Standard curve, saved earlier in the LightCycler® 480 software, by Dr. E. Beert. Of the respective Standard 1 μL of cDNA was added together with 10 ng of salmon sperm DNA (Thermo Fisher Scientific).

Finally, the wells were covered with a Lightcycler® 480 Sealing Foil (Roche Life Science). The plate was shortly centrifuged prior to placement into the Lightcycler® 480 Instrument (Roche Life Science). The qPCR program can be found in Addendum B1 (C). The multiwell plate was subsequently discarded.

5.4. Analysis of qPCR data

The obtained data were analyzed with the LightCycler® 480 software (Roche Life Science). For each qPCR, an Absolute Quantification Analysis was performed to investigate if the curves showed a normal course and if the NTCs showed no signal, using an external standard if possible. If not the indicated qPCR efficiency was used. If one of the three replicates showed a striking deviant course as compared to the other curves, this curve was

excluded from further analyses. Subsequently, for each qPCR a Melt Curve Genotyping analysis was done for all genes to validate if primer dimers, contamination or non-specific fragments were present, visualized by abnormal melting peaks and to validate if the fragment length was accurate. Finally, High Specificity Advanced Relative Quantification Analysis for the target genes compared to the reference gene was run. Here, the ratio of the mean Cp of each time point of each target gene over the mean Cp of each respective time point of the reference gene was normalized, with the positive calibrator Cp ratio set as 1. The normalized ratios were visualized via bar plots in MS Excel®. Due to the absence of replicate exposure treatments, as these were pooled during RNA precipitation for whole *Daphnia* and during sampling for the *Daphnia* guts, no statistical analysis was possible.

6. Gut microbiome composition

Experimental set-up and analysis were performed by Emile Clappaert, egg surface sterilization, DNA isolation and library preparation by dr. Emilie Macke and Isabel Vanoverberghe.

6.1. Experimental set-up

In order to investigate the changes in gut microbial community, living in symbiosis with *Daphnia magna* after exposure to hypoxic conditions, the KNO 15.04 clone was used. The eggs of adult *Daphnia magna* were dissected using the same equipment as in 3. The eggs were placed in a petridish with 8 mL of 0.01% peracetic acid (PAA, Sigma-Aldrich ®) for 10 min to make them axenic. After a short wash step in a petridish with sterile ADaM, 25-30 eggs were placed in a 6 well plate filled with sterile ADaM. These plates were placed in a 20°C incubator until hatching. PAA sterilizes the shell of the egg and as there are no bacteria present inside the egg, the juveniles were germ-free (protocol as in Callens *et al.*, 2016).

Fifteen five days old axenic *Daphnia* were distributed over six 80 mL jars filled with 30 mL of sterile ADaM for each condition, i.e. normoxia or hypoxia. This equals a total of 30 *Daphnia magna*, 15 individuals per treatment. The six jars were separated into three groups with each five *Daphnia*. To each jar, 100 µL of in water homogenized *Daphnia* was added in order to supply a standard microbiome to the axenic juveniles.

The jars of the hypoxic treatment were exposed to 0,85 mg/L of atmospheric oxygen saturation in the Biospherix 'C-chamber sub chamber' (Figure 13) with ProOx 110 O₂ controller to obtain a 1,7 mg/L oxygen saturation in the ADaM. The control treatment was placed under normal oxygen conditions (9 mg/L O₂). After 14 days, the guts of *Daphnia* were dissected following instructions in 3., with the guts deposited per five for each group in 200 µL of Milli-Q® in an Eppendorf and stored at -80°C until DNA isolation.

6.2. DNA isolation

Cell lysis and protein removal - The *Daphnia magna* guts were thawed and Milli-Q® water was added until a volume of 500 µL was reached. Sterilized glass beads were added (30 µL) and the Eppendorf tubes were placed in a bead-beater (TissueLyser, Qiagen) for 3 x 30 s at 30 beats/s. Subsequently, 30 µL of lysozyme (50 mg/mL, Sigma-Aldrich ®) was added and the samples were incubated for 1 h at 37°C. After incubation, 25 µL of 10% sodium dodecyl sulfate solution and 20 µL of 0.5 M EDTA were added to the mixture and followed by another 3 x 30 s at 30 beats/s in the bead-beater. Before incubation at 55°C for 1 h, 25 µL of proteinase K (1 mg/mL, Sigma-Aldrich ®) was added.

To the tubes, 500 µL of phenol-chloroform-isoamylalcohol (25-24-1, Carl Roth GmbH + Co.) was added and inverted by hand. After this, the tubes were centrifuged for 10 min at 4°C (13300 rpm). Subsequently, the upper aqueous phase was placed in a new tube and another 500 µL of phenol-chloroform-isoamylalcohol (25-24-1) was added. This was followed by another centrifugation for 10 min at 4°C (13300 rpm) and transfer of the upper aqueous phase to a new tube.

DNA precipitation - To the tubes, 20 µL of NaCl solution (5M) and 500 µL of isopropanol was administered, mixed and centrifuged for 25 min at 4°C (13300 rpm). Subsequently, the supernatant was removed and the pellet washed with 200 µL of 75% ice-cold ethanol. After another centrifugation step for 10 min at 4°C (13300 rpm), all ethanol was removed from the tube and the tube was left open 10 min to air-dry. The pellet was dissolved in 30 µL of Milli-Q® water and the DNA concentration measured with the Qubit™ 2.0 Fluorometer (Thermo Fisher Scientific) as in 4.1., using the Qubit dsDNA BR kit. Finally, DNA was stored at -20°C.

6.3. Library preparation and Illumina Sequencing

In this sequencing process, the full length 16S rRNA gene was analyzed. All steps were performed at RT unless mentioned otherwise. This 16S rRNA is typically for prokaryotes and gives an overview of the bacterial species present in the gut of *Daphnia magna*. The 16S rRNA gene was amplified with a standard PCR, using 16S rRNA specific primers 27F (0,3 µM) and 1492R (0,3 µM) (Table 3) and the Platinum Pfx® protocol (Thermo Fisher Scientific) (1X Reaction buffer, dNTP mix (0,3 mM), MgSO₄ (1 mM), Pfx DNA polymerase (1 U), DNA template (0,4272ng/µL) and water till 25µL). The program can be found in Table Addendum B1 (D). The PCR product was purified with the QIAquick PCR purification kit (Qiagen). To the PCR product 100 µL of PB buffer from the kit and 10 µL of sodium acetate (3 M, pH 5,0) was added. Then, the mixture was loaded onto a QIAquick column and centrifuged for 1 min at 13000 rpm. After discarding the flow-through, 0,75 mL of PE buffer from the kit was administered to the QIAquick column and again centrifuged for 1 min at 13000 rpm. Subsequently, the flow-through was discarded, centrifuged for 1 min at 13000 rpm and the

column placed in a new Eppendorf. Finally, 30 μ L of EB from the kit was added to the column and incubated 1 - 5 min before centrifugation (1 min at 13000 rpm) and storage at -20°C .

(i) Dual-index amplicons of the fourth variable region of the 16S rRNA gene (V4), (ii) Illumina adapters and (iii) an 8nt-barcode at the 5'-end were obtained through a second amplification round. Analogous to Kozich *et al.* (2013), to 5 μ L of the PCR product primer 515F (0,15 μ M) and a modified version of 806R (0,15 μ M) (Aprill *et al.*, 2015) was added (Table 3). The PCR program can be found in Table Addendum B1 (E) and again the Platinum *Pfx*[®] protocol was used. For each sample, the PCRs were performed in triplicate and pooled afterwards. The PCR product was run on a 1,5 % agarose gel/0.75X GelRed (135V) and purified with the QIAquick extraction kit (Qiagen) as in 5.2.

Through normalizing the amplicon concentrations with the SequelPrep Normalization Plate (Applied Biosystems), an equimolar library was prepared. The amplicons were sequenced with a v2 PE500 kit with custom primers on the Illumina Miseq platform (KU Leuven Genomics Core), resulting in 2x250-nt paired-end reads.

6.4. Analysis

In order to analyze the data, R 3.4.0 was used (R Core Team, 2017) as performed for microbiome analysis in Callahan *et al.*, 2016. First, the sequences were trimmed (first 10 nucleotides and nucleotides from which the mean quality score dropped below Q25 were removed). Secondly, the sequences were filtered (only maximum two expected errors per read). With the high-resolution DADA2 method, the sequence variants were inferred and chimeras removed. With the RDP training set, taxonomy was assigned to the sequences until class level. Unweighted and weighted UniFrac plots were generated (Lozupone & Knight, 2005), respectively placing the sequences into the phylogenetic tree and investigating the relatedness between the samples. Using a bar plot diagram, the relative abundance of different Operational Taxonomical Units over the different samples was set.

Table 3: Primer sequences of the primers 27F and 1492R used for the amplification of the 16S rRNA gene and the primers 515F and modified 809R used for the preparation of the sequences for the Illumina sequencing containing (i) Dual-index amplicons of the fourth variable region of the 16S rRNA gene (V4), (ii) Illumina adapters and (iii) an 8nt-barcode at the 5'-end.

Primer	Forward/Reverse	Sequence (5'-3')
27F	Forward	agaagtttgatcctggctcag
1492R	Reverse	ggttacctgttacgactt
515F	Forward	gtgccagcmgccgcggta
Modified 809R	Reverse	ggactacnvgggtwtctaata

PART III: Results

1. qPCR primer optimization: *ECAD*, *NCAD*, *SNAI1* and *TWIST*

At first, several PCRs were run with different annealing temperatures (54°C, 56°C, 57°C, 58°C, 60°C, 62°C) to find the optimal annealing temperature for the *ECAD*, *NCAD*, *SNAI1* and *TWIST* primers. The optimal annealing temperature was 58°C (Figure 15) and used during the qPCR. The PCR on *NCAD* and *TWIST* showed minor formation of primer dimers (white squares, Figure 15). In the qPCR, this formation was confirmed, however only occurring at a very low rate (in 5 of 93 reactions) (Addendum 3). The *Small Fragments SmartLadder* showed a deviant running pattern, present in all performed gel electrophoreses. The fragment length of each gene cDNA was correspondent to the actual length (Table 2).

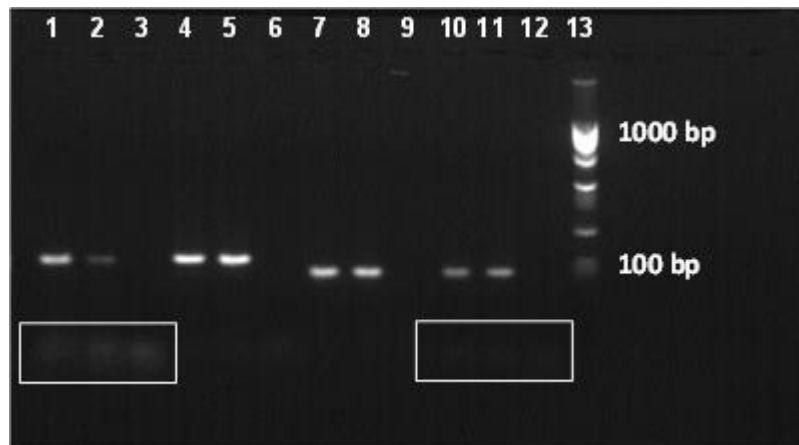


Figure 15: Agarose gel representing the succeeded PCR with annealing temperature at 58°C. Lanes 1 - 3: *NCAD* Normoxia, Hypoxia and Control (water); Lanes 4 – 6: *ECAD* Normoxia, Hypoxia and Control; Lanes 7 - 9: *SNAI1* Normoxia, Hypoxia and Control; Lanes 10 – 12: *TWIST* Normoxia, Hypoxia and Control; Lane 13: *Small Fragments SmartLadder*. White squares represent formation of primer dimers.

2. Real-time expression level of *HIF α* and EMT marker genes *SNAI1*, *TWIST*, *NCAD* and *ECAD* via qPCR

Only the cDNA from selected time points obtained from the 1st, 2nd and 3rd LTH exposure experiment and the 1st and 2nd STM experiment were used for qPCR in this thesis. Levels of cDNA of the STH treatment were too low (<13 ng/ μ L) to perform qPCR. With respect to all qPCR analyses below important to note is that the control treatments were supposed to have a normalized Cp ratio (i.e. the ratio of the mean Cp of the target gene and mean Cp of the reference gene (RPL32)) from around 1 according to the positive calibrator, which was not the case in these qPCR analyses, so validation of the observed trends needs further research.

The effect of hypoxia

The expression of *HIF α* showed initially an increasing trend when the *Daphnia* were exposed to hypoxia (1,7 mg/L oxygen saturation) (Figure 16 (A)&(B)). Thereafter, a decrease in the *HIF α* expression was present in the 1st, but not repeated in the 2nd LTH exposure (Figure 16 (B)&(C)). In the *Daphnia* gut, the expression of *HIF α* increased until day 28 (Figure 16 (C)).

The expression of *SNAI1* showed an increase in the whole *Daphnia* tissue, especially after day 14 (Figure 16 (D)). In the *Daphnia* gut, there was an increase until day 14, which decreased after day 14 (Figure 16 (E)). This was measured in the 2nd and 3rd LTH exposure.

The expression levels of *TWIST* and *NCAD* were only measured in whole *Daphnia* tissue because of the occurrence of deviant melting peaks during the qPCR program (Figure Addendum 3).

The expression of *TWIST* was relatively stable in the whole *Daphnia* (Figure 16 (F)).

NCAD showed a decreasing trend, especially until day 14 in the whole *Daphnia* tissue (Figure 17 (A) and Figure 17 (B)). After that no consistent pattern was present in the different LTH experiments.

In the different LTH experiments, an increasing trend was observed of the *ECAD* expression level, especially at later time points (Figure 17 (C) and Figure 17 (D)). This increasing trend at start (before day 14) was also present in the *Daphnia* gut, but was reversed after day 14 (Figure 17 (E)). The ratio of the mean normalized Cp ratios of *ECAD/NCAD*, combined over all three LTH shows a clear increasing trend (Figure 17 (F)).

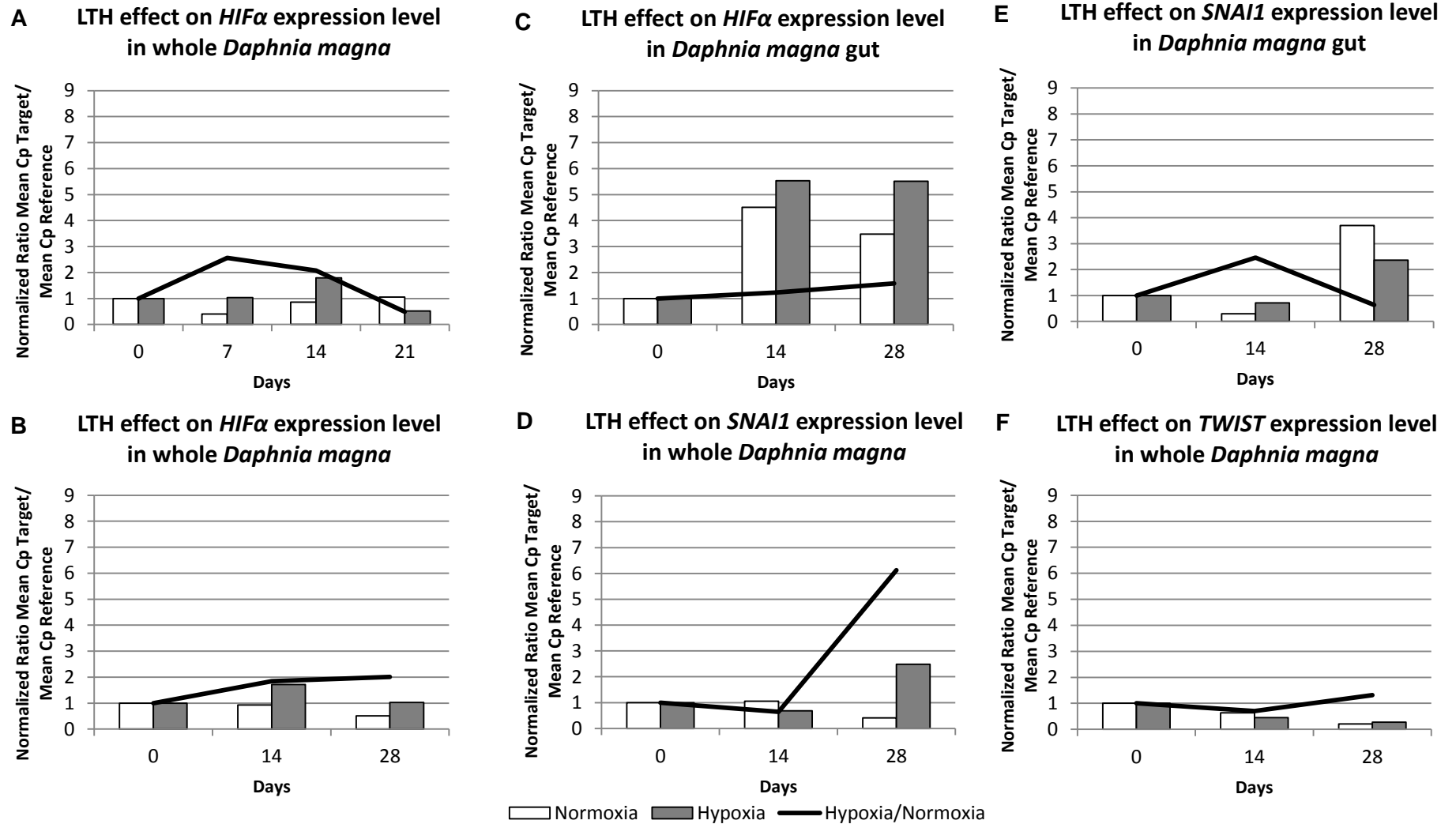


Figure 16: Relative quantification of *HIFα*, *SNAI1* and *TWIST* gene expression level during long term exposure to hypoxia in the F clone. Gene expression of: **(A)** *HIFα* in whole *Daphnia* (1st LTH), **(B)** *HIFα* in whole *Daphnia* (2nd LTH), **(C)** *HIFα* in *Daphnia* gut (2nd LTH), **(D)** *SNAI1* in whole *Daphnia* (2nd LTH), **(E)** *SNAI1* in *Daphnia* gut (3rd LTH) and **(F)** *TWIST* in whole *Daphnia* (3rd LTH). This is depicted by bar plots representing the normalized Cp ratio over time (days). The curve depicts the ratio of the Hypoxia treatment over the Normoxia treatment, giving the net effects on gene expression of the Hypoxia treatment.

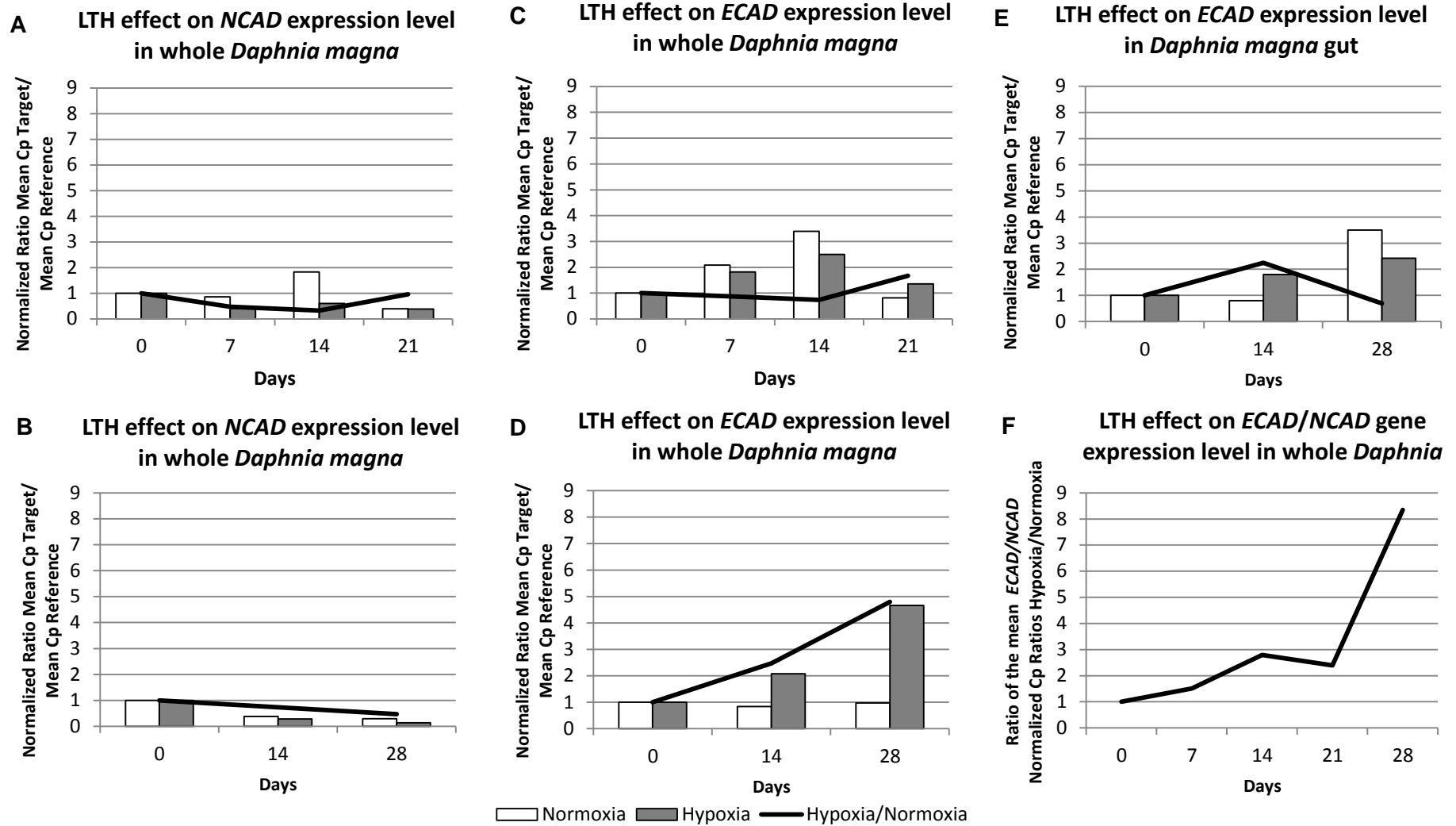


Figure 17: Relative quantification of gene expression level of *ECAD* and *NCAD* during long term exposure to hypoxia in the F clone. Gene expression level of: **(A)** *NCAD* in whole *Daphnia* (1st LTH), **(B)** *NCAD* in whole *Daphnia* (3rd LTH), **(C)** *ECAD* in whole *Daphnia* (1st LTH), **(D)** *ECAD* in whole *Daphnia* (2nd LTH), **(E)** *ECAD* in *Daphnia* gut (3rd LTH). This is depicted by bar plots representing the normalized Cp ratio over time (days). The curve depicts the ratio of the Hypoxia treatment over the Normoxia treatment, giving the net effects on gene expression of the Hypoxia treatment. **(F)** Ratio of *ECAD/NCAD* gene expression level. Mean Cp ratios were taken from 1st, 2nd and 3rd LTH.

The effect of the *Microcystis aeruginosa* diet

Daphnia exposed to *M. aeruginosa* showed an initial increase in the expression level of *HIF α* , in the whole *Daphnia* tissue as well as in the gut during the 1st STM exposure. This increasing trend was reversed at day 4 (Figure 18(A)&(B)). This decreasing trend restored the initial level of expression.

The expression of *SNAI1* showed an initial decrease in the whole (1st STM) and in the gut of the *Daphnia* (2nd STM). This was followed by an increase until initial levels (Figure 18 (C)&(D)). A similar pattern was observed for *TWIST* (Figure 18 (E)) during the 2nd STM.

No statements can be made out of the expression level of *NCAD* in whole *Daphnia* tissue, as the normalized Cp ratio at day 4 was very low (0,0723) (Figure 19 (A)).

The expression of *ECAD* showed a decreasing trend in the whole *Daphnia* tissue (Figure 19 (B)). However, in the gut, this decreasing trend was reversed at day 4, leading to restoration of the initial expression level (Figure 19 (C)). When the ratio of the mean normalized Cp ratio of *ECAD/NCAD* was taken, an initial decrease was followed by an increase until the original *ECAD/NCAD* ratio (Figure 19 (D)).

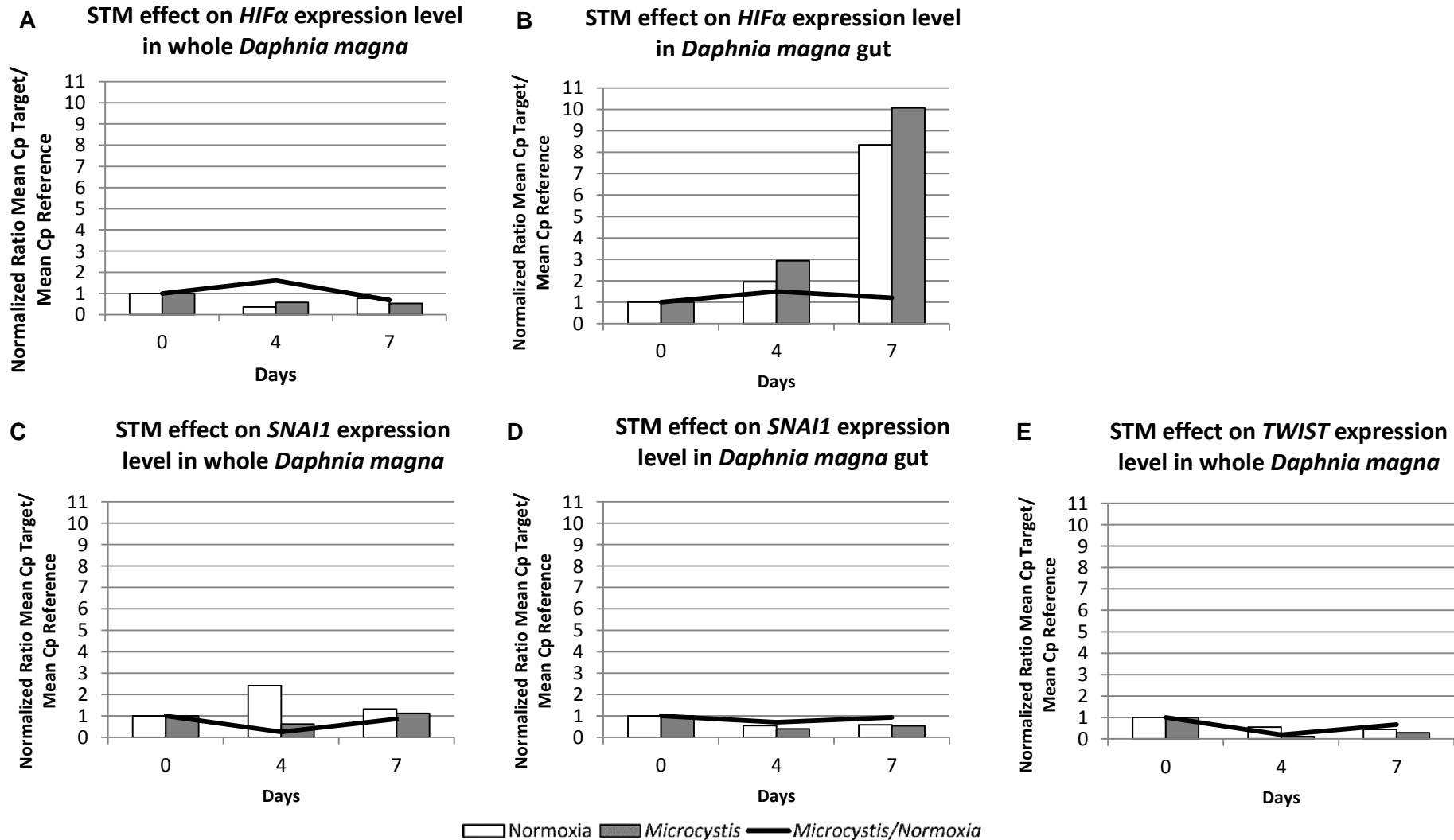


Figure 18: Relative quantification of gene expression level of *HIFα* and EMT marker genes during a short term exposure to *Microcystis aeruginosa* diet in the F clone. Gene expression level of: **(A) *HIFα* in whole *Daphnia* (1st STM), (B) *HIFα* in *Daphnia* gut (1st STM) (C) *SNAI1* in whole *Daphnia* (1st STM), (D) *SNAI1* in *Daphnia* gut (2nd STM) and (E) *TWIST* in whole *Daphnia* (2nd STM).** This is depicted by bar plots representing the normalized Cp ratio over time (days). The curve depicts the ratio of the *M. aeruginosa* treatment over the Normoxia treatment, giving the net effects on gene expression of the *M. aeruginosa* treatment.

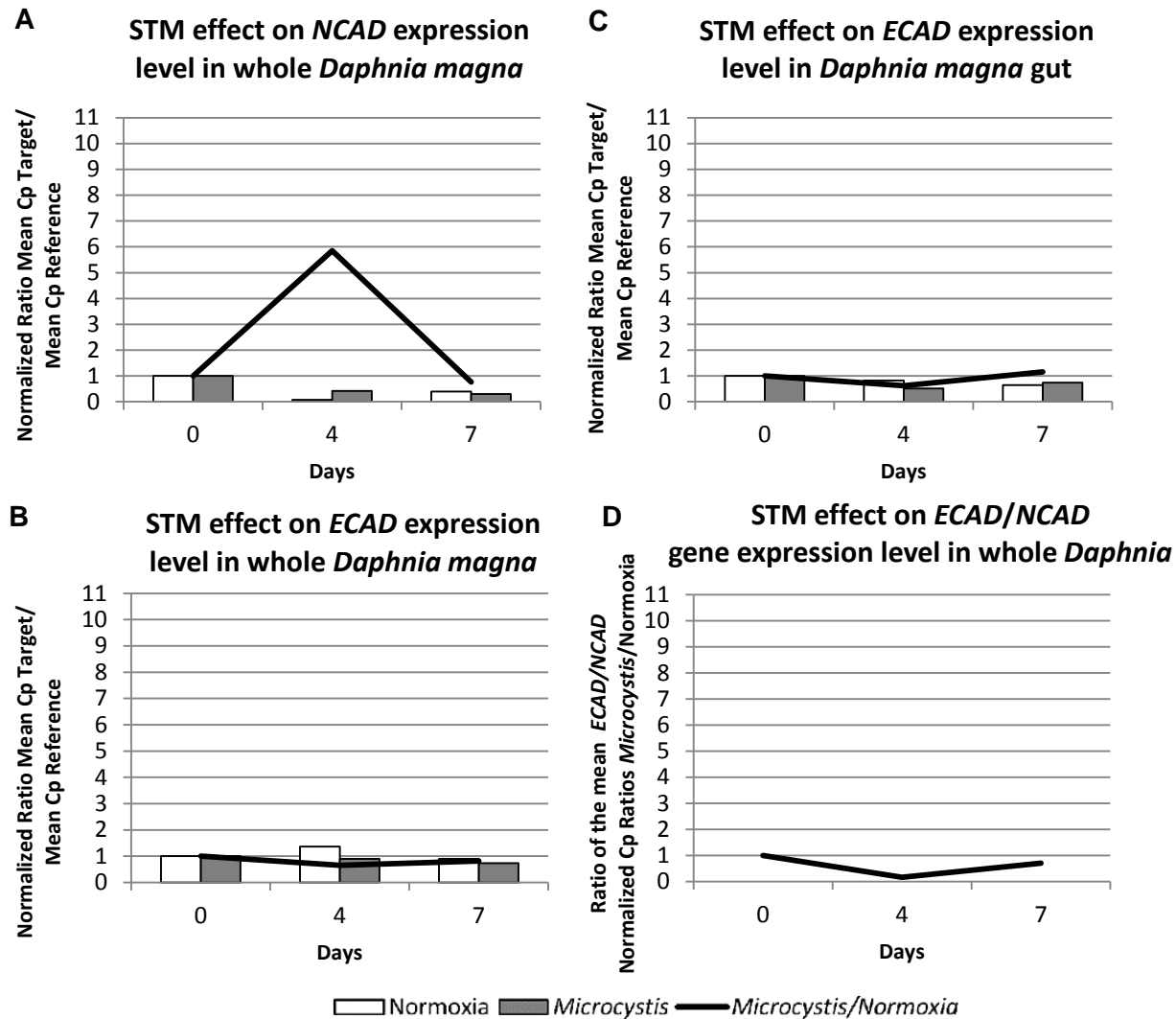


Figure 19: Relative quantification of gene expression level of *HIF α* and EMT marker genes *ECAD* and *NCAD* during a short term exposure to *Microcystis aeruginosa* diet in the F clone. Gene expression level of: (A) *NCAD* in whole *Daphnia* (2nd STM), (B) *ECAD* in whole *Daphnia* (1st STM) and (C) *ECAD* in *Daphnia* gut. This is depicted by bar plots representing the normalized Cp ratio over time (days). The curve depicts the ratio of the Hypoxia treatment over the Normoxia treatment, giving the net effects on gene expression of the Hypoxia treatment. (D) Ratio of *ECAD/NCAD* gene expression level. Mean Cp ratios were taken from 1st STM.

3. Gut microbiota composition in *Daphnia magna* after exposure to hypoxia

The unweighted UniFrac β -diversity measure (Luzopone and Knight, 2005) shows a difference in microbial composition in the gut of *Daphnia magna* between the two treatments, hypoxia and normoxia (Figure 20(A)). However, when the abundance was taken into account in the weighted UniFrac measure (Figure 20(B)), this difference was less clear. The effect of the treatment was not significant (Adonis test, P-value: $p=0,1$). In Figure 21 (A), the effect of the treatment on the relative abundance of the different classes of bacteria present in the gut of *Daphnia magna* is depicted. Here, an effect of the hypoxia on the composition of the bacterial classes can be observed. A clear increase in Sphingobacteria was present, together with a decrease of γ -Proteobacteria in all hypoxia samples and a decrease of β -Proteobacteria in two of the three hypoxia samples. In one of the normoxia samples a decrease is present in the Flavobacteria. When the changes on order level were investigated (Figure 21 (B)), an increase in Sphingobacteriales was observed, according to the increase of the order Sphingobacteria. The order of the Burkholderiales was clearly reduced in two of the three hypoxia samples.

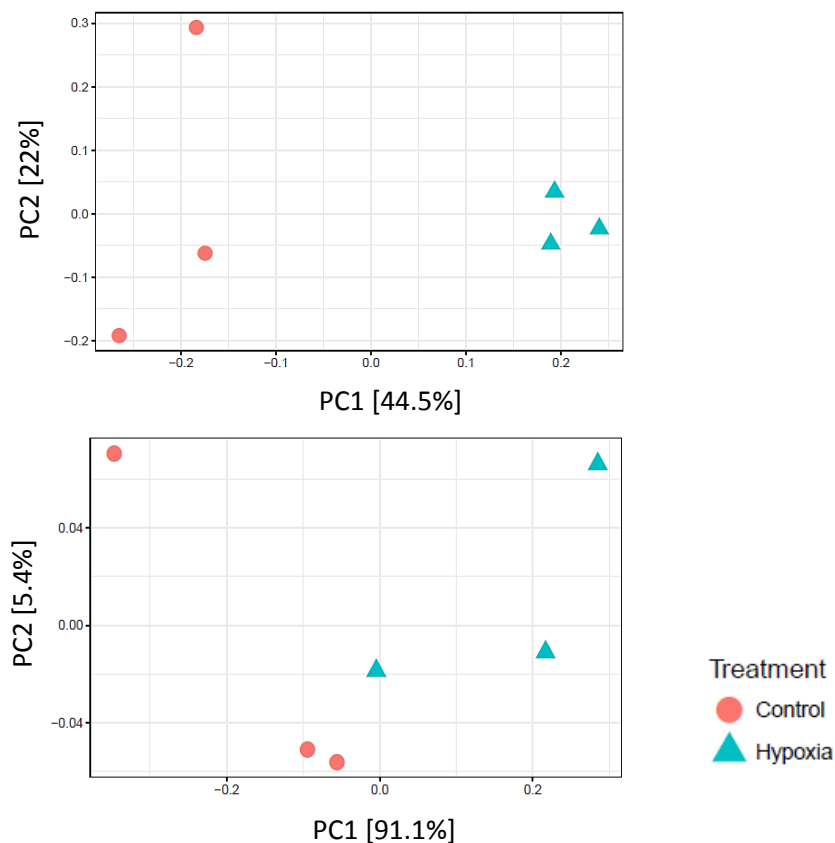


Figure 20: Unweighted and weighted UniFrac analysis of the gut microbiota composition in *Daphnia* (F clone) in normoxia (control) or in hypoxia. The UniFrac β -diversity measure shows a clear difference between gut microbiota composition in the *Daphnia* gut of after exposure to hypoxia. However, this treatment effect on the gut microbiota composition was not present in the weighted UniFrac analysis and not significant (Adonis test, P-value: $p=0,1$).

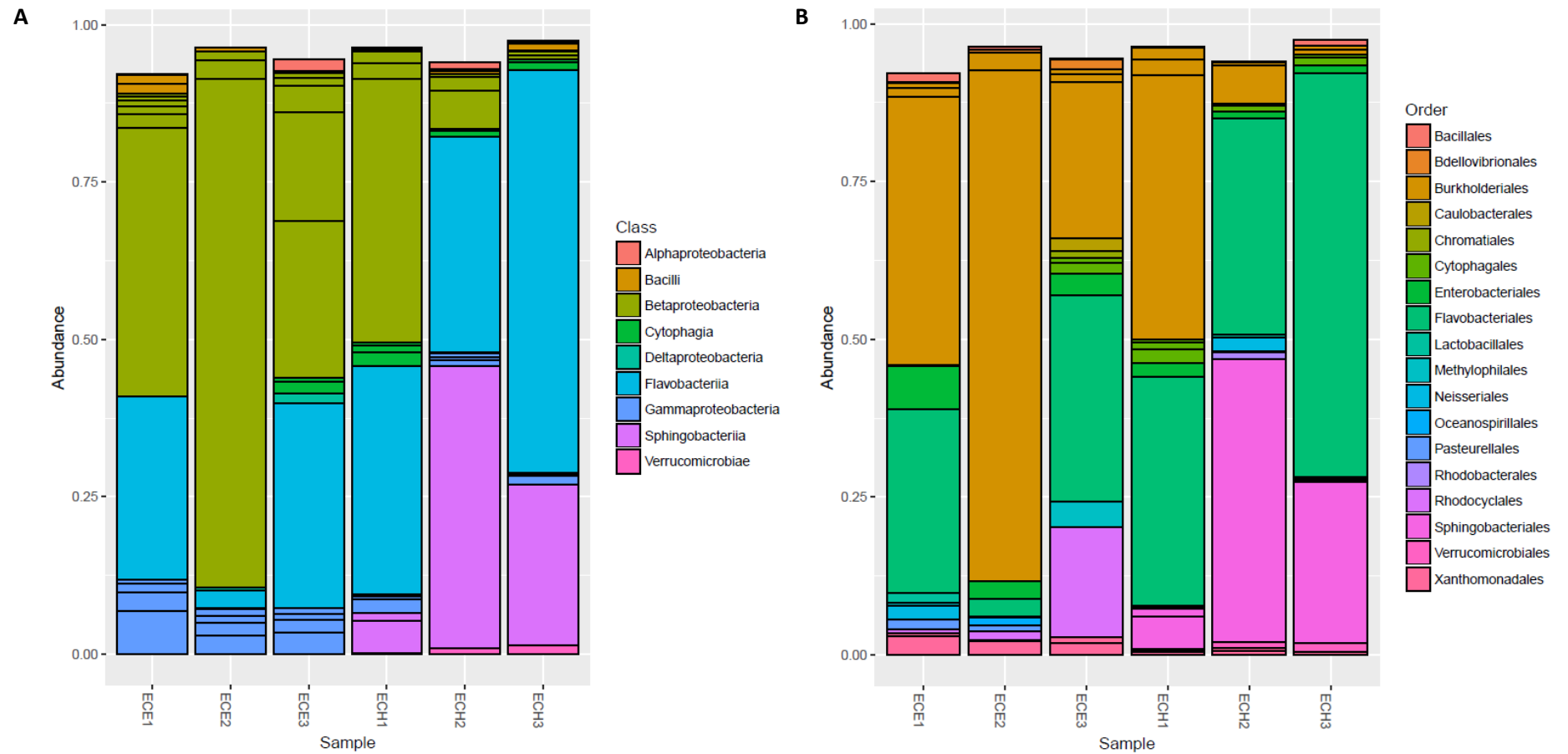


Figure 21: The effect of the treatment (ECE = Normoxia, ECH = Hypoxia) on the relative abundance of the gut microbiota in the gut of *Daphnia magna* (F clone) on class (A) and order level (B).

PART IV: Discussion

1. Effect of hypoxia and *Microcystis aeruginosa* on the expression level of *HIF α* and EMT marker genes in *Daphnia magna*

For both stressors tested, hypoxia and *M. aeruginosa*, *Daphnia* shows strong phenotypic plasticity and adaptation (Smirnov 2017). In addition, both stressors are associated with EMT, Epithelial-to-Mesenchymal Transition, a crucial process in cancer metastasis. Hypoxia is a proven inducer of EMT in cancer cells (Imai *et al.*, 2003). The addition of microcystin produced by *Microcystis sp.* is associated with an increased cell junction loss in mice (Wang *et al.*, 2016) and the promotion of EMT *in vitro* in colorectal cancer cells (Ren *et al.*, 2017). Nevertheless, clear cut evidence and the exact mechanisms at the gene expression level *in vivo* are not unraveled yet and therefore tested in this thesis in the invertebrate *Daphnia*.

Hypoxia exposure

In the whole *Daphnia* tissues of the F clone, the expression of *HIF α* initially increased upon hypoxia. This is described to be associated with an increase in Hb expression, probably as a result of HIF stabilization (Gorr, 2004, Smirnov, 2017). This assumed increase in Hb was confirmed in the phenotypic outcome, given that the *Daphnia* hemolymph turned red. After 14 days, there was a trend to stagnation and even decrease of *HIF α* expression in the whole *Daphnia* tissue. The decreasing trend after a first increase in *HIF α* expression was also observed in a previous experiment of the clone KNO 15.04 to hypoxia done by dr. E. Beert on whole *Daphnia magna* tissue. These results are in agreement with observations that the role of *HIF α* is mainly situated in the acute phase of hypoxia, but diminishes in the chronic hypoxic state when a new homeostasis is reached (Uchida *et al.*, 2004). This result also assumes the activation of a protection mechanism or negative feedback loop, protecting the organism against the possible harmful effects of *HIF α* during chronic hypoxia. Such a feedback mechanism has been described by Cavadas *et al.* (2015) in human cells: REST silences the *HIF-1 α* gene expression by binding to the 21bp RE1 in the *HIF-1 α* promotor. A corepressor of REST is also found in *Daphnia magna*, indicating the possible existence of a similar mechanism (wFleaBase.org). Other negative regulators of HIF might also play a role in the *Daphnia* cells such as upregulation of PHDs (Metzen *et al.*, 2005), antisense HIF mRNA strands (Rossignol *et al.*, 2002) or miRNAs (Bruning *et al.*, 2011). In the guts of *Daphnia*, a slightly increasing trend persisted until day 28 during the 2nd LTH experiment, which suggests that no negative feedback mechanisms with respect to *HIF α* expression are present in the *Daphnia* gut.

Additionally, the role of the transcription factors SNAI1 and TWIST in the activation of EMT was investigated. *SNAI1* is an important transcription factor for the activation of genes involving EMT, especially in downregulating E-cadherin (Ohkubo & Ozawa, 2004; Kume *et*

al., 2013), and its expression should be lowered in order to prevent EMT from happening. An increased expression of *SNAI1* was observed in the whole *Daphnia* tissue, but not in the gut cells, where a decreasing trend was observed. The decreasing trend in the gut thus rather reflects a protective mechanism against EMT in this F clone. The expression of *TWIST* in the whole *Daphnia* tissue was rather stable and did not show the expected increasing trend under EMT (Yang *et al.*, 2008; Xu *et al.*, 2009).

Next to the changes in *HIF α* , *SNAIL* and *TWIST*, the loss of E-cadherin (*ECAD*) and the gain of N-cadherin (*NCAD*) expression, as expected under EMT, were studied. This was performed in order to relate the EMT process to the transcription factor expression. The most important trends were that *ECAD* expression increased and *NCAD* expression decreased in the chronic hypoxia treatment in the whole *Daphnia*, which is thus contrary to what is expected during EMT (Kume *et al.*, 2013; Qian *et al.*, 2014). The increased *ECAD* expression may have tightened the junctions between the epithelial cells. This is in agreement with the assumption of the existence of a protection mechanism in the *Daphnia*, increasing the cell-cell interaction to prevent EMT from occurring, as described *in vitro* by Furuta *et al.* (2001). This effect was confirmed in a phenotypic effect that was detected upon performing the dissections. In the dissections, the guts of the hypoxia treatment were much more stable than in normoxia, suggesting strong cell junctions like E-cadherin. HIF-mediated upregulation of *ECAD* may also have been activated in the gut first as this organ first encounters hypoxia. When the cell junctions are sufficiently reinforced in the gut, the expression may afterwards be downregulated again. However, as E-cadherin is not the only cell junction protein and only part of adherens junctions, other proteins of tight junctions and desmosomes could also be up-regulated by HIF to counteract the presumptive negative effect of hypoxia.

As conclusion, we can state that we could not confirm EMT to occur upon hypoxia stress in this F clone, but that rather protective mechanisms are present. The fact that *HIF α* is only downregulated after several weeks in this F clone, can be accredited to the opportunity for *Daphnia magna* to set on *HIF α* to gain enough oxygen in its natural environment, where hypoxia occurs as a normal abiotic stress factor (Gorr *et al.*, 2004). If this increased HIF expression would be associated with EMT, it would not be an efficient fitness strategy, given that EMT is harmful to the organism. An increase in *HIF-1 α* expression during long-term hypoxia was also described *in vivo* in the liver of hypoxia-tolerant sea bass (Terova *et al.*, 2008). Furuta *et al.* (2001) proposed that HIF might be the protection mechanism itself against EMT, strengthening the epithelial barrier under influence of hypoxia through the activation of the barrier-protecting intestinal trefoil factor, specific for epithelial cells. Also, the gut microbiota may set on this mechanism through SCFAs, in this way protecting their host's gut from EMT (Kelly *et al.*, 2015). The question that rises here is how HIF in *Daphnia* is

prevented from inducing EMT under hypoxic circumstances as seen in tumor cells and why this does occur in tumor cells. The search for the exact mechanisms and pathways promoting cell survival during hypoxia in which HIF plays a role can be performed in *Daphnia*, as these possibly counteract the occurrence of EMT. Further research on the existence and action of this possible protection mechanism against EMT through experimental *HIF α* downregulation is needed to validate this hypothesis. Then, through specific knock-out experiments of players of this protection pathway, the real role of hypoxia in the induction of EMT can be elucidated and can *Daphnia* serve as a credible model in further cancer metastasis research.

Important to note methodologically is that the PCR and qPCR on *NCAD* and *TWIST* showed primer dimer peaks in the melting curve analysis (Addendum 3). This questions the use of the primers, as they also showed minor presence of primer dimers in the optimization process. The primer dimer formation may be due to low concentrations of *NCAD* and *TWIST* present in the cells as well. Because of this, the primers formed dimers because not enough matching cDNA was present. Therefore, a qPCR on the expression of both *NCAD* and *TWIST* was not yet performed on the cDNA from the gut. After further optimization and clearance of the peaks, more reliable results might be obtained, validating the use of the primers in the investigation of the expression in the gut cells.

***M. aeruginosa* diet**

In whole *Daphnia* tissues as well as in the gut cells, the expression of *HIF α* showed an increasing trend followed by a decreasing trend after four days. The fact that exposure to *Microcystis* activates *HIF α* expression is intriguing. This could be due to a changed oxygen level in the *Microcystis* treatment (which needs to be measured upon new exposures) or it could be that *Microcystis* exposure initiates an equal stress mechanism as hypoxia in *Daphnia* that are adapted to the co-occurring stressors (Smirnov, 2017). The activation might also be caused by the decrease in ADaM level in the jars due to evaporation, initiating stress pathways. In Ren *et al.* (2017), the activation of the EMT pathway by microcystin is regulated through the activation of PI3K/Akt and SMAD2 pathways and not the HIF pathway. These pathways are thus interesting to investigate in further experiments.

For the expression level of the EMT marker gene *ECAD*, a decreasing trend is observed which might explain possible occurrence of EMT (Wang *et al.*, 2016). However, in the gut cells this decreasing trend is reversed until initial levels were obtained at day 7, refuting the possibility of EMT occurring in the gut cells. Another possibility is that the cells, in which EMT occurred, already migrated out of the epithelium. This possibility, however, is questionable as no other EMT marker genes, namely *NCAD*, *SNAI1* and *TWIST*, showed the necessary increase in expression neither in the whole organism, nor in the gut cells. The strong outlier

for *NCAD* expression in the whole *Daphnia* at day 4 was due to the very low control Cp value, possibly masking another trend (see further).

From these results, we cannot confirm that *M. aeruginosa*-induced EMT occurred in *Daphnia*. This counteracts the observations done in previous research (Wang *et al.*, 2016; Ren *et al.*, 2017). However, in those experiments, only pure microcystin toxin was used, in contrary to the living algae in this thesis. In future research, administration of this toxin might contribute more to our understanding of the EMT inducing mechanism of microcystin observed in other studies. Another explanation why no EMT was observed, might have been the presence of microcystin degrading bacteria in the gut of *Daphnia*, leading to too low concentrations of the toxin and making the host *Daphnia* resistant to the toxin (Macke *et al.*, in revision). Therefore, the experiment should be repeated using susceptible *Daphnia* clones or axenic *Daphnia*. Also, the first time point used in this thesis was four days. In the future, time points closer to the first administration should be analyzed in order to observe earlier effects that were not visible in this thesis.

Experimental set-up

In many of the qPCRs for both the effects of hypoxia as the effects of *M. aeruginosa*, the normalized ratio of the Cp values of the control treatment showed a value ranging from 0,0723 till 8,348. That was very deviant from the expected control normalized Cp value, normally situated around 1. This observation places a question mark with every trend that was seen in these qPCRs. The reason possibly lay in the experimental set-up. The placing of three *Daphnia* in 30 mL of ADaM in 20°C, led to the evaporation of the ADaM, increasing the salt concentration in the remaining medium. As *Daphnia* are very sensitive to any environmental stress and therefore often used in eco-toxicology studies, the higher salt concentration due to the evaporation might have activated stress associated molecular pathways, deforming the expression levels observed in the qPCR (Gonçalves *et al.*, 2007). Only the jars present in the hypoxia chamber did not encounter this evaporation as it was possible to create a humid micro-environment in the chamber, counteracting evaporation. Another factor that might play a role is the occurrence of a yet unidentified fungal infection of the *Daphnia* breeding facility. Due to this infection, *Daphnia* from the 3rd LTH exposure might have set on protective pathways, in this way masking or influencing the effect of the hypoxia/*M. aeruginosa*. However, the fungus did not manage to survive in the hypoxic conditions created in the hypoxia chamber, leaving only the control and the *Microcystis* treatment subject to the infection. This might also explain the much lower control Cp values in the qPCR on *NCAD* and *TWIST* in the 3rd LTH. Again HIF could have played a role in the arrest of the fungal infection in hypoxic conditions, upregulating defense mechanisms in the *Daphnia* (Friedrich *et al.*, 2017) and questioning the trends observed in the 3rd LTH exposure.

Daphnia in all of the exposures and controls tend to show a much lower body size (no data available) and reproduction was also severely diminished as compared to *Daphnia* who remained in the 2L jars. Only very few *Daphnia* in the hypoxia treatment were able to reproduce, and if so, in very low quantities. In normal conditions a *Daphnia* is able to reproduce every 3 to 4 days carrying up to 30-40 parthenogenetic eggs (Ebert, 2005). On the other hand, the *Daphnia* in the experiment were not so much stressed that they induced ephippia formation. The reason for these first hand observations is not yet clear. In the control treatment, the higher salinity level due to evaporation of ADaM should not play a role as the concentration should be quite high (Gonçalves *et al.*, 2007). However, it may be a result of the decision to put three *Daphnia* in only 30 mL in all the experiments. This 30 mL was a profound choice, as the diffusion rate of oxygen out of this amount of ADaM, at an atmospheric oxygen saturation of 0,85 mg/L, until a ADaM oxygen saturation level of 1,7 mg/L, was monitored by dr. E. Beert to be 24h. As the *Daphnia* suffer from this high density of organisms in such a small environment, it might be an option in the future to use larger aquaria containing a representative level of ADaM. The *Daphnia* would have more space and the population stress factors might be diminished.

Statistics were not applied in this master thesis on the results obtained from the qPCR, given that the optimization protocol for the qPCR was the central focus of this project. There were replica set-up, but as there was not enough material to perform the qPCRs, replica were pooled during the RNA precipitation for the whole *Daphnia* and during sampling for the *Daphnia* guts. For this reason, no significant results could be concluded and the trends witnessed only led to assumptions that need further testing. A larger set-up with different simultaneous exposures to hypoxia/*M. aeruginosa* would be advised in order to analyze the data with statistical relevance, using the LightCycler® 480 software or external software like for instance qbase+ (Biogazelle). However, only a limited number of 80 mL jars can be placed in the hypoxia chamber. A larger set-up would therefore implicate the acquirement of additional lab equipment in order to subject larger amount of *Daphnia magna* to hypoxia. The exposures performed in this thesis were done on separate dates, leading to possible temporal variability in the gene expression in *Daphnia magna*. For this reason, no assumptions can be made between the several LTH or STM exposures. Future experiments with multiple replicates should spread variation over time over the different replicates.

On the other hand, also exposures comparing different lab clones can add credibility to the general aspect of the mechanism, making it not a mechanism seen once in only a single particular lab clone. The F clone, used in the LTH experiments might just be resistant to hypoxia through mechanisms described earlier or harbor bacteria making him resistant to microcystins. The STH experiment in this master thesis, wherein different lab clones (F clone and KNO 15.04) were compared, failed as the cDNA concentrations were too low. This

sudden drop in cDNA concentration might be attributed the use on E.Z.N.A. © RNA Lock Stabilizer Reagent (Omega Bio-tek) instead of RNA $later$ (Qiagen). The reason for this is unclear, but when RNA $later$ was used in the single clone exposures, cDNA concentrations were much higher and ready to use in further experiments. The cDNA extracted from samples from the 1st LTH exposure had a lower quality. This was assumed after the observation that the measurement with the QubitTM showed a higher concentration than the qPCR results showed. This led to a lower Cp than the samples from the 2nd and 3rd LTH exposure. Only results from the *HIF α* , *ECAD* and *NCAD* qPCRs of the 1st LTH were reliable, those of *SNAI1* showed irregular fluorescence measurements and melting peaks. In order to solve this, a gel electrophoresis or quality measurement could be performed, using for instance a NanoDropTM (Thermo Fisher Scientific), leading to more accurate concentration determination.

In order to visualize the protein translation of the EMT markers resulting from the witnessed gene expression levels, a western blot can be performed on the protein content in the *Daphnia* exposed to hypoxia or *M. aeruginosa* and compared with a control treatment. In the Aquatic Biology lab @ IRF-KULAK, Isabel Vanoverberghe is already performing immunohistochemistry on coupes of paraffin-imbedded *Daphnia magna*, exposed to hypoxia/*Microcystis*. Also the amount of mesenchymal cells travelling in the hemolymph of the *Daphnia* could be measured through Fluorescence-Activated Cell Sorting, specific for possible mesenchymal cell surface proteins. This might clarify whereto the mesenchymal cells have migrated after they underwent EMT. Investigating the migration path can be done via staining of specific epithelial cells and observing the migration using fluorescence microscopy. To a further extent, the cells undergoing hypoxia could be visualized using a reversible oxygen-influenced off-on fluorescence probe based on the Förster resonance energy transfer technology (Takahashi *et al.*, 2012). Here, an oxygen sensitive quencher is inhibited at low oxygen levels, allowing a fluorescent dye to emit signals. In the future, the effect of hypoxia in *Daphnia* could also be investigated on the level of the epigenome. Research on epigenetics in *Daphnia* has already been performed by Asselman, *et al.* (2017) on the effects of *Microcystis* on the methylation of serine and threonine amino acids. Herein, they state that as DNA methylation is modulated by environmental stressors such as *Microcystis sp.*, it will shed new light on regulatory mechanisms when taken into account in further toxicity and hypoxia research studies.

When the EMT is found to be present in *Daphnia* after exposure to hypoxia/*M. aeruginosa* and the cellular pathway involved in inducing EMT is elucidated, the next step would be to test drugs in counteracting this mechanism. Performing drug testing on *Daphnia* is not easily carried out, as these crustaceans are very sensitive to toxins, already dying at low concentrations (Parella *et al.*, 2014). In addition to that, as an aquatic organism, the drugs

should be administered to the water, making it difficult to investigate the uptake of the drug (but solutions for increased solubility and bioavailability are present, e.g. via the use of liposomes or nanoparticles). However, this is still a relatively easy way of administration in comparison to e.g. injection in vertebrates. Based on the concentration in the water, an estimation on the uptake could be made, however more research should be performed to investigate how much is really taken up by the *Daphnia* and at which rate. The filtering rate was found to correlate with the body size of the *Daphnia* and the temperature of the medium (Burns, 1969). An additional point to consider is that *Daphnia* only filters particles until a certain size (max. 70 μm diameter) (Ebert, 2005).

In the context of hypoxia-induced EMT, several experimental drugs could be tested, already proven to counteract hypoxia-induced EMT at different occasions, like paeoniflorin and acriflavin. Paeoniflorin, a monoterpene glycoside that is extracted from the *Paeonia lactiflora* Pall. or Chinese peony, was proven to retain hypoxia-induced EMT in breast cancer (Zhou, *et al.*, 2016). The inhibitory effect from paeoniflorin on hypoxia-induced EMT is obtained through the inhibition of HIF-1 α . Such results could also be expected for the hypoxia-induced EMT in *Daphnia* if the active site at HIF α in *Daphnia* is alike. Acriflavine, originally developed from a heterochromic dye, is now known for the inhibition of dimerization of HIF-1 α with HIF-1 β in the downstream hypoxia response-pathway in human cells. Recent research by Dekervel *et al.* (2017) showed that acriflavine successfully inhibited EMT induced by TGF β and by CoCl $_2$, a hypoxia-inducer. It has also been proven to successfully inhibit EMT induced drug resistance (Dekervel *et al.*, 2017). As these two drugs already prove to inhibit hypoxia-induced EMT, it might be interesting to use *Daphnia* to investigate in an *in vivo* high-throughput way, the exact functions of these and other HIF inhibiting drugs (Semenza, 2012) drugs on the mechanism. Furthermore, through this HIF-inhibition, the possible protective effect of HIF as presented in (Kelly *et al.*, 2015) can be further elucidated.

2. Effect of hypoxia on the microbiota composition in *Daphnia magna*

The hypoxia treatment showed to imply an effect on the β -diversity of the bacterial community in *Daphnia magna* as compared to the normoxia control treatment, as was seen in mice subjected to hypoxia during sleep apnoea (Moreno-Indias *et al.*, 2015). However, the result in this thesis was not significant. This might be due to the lack of sufficient samples used for the analysis. Additionally, one of the hypoxia samples showed an increased presence of β -Proteobacteria, compared to the other hypoxia samples. This might have biased the outcome of the analysis. Future experiments with a higher number of replicates will need to confirm the obtained results.

In *Daphnia*, β -Proteobacteria showed to be the most abundant bacteria species (Qi *et al.*, 2009). In this thesis, this was confirmed in the normoxia treatment. However the relative abundance in *Daphnia* subjected to hypoxia, showed almost all of these bacteria being replaced by Sphingobacteria. The β -Proteobacteria comprise *Limnohabitans sp.*, proven to be one of the main symbionts of *Daphnia magna* (Peerakietjahorn *et al.*, 2015). The decrease of these bacteria species may also explain the lowered fecundity observed in *Daphnia* under hypoxic stress, as these bacteria improve the reproduction (Peerakietjahorn *et al.*, 2015). The reason why Sphingobacteria are more abundant in the hypoxic gut is not clear. This class of bacteria is naturally present in *Daphnia* (Qi *et al.*, 2009), however not much was found in literature about the link between Sphingobacteria and hypoxia.

The bacteria present in the gut of *Daphnia* may have even protected the epithelium from the harmful effects of hypoxia (Kelly *et al.*, 2015). SCFAs, like butyrate, produced by bacteria living in the vertebrate hypoxic colon, activate HIF that increases the barrier function (Furuta *et al.*, 2001). In *Daphnia*, the existence of this butyrate-production is not yet elucidated. However, it gives, together with a possible protective role of the microbiota, an interesting starting point for future research. Inhibiting this butyrate signaling, by administering antibiotics to eradicate the microbiota or by investigating how axenic *Daphnia* (Callens *et al.*, 2016) react to these hypoxic conditions, might give further insights in the mechanism.

The microbiome composition is dynamic, leading to the assumption that *Daphnia* will only keep the bacteria that are suited for a symbiosis in that particular situation. During hypoxia this might have been the bacteria protecting the *Daphnia* through SCFA-production, maybe the Sphingobacteria. This is possible as the host-microbiota interaction is dependent on the host genotype. The environment can therefore influence *Daphnia* to discard bacteria or feed on them instead of living in symbiosis. *Daphnia* is able to choose its microbiota through the secretion of antimicrobial peptides. In many animals, these peptides are part of the innate immune system and play an important role in shaping the microbiome (Tasiemski *et al.*, 2015). However, the existence of these peptides still has to be elucidated in *Daphnia magna*.

In addition to this, not all of the bacteria found in the sequencing are symbiotic. Some might just survive low oxygen and serve as food, therefore implicating caution when analyzing the sequencing results. A possibility to improve the fitness of *Daphnia* during hypoxia might also be the increase of photosynthetic oxygen-producing bacteria living in symbiosis. However, in earlier research no clear evidence was found that these kinds of bacteria live in symbiosis with *Daphnia* (Qi *et al.*, 2009).

In the future, it would be interesting to perform the exposure on a longer time span than two weeks and observe a more established hypoxia-specific microbiota composition. In this way the transgenerational effect could be measure as well, looking at the possible vertical transmission of bacteria that arm the *Daphnia* against hypoxia to their offspring. Also in aquatic and marine systems, different bacteria populations are present when oxygen levels are lower (Wilhelm *et al.*, 2013). It might be interesting to investigate the gut microbiota in *Daphnia* living in these hypoxic ponds to look if the same bacteria live in symbiosis as in this thesis. With this in mind, additionally the ADaM in which the hypoxic *Daphnia* live should be analyzed, to investigate the presence of a shift in microbial community in the medium. Another possibility for the future is to conduct mono-association experiments, where specific bacteria species, cultured from previous *Daphnia* subjected to hypoxia, are administered to the *Daphnia* and the role of the specific bacteria in the survival and adaptation of *Daphnia* during hypoxia, i.e. the activation of HIF, is investigated. The interaction between the host and the microbiota can then be investigated through *in vivo* tracking (Geva-Zatorsky *et al.*, 2015). The ability of *Daphnia* to survive low-oxygen conditions makes it also suitable as a model organism to investigate and understand human gut microbiota that normally live in hypoxic parts of the gut and the relation to their host. These anaerobe bacteria do not stand oxygen and can induce dysbiosis and inflammatory bowel disease when the oxygen levels increase (Rigottier-Gois, 2013). The contribution of these bacteria in gastric or colon cancer can be investigated in *Daphnia* subjected to hypoxia, resembling the hypoxic environments observed in the vertebrate gut.

Conclusions and future perspectives

Out of the results obtained in this master thesis, no clear conclusions can be made on the occurrence of EMT in *Daphnia magna* subjected to hypoxia or *Microcystis aeruginosa*. Here, a possible protective role of HIF during hypoxia is assumed that protects the epithelial barrier through upregulation of cell junction protein expression and inhibition of the expression of EMT marker genes. However, this was only seen in one *Daphnia* clone and without statistical significance, urging for the validation in different clones with sufficient replicates in the future. The investigation of changes of these marker genes in protein level will give a more complete picture on the occurrence of EMT.

The microbiota composition in *Daphnia magna* subjected to hypoxia for two weeks showed a shift from a β -Proteobacteria-rich to a Sphingobacteria-rich community, however without significance. This was possibly due to the low amount of replicates in this experiment. A possible role of the microbiota is assumed in the activation of the HIF-mediated protection of the epithelial cell identity, with *Daphnia* selecting those specific bacteria. A repeat of the experiment with more replicates and for a longer time period is needed to make further conclusions.

Using *Daphnia* in biomedical research encounters multiple issues seen in this study. However, if these problems are overcome and more tools become available, this invertebrate might serve as a valid model organism for high-throughput cancer research because of its characteristics, with the possibility of lowering the amounts of vertebrate organisms used nowadays. However, in order to extrapolate the results observed in *Daphnia* to humans, the vertebrate model step is still essential as they are more closely related to humans and *Daphnia* do not show an adaptive immune system. Additionally, the use of *Daphnia* in toxicity studies gives an extra dimension for testing experimental drugs in this model.

References

1. Abreu, M. T., Peek, R. M. (2014). Gastrointestinal Malignancy and the Microbiome. *Gastroenterology*, 146(6), 1534-46.
2. Acloque, H., Adams, M. S., Fishwick, K., Bronner-Fraser, M., Nieto, M. A. (2009). Epithelial-mesenchymal transitions: The importance of changing cell state in development and disease. *Journal of Clinical Investigation*, 119(6), 1438-49.
3. Apprill, A., McNally, S., Parsons, R., Weber, L. (2015). Minor revision to V4 region SSU rRNA 806R gene primer greatly increases detection of SAR11 bacterioplankton. *Aquatic Microbial Ecology*, 75, 129-37.
4. Aragonés, J., Schneider, M., Van Geyte, K., Fraisl, P., Dresselaers, T., Mazzone, M., Dirkx, R., Zacchigna, S., Lemieux, H., Jeoung, N. H., *et al.* (2008). Deficiency or inhibition of oxygen sensor Phd1 induces hypoxia tolerance by reprogramming basal metabolism. *Nature Genetics*, 40(2), 170-80.
5. Arthur, J. C., Perez-Chanona, E., Mühlbauer, M., Tomkovich, S., Uronis, J. M., Fan, T.-J., Campbell, B. J., Abujamel, T., Dogan, B., Rogers, A. B., *et al.* (2012). Intestinal Inflammation Targets Cancer-Inducing Activity of the Microbiota. *Science*, 338, 120-23.
6. Asselman, J., De Coninck, D. I. M., Beert, E., Janssen, C. R., Orsini, L., Pfrender, M. E., Decaestecker, E., De Schampelaere, K. A. C. (2017). Bisulfite Sequencing with *Daphnia* Highlights a Role for Epigenetics in Regulating Stress Response to *Microcystis* through Preferential Differential Methylation of Serine and Threonine Amino Acids. *Environmental Science & Technology*, 51(2), 924-31.
7. Au, S. H., Storey, B. D., Moore, J. C., Tang, Q., Cheng, Y.-L., Javaid, S., Sarioglu, A. F., Sullivan, R., Madden, M. W., O'Keefe, R., *et al.* (2016) Clusters of circulating tumor cells traverse capillary-sized vessels. *PNAS*, 113(18), 4947-52.
8. Barrallo-Gimeno, A., Nieto, M. A. (2005). The Snail genes as inducers of cell movement and survival: implications in development and cancer. *Development (Cambridge, England)*, 132(14), 3151-61.
9. Boulay, J. L., Dennefeld, C., Alberga, A. (1987). The *Drosophila* developmental gene snail encodes a protein with nucleic acid binding fingers. *Nature*, 330(6146), 395-8.
10. Broihier, H. T., Moore, L. A., Van Doren, M., Newman, S., Lehmann, R. (1998) zfh-1 is required for germ cell migration and gonadal mesoderm development in *Drosophila*. *Development*, 125(4), 655-66.
11. Bruning, U., Cerone, L., Neufeld, Z., Fitzpatrick, S. F., Cheong, A., Scholz, C. C., Simpson, D. A., Leonard, M. O., Tambuwala, M. M., Cummins, E. P., *et al.* (2011). MicroRNA-155 Promotes Resolution of Hypoxia-Inducible Factor 1 alpha Activity during Prolonged Hypoxia. *Molecular and Cellular Biology*, 31(19), 4087-96.
12. Burns, C. W. (1969). Relation Between Filtering Rate, Temperature, and Body Size in Four Species of *Daphnia*. *Limnology and Oceanography*, 14(5), 693-700.
13. Callahan, B. J., Sankaran, K., Fukuyama, J. A., McMurdie, P. J., Holmes, S. P. (2016). Bioconductor Workflow for Microbiome Data Analysis: from raw reads to community analyses. *F1000Research*, 5, 1492.

14. Callens, M., Macke, E., Muylaert, K., Bossier, P., Lievens, B., Waud, M., Decaestecker, E. (2016). Food availability affects the strength of mutualistic host–microbiota interactions in *Daphnia magna*. *ISME*, 10(4), 911–20.
15. Campos, A., Vasconcelos, V. (2010). Molecular mechanisms of microcystin toxicity in animal cells. *International Journal of Molecular Sciences*, 11(1), 268–87.
16. Cane, G., Ginouvès, A., Marchetti, S., Buscà, R., Pouysségur, J., Berra, E., Hofman, P., Valérie, V.-C. (2010). HIF-1a mediates the induction of IL-8 and VEGF expression on infection with Afa/Dr diffusely adhering *E. coli* and promotes EMT-like behaviour. *Cellular Microbiology*, 12(5), 640-53.
17. Carmeliet, P., Jain, R. K. (2011). Principles and mechanisms of vessel normalization for cancer and other angiogenic diseases. *Nature Reviews. Drug Discovery*, 10, 417-27.
18. Castellone, M. D., Teramoto, H., Williams, B. O., Druet, K. M., Gutkind, J. S. (2005). Prostaglandin E2 promotes colon cancer cell growth through a Gs-axin-beta-catenin signaling axis. *Science* 310, 1504–10.
19. Cavadas, M. A. S., Mesnieres, M., Crifo, B., Manresa, M. C., Selfridge, A. C., Scholz, C. C., Cummins, E. P., Cheong, A., Taylor, C. T. (2015). REST mediates resolution of HIF-dependent gene expression in prolonged hypoxia. *Scientific Reports*, 5, 17851.
20. Chaffer, C. L., Thompson, E. W., Williams, E. D. (2007). Mesenchymal to epithelial transition in development and disease. *Cells, Tissues, Organs*, 185(1-3), 7–19.
21. Chang, H., Kim, N., Park, J. H., Nam, R. H., Choi, Y. J., Park, S. M., Choi, Y. J., Yoon, H., Shin, C. M., Lee, D. H. (2015). *Helicobacter pylori* Might Induce TGF- β 1-Mediated EMT by Means of *cagE*. *Helicobacter*, 20(6), 438-48.
22. Cheung, M. Y., Liang, S., Lee, J. (2013). Toxin-producing cyanobacteria in freshwater: a review of the problems, impact on drinking water safety, and efforts for protecting public health. *Journal of Microbiology (Seoul, Korea)*, 51(1), 1–10.
23. Cobaleda, C., Pérez-Caro, M., Vicente-Dueñas, C., Sánchez-García, I. (2007). Function of the zinc-finger transcription factor SNAI2 in cancer and development. *Annual Review of Genetics*, 41, 41–61.
24. Colbourne, J.K., Pfrender, M.E., Gilbert, D., Thomas, W.K., Tucker, A., Oakley, T.H. Tokishita, S., Aerts, A., Arnold, G., Basu, M., et al. (2011). The ecoresponsive genome of *Daphnia pulex*. *Science*, 331(6017), 555-61.
25. Crea, F., Clermont, P. L., Parolia, A., Wang, Y., Helgason, C. D. (2014). The non-coding transcriptome as a dynamic regulator of cancer metastasis. *Cancer and Metastasis Reviews*, 33(1), 1–16.
26. Decaestecker, E., De Meester, L., Ebert, D. (2002). In deep trouble: Habitat selection constrained by multiple enemies in zooplankton. *Proceedings of the National Academy of Sciences of the United States of America*, 99(8), 5481-85.
27. Decaestecker, E., De Meester, L., Mergeay, J. (2009). Cyclical parthenogenesis in *Daphnia*: Sexual versus asexual reproduction. In: Van Dijk P., Maertens K., Schoen I. (Eds.), *Lost sex: the evolutionary biology of parthenogenesis*. Dordrecht: Springer Netherlands, 295-316.

28. Decaestecker, E., Labbé, P., Ellegaard, K., Allen, J., Little, T. (2011). Candidate immune gene expression in the ecological genetics model *Daphnia*. *Developmental and Comparative Immunology*, 35(10), 1068-77.
29. Dekervel, J., Bulle, A. S., Windmolders, P., Lambrechts, D., Van Cutsem, E., Verslype, C., van Pelt, J. (2017). Acriflavine Inhibits Acquired Drug Resistance by Blocking the Epithelial-to-Mesenchymal Transition and the Unfolded Protein Response. *Translational Oncology*, 10(1),59-69.
30. de Martel, C., Ferlay, J., Franceschi, S., Vignat, J., Bray, F., Forman, D., Plummer, M. (2012). Global burden of cancers attributable to infections in 2008: a review and synthetic analysis. *Lancet Oncology*, 13(6), 607-15.
31. Deplancke, B., Gaskins, H.R. (2003). Hydrogen sulfide induces serum-independent cell cycle entry in nontransformed rat intestinal epithelial cells. *FASEB J*, 17, 1310–12.
32. Diaz, R.J., Rosenberg, R. (1995). Marine benthic hypoxia: A review of its ecological effects and the behavioural responses of benthic macrofauna. *Oceanography and Marine Biology*, 33, 245–303.
33. Diaz Heijtz, R., Wang, S., Anuar, F., Qian, Y., Björkholm, B., Samuelsson, A., Hibber, M. L., Forssberg, B. E., Pettersson, S. (2011). Normal gut microbiota modulates brain development and behavior. *PNAS*, 108(7), 3047–52.
34. Díaz-López, A., Moreno-Bueno, G., Cano, A. (2014). Role of microRNA in epithelial to mesenchymal transition and metastasis and clinical perspectives. *Cancer Management and Research*, 6, 205–16.
35. Diepenbruck, M., Christofori, G. (2016). Epithelial-mesenchymal transition (EMT) and metastasis: yes, no, maybe? *Current Opinion in Cell Biology*, 43, 7–13.
36. Dillon, R. J., Vennard, C.T., Buckling, A., Charnley, A.K. (2005). Diversity of locust gut bacteria protects against pathogen invasion. *Ecology Letters*, 8, 1291-98.
37. Du, W., Liu, X., Fan, G., Zhao, X., Sun, Y., Wang, T., Zhao, R., Wang, G., Zhao, C., *et al.* (2014). From cell membrane to the nucleus: An emerging role of E-cadherin in gene transcriptional regulation. *Journal of Cellular and Molecular Medicine*, 18(9), 1712–19.
38. Dziga, D., Wasylewski, M., Wladyka, B., Nybom, S., Meriluoto, J. (2013). Microbial Degradation of Microcystins. *Chemical research in Toxicology*, 26, 841-52.
39. Dzutsev, A., Goldszmid, R.S., Viaud, S., Zitvogel, L., Trinchieri, G. (2015) The role of the microbiota in inflammation, carcinogenesis, and cancer therapy. *European Journal of Immunology*, 45, 17–31.
40. Ebert, D. (2005). *Ecology, Epidemiology, and Evolution of Parasitism in Daphnia*. Bethesda (MD): National Library of Medicine (US), National Center for Biotechnology Information. <http://www.ncbi.nlm.nih.gov/entrez/query.fcgi?db=Books>
41. Ebos, J. M. L., Lee, C. R., Kerbel, R. S. (2009). Tumor and Host-Mediated Pathways of Resistance and Disease Progression in Response to Antiangiogenic Therapy. *Clinical Cancer Research*, 15(16), 5020-25.
42. Estrella, V., Chen, T., Lloyd, M., Wojtkowiak, J., Cornell, H. H., Ibrahim-Hashim, A., Bailey, K., Balagurunathan, Y., Rothberg, J. M., Sloane, B. F., *et al.* (2013). Acidity

- generated by the tumor microenvironment drives local invasion. *Cancer Research*, 73(5), 1524–35.
43. Fabbri, M., Paone, A., Calore, F., Galli, R., Gaudio, E., Santhanam, R., Lovat, F., Fadda, P., Mao, C., Nuovo, G. J., *et al.* (2012). MicroRNAs bind to Toll-like receptors to induce prometastatic inflammatory response. *PNAS*, 109(31), E2110-6.
 44. Fischer, K. R., Durrans, A., Lee, S., Sheng, J., Li, F., Wong, S. T. C., Choi, H., El Rayes, T., Ryu, S., Troeger, J., *et al.* (2015). Epithelial-to-mesenchymal transition is not required for lung metastasis but contributes to chemoresistance. *Nature*, 527, 472-88.
 45. Fox, H. M. (1948) The Haemoglobin of *Daphnia*. *The Royal Society*, 135(879).
 46. Freese, H. M., Schink, B. (2011). Composition and stability of the microbial community inside the digestive tract of the aquatic crustacean *Daphnia magna*. *Microbial Ecology*, 62(4), 882–94.
 47. Friedrich, D., Fecher, A.R., Rupp, J., Deepe, G.S.J. (2017). Impact of HIF-1 α and hypoxia on fungal growth characteristics and fungal immunity. *Microbes and Infection*, 19(3), 204-9.
 48. Furuta, G.T., Turner, J.R., Taylor, C.T., Hershberg, R.M., Comerford, K., Narravula, S., Podolsky, D.K., Colgan, S.P. (2001). Hypoxia-inducible Factor 1–dependent Induction of Intestinal Trefoil Factor Protects Barrier Function during Hypoxia. *Journal of Experimental Medicine*, 193 (9), 1027–34.
 49. Garrett, W. S. (2015). Cancer and the Microbiota. *Science*, 348 (6230), 80-86.
 50. Gatesoupe, F.-J., Huelvan, C., Le Bayon, N., Le Delliou, H., Madec, L., Mouchel, O, *et al.* (2016) The highly variable microbiota associated to intestinal mucosa correlates with growth and hypoxia resistance of sea bass, *Dicentrarchus labrax*, submitted to different nutritional histories. *BMC Microbiology*, 16(266), 1-13.
 51. Gehringer, M. M., Shephard, E. G., Downing, T. G., Wiegand, C., Neilan, B. A. (2004). An investigation into the detoxification of microcystin-LR by the glutathione pathway in Balb/c mice. *International Journal of Biochemistry and Cell Biology*, 36(5), 931-41.
 52. Geva-Zatorsky, N., Alvarez, D., Hudak, J.E., Reading, N.C., Erturk-Hasdemir, D., Dasgupta, S., *et al.* (2015). In vivo imaging and tracking of host-microbiota interactions via metabolic labeling of gut anaerobic bacteria. *Nature Medicine*, 21(9), 1091-100.
 53. Gilkes, D. M., Semenza, G., L. (2013). Role of hypoxia-inducible factors in breast cancer metastasis. *Future Oncology*, 9(11), 1623–1636.
 54. Gjorevski, N., Boghaert, E., Nelson, C. M. (2012). Regulation of epithelial-mesenchymal transition by transmission of mechanical stress through epithelial tissues. *Cancer Microenvironment*, 5(1), 29–38.
 55. Gonçalves, A.M.M., Castro, B.B., Pardal, M.A., Gonçalves, F. (2007). Salinity effects on survival and life history of two freshwater cladocerans (*Daphnia magna* and *Daphnia longispina*). *International Journal of Limnology*, 43(1), 13-20.
 56. Gorr, T. A. (2004). *Daphnia* and *Drosophila*: two invertebrate models for O₂ responsive and HIF-mediated regulation of genes and genomes. *International Congress Series*, 1275, 55–62.

57. Gonzalez, C. (2013) *Drosophila melanogaster*: a model and a tool to investigate malignancy and identify new therapeutics. *Nature Reviews Cancer*, 13(3), 172-83.
58. Gros, J., Tabin, C. J. (2014). Vertebrate Limb Bud Formation Is Initiated by Localized Epithelial-to-Mesenchymal Transition. *Science*, 343(6176), 1253-56.
59. Hanahan, D., Weinberg, R. a. (2011). Hallmarks of cancer: the next generation. *Cell*, 144(5), 646–74.
60. Harris, T. J. C., Tepass, U. (2010) Adherens junctions: from molecules to morphogenesis. *Nature reviews: Molecular Cell Biology*, 11, 502-14.
61. Heckmann, L.- H., Sibly, R. M., Connon, R., Hooper, H. L., Hutchinson, T. H., Maund, S. J., Hill, C. J., Bouetard, A., Callaghan, A. (2008). Systems biology meets stress ecology: linking molecular and organismal stress responses in *Daphnia magna*. *Genome Biology*, 9(R40), R40.
62. Herrero, A., Muro-Pastor, A. M., Flores, E. (2001). Nitrogen Control in Cyanobacteria. *Journal of Bacteriology*, 183(2), 411–25.
63. Homer, D. H., Waller, W. (1983). Chronic effect of reduced dissolved oxygen on *Daphnia magna*. *Water Air Soil Pollution*, 20(1), 23-8.
64. Hudnell, H. K. (2010). The state of U.S. freshwater harmful algal blooms assessments, policy and legislation. *Toxicon*, 55(5), 1024–1034.
65. Hwang, W.-L., Jiang, J.-K., Yang, S.-H., Huang, T.-S., Lan, H.-Y., Teng, H.-W., *et al.* (2014). MicroRNA-146a directs the symmetric division of Snail-dominant colorectal cancer stem cells. *Nature Cell Biology*, 16(3), 268–80.
66. Imai, T., Horiuchi, A., Wang, C., Oka, K., Ohira, S., Nikaido, T., Konishi, I. (2003). Hypoxia attenuates the expression of E-cadherin via up-regulation of SNAIL in ovarian carcinoma cells. *The American Journal of Pathology*, 163(4), 1437–47.
67. Imamichi ,Y., Menke, A. (2007). Signaling pathways involved in collagen-induced disruption of the E-cadherin complex during epithelialmesenchymal transition. *Cells Tissues Organs*, 185, 180-90.
68. Irrazábal, T., Belcheva, A., Girardin, S.E., Martin, A., Philpott, D.J. (2014). The Multifaceted Role of the intestinal Microbiota in Colon Cancer. *Molecular Cell*, 54, 309-20.
69. Jiang, J., Tang, Y. L., Liang, X. H. (2011). EMT: A new vision of hypoxia promoting cancer progression. *Cancer Biology and Therapy*, 11(8), 714–23.
70. Johnston, D. S., Ahringer, J. (2010). Cell Polarity in Eggs and Epithelia: Parallels and Diversity. *Cell*, 141(5), 757-74.
71. Kalluri, R., Weinberg, R. A. (2009). The basics of epithelial-mesenchymal transition. *Journal of Clinical Investigation*, 119(6), 1420-28.
72. Kelly, C.J., Zheng, L., Campbell, E.L., Saeedi, B., Scholz, C.C., Bayless, A.J., *et al.* (2015). Crosstalk between Microbiota-Derived Short-Chain Fatty Acids and Intestinal Epithelial HIF Augments Tissue Barrier Function. *Cell Host & Microbe*, 17, 662–67.
73. Kirienko, N. V., Mani, K., Fay, D. S. (2010). Cancer models in *Caenorhabditis elegans*. *Developmental Dynamics*, 239(5), 1413–48.

74. Klüttgen, B., Dulmer, U., Engels, M., Ratre, H. T. (1994). ADaM , An Artificial Freshwater for the Culture of Zooplankton. *Water Research*, 28(3), 743–46.
75. Kohl, K. D., Weiss, R. B., Cox, J., Dale, C., Dearing, M. D. (2014). Gut microbes of mammalian herbivores facilitate intake of plant toxins. *Ecol. Lett.*, 17, 1238-46.
76. Kokkinos, M. I., Murthi, P., Wafai, R., Thompson, E. W., Newgreen, D. F. (2010). Cadherins in the human placenta--epithelial-mesenchymal transition (EMT) and placental development. *Placenta*, 31(9), 747–55.
77. Komarova, Y. A., Mehta, D., Malik, A. B. (2007). Dual regulation of endothelial junctional permeability. *Science Signaling*, 412, re8.
78. Kozich, J.J., Westcott, S.L., Baxter, N.T., Highlander, S.K., Schloss, P.D. (2013). Development of a Dual-Index Sequencing Strategy and Curation Pipeline for Analyzing Amplicon Sequence Data on the Miseq Illumina Sequencing Platform. *Applied and Environmental Microbiology*, 79, 5112–20.
79. Kume, K., Haraguchi, M., Hijioka, H., Ishida, T., Miyawaki, A., Nakamura, N., Ozawa, M. (2013). The transcription factor Snail enhanced the degradation of E-cadherin and desmoglein 2 in oral squamous cell carcinoma cells. *Biochemical and Biophysical Research Communications*, 430(3), 889–94.
80. Kump, L. R., Junium, C., Arthur, M. a., Brasier, A., Fallick, A. E., Melezhik, V., Lepland, A., Črne, A. E., Luo, G. (2011). Isotopic evidence for massive oxidation of organic matter following the great oxidation event. *Science*, 334(December), 1694–96.
81. Lai, K.-P., Li, J.-W., Chan, C. Y.-S., Chan, T.-F., Yuen, K. W.-Y., Chiu, J. M.-Y. (2016). Transcriptomic alterations in *Daphnia magna* embryos from mothers exposed to hypoxia. *Aquatic Toxicology (Amsterdam, Netherlands)*, 177, 454–63.
82. Lamkemeyer, T., Zeis, B., Decker, H., Jaenicke, E., Waschbüsch, D., Gebauer, W., Markl, J., Meissner, U., Rousselot, M., Zal, F., *et al.* (2006). Molecular mass of macromolecules and subunits and the quaternary structure of hemoglobin from the microcrustacean *Daphnia magna*. *FEBS Journal*, 273(14), 3393–10.
83. Lamouille, S., Xu, J., Derynck, R. (2014). Molecular mechanisms of epithelial-mesenchymal transition. *Nature Reviews. Molecular Cell Biology*, 15(3), 178–96.
84. Leopold, P. L., Vincent, J., Wang, H. (2012). A comparison of epithelial-to-mesenchymal transition and re-epithelialization. *Seminars in Cancer Biology*, 22(5–6), 471–83.
85. Li, Q., Sodroski, C., Lowey, B., Schweitzer, C. J., Cha, H., Zhang, F., Liang, T. J. (2016). Hepatitis C virus depends on E-cadherin as an entry factor and regulates its expression in epithelial-to-mesenchymal transition. *Proceedings of the National Academy of Sciences of the United States of America*, 113(27), 7620–5.
86. Lin, F., Wang, N., Zhang, T.-C. (2012). The role of endothelial-mesenchymal transition in development and pathological process. *IUBMB Life*, 64(9), 717–23.
87. Little, T. J., O'Connor, B., Colegrave, N., Watt, K., Read, A. F. (2003). Maternal transfer of strain-specific immunity in an invertebrate. *Current Biology*, 13, 489–92.
88. Lozupone, C., Knight, R. (2005). UniFrac: a New Phylogenetic Method for Comparing Microbial Communities. *Applied and Environmental Microbiology*, 71(12), 8228–35.

89. Lundgren, K., Nordenskjöld, B., Landberg, G. (2009). Hypoxia, Snail and incomplete epithelial-mesenchymal transition. *British Journal of Cancer*, 101, 1769-81.
90. Leatherman, J. L., DiNardo, S. (2008). Zfh-1 Controls Somatic Stem Cell Self-Renewal in the *Drosophila* Testis and Nonautonomously Influences Germline Stem Cell Self-Renewal. *Cell Stem Cell*, 3(1), 44–54.
91. Macke, E., Callens, M., De Meester, L., Muylaert, K., Decaestecker, E. (in revision) Microbiome-mediated adaptation to climate change: how gut microbes drive resistance to toxic algal blooms.
92. Mani, S. a, Guo, W., Liao, M., Eaton, E. N., Ayyanan, A., Zhou, Y., Brooks, M., Reinhard, F., Zhang, C. C., Shipitsin, M., *et al.* (2009). The epithelial-mesenchymal transition generates cells with properties of stem cells. *Cell*, 133(4), 704–15.
93. Manzanares, M., Locascio, A., Nieto, M. A. (2001). The increasing complexity of the Snail gene superfamily in metazoan evolution. *TRENDS in Genetics*, 17(4), 178–81.
94. Marcucci, F., Bellone, M., Caserta, C. A., Corti, A. (2014). Pushing tumor cells towards a malignant phenotype: Stimuli from the microenvironment, intercellular communications and alternative roads. *International Journal of Cancer*, 135(6), 1265-76.
95. Metchnikoff, E., 1893. Lectures on the Comparative Pathology of Inflammation. (Translated from the French by F.A. and E.H. Starling) Kegan Paul, Trench Trubner and Co., Ltd., London.
96. Metzen, E., Stiehl, D.P., Doege, K., Marxsen, J.H., Hellwig-Bürgel, T., Jelkmann, W. (2005). Regulation of the prolyl hydroxylase domain protein 2 (phd2/egln-1) gene: identification of a functional hypoxia responsive element. *The Biochemical Journal*, 387(3), 711-17.
97. Mimeault, M., Batra, S. K. (2013). Hypoxia-inducing factors as master regulators of stemness properties and altered metabolism of cancer- and metastasis-initiating cells. *Journal of Cellular and Molecular Medicine*, 17(1), 30–54.
98. Miner, B. E., De Meester, L., Pfrender, M. E., Lampert, W., Hiarston, N. G. (2012). Linking genes to communities and ecosystems: *Daphnia* as an ecogenomic model. *Proceedings of the Royal Society B: Biological Sciences*, 279(1735), 1873-82.
99. Moreno-Indias, I., Torres, M., Montserrat, J. M., Sanchez-Alcoholado, L., Cardona, F., Tinahones, F. J., Gozal, D., Poroyko, V. A., Navajas, D., Queipo-Ortuño, M. I., *et al.* (2015). Intermittent hypoxia alters gut microbiota diversity in a mouse model of sleep apnoea. *The European respiratory journal*, 45(4), 1055-65.
100. Nakajima, Y., Yamagishi, T., Hokari, S., Nakamura, H. (2000). Mechanisms Involved in Valvuloseptal Endocardial Cushion Formation in Early Cardiogenesis: Roles of Transforming Growth Factor (TGF)- β and Bone Morphogenetic Protein (BMP). *The Anatomical Record*, 258(2), 119–27.
101. Narumiya, S., Tanji, M., Ishizaki, T. (2009). Rho signaling, ROCK and mDia1, in transformation, metastasis and invasion. *Cancer Metastasis Rev*, 28(1), 65–76.
102. Natzle, J. E., Kiger, J. A., Green, M. M. (2008). Bursicon signaling mutations separate the epithelial-mesenchymal transition from programmed cell death during *Drosophila melanogaster* wing maturation. *Genetics*, 180(2), 885–93.

103. Nicholson, J. K., Holmes, E., Kinross, J., Burcelin, R., Gibson, G., Jia, W., Pettersson, S. (2012). Host-gut microbiota metabolic interactions. *Science*, 336(6086), 1262–7.
104. Nieto, M. A., Huang, R. Y.-J., Jackson, R. a., Thiery, J. P. (2016). EMT: 2016. *Cell*, 166(1), 21–45.
105. Nistico, P., Bissell, M. J., Radisky, D. C. (2009). Epithelial-Mesenchymal Transition: General Principles and Pathological Relevance with Special Emphasis on the Role of Matrix Metalloproteinases. *Cold Spring Harbor Perspectives in Biology*, 4(2), a011908.
106. Ohkubo, T., Ozawa, M. (2004). The transcription factor Snail downregulates the tight junction components independently of E-cadherin downregulation. *Journal of Cell Science*, 117(9), 1675–85.
107. Ozdemir, A., Fisher-Aylor, K. I., Pepke, S., Samanta, M., Dunipace, L., Mccue, K., Zeng, L., Ogawa, N., Wold, B. J., Stathopoulos, A. (2011). High resolution mapping of Twist to DNA in *Drosophila* embryos : Efficient functional analysis and evolutionary conservation. *Genome research*, 21, 566–77.
108. Parrella, A., Kundi, M., Lavorgna, M., Criscuolo, E., Russo, C., Isidori, M. (2014). Toxicity of exposure to binary mixtures of four anti-neoplastic drugs in *Daphnia magna* and *Ceriodaphnia dubia*. *Aquatic Toxicology*, 157, 41–6.
109. Peerakietkhajorn, S., Kato, Y., Kasalický, V., Matsuura, T., Watanabe, H. (2016). Betaproteobacteria *Limnohabitans* strains increase fecundity in the crustacean *Daphnia magna*: symbiotic relationship between major bacterioplankton and zooplankton in freshwater ecosystem. *Environmental Microbiology*, 18(8), 2366–74.
110. Peinado, H., Olmeda, D., Cano, A. (2007). Snail, Zeb and bHLH factors in tumour progression: an alliance against the epithelial phenotype? *Nature Reviews. Cancer*, 7(6), 415–28.
111. Pilli, V. S., Gupta, K., Kotha, B. P., Aradhyam, G. K. (2015). Snail-mediated Cripto-1 repression regulates the cell cycle and epithelial-mesenchymal transition-related gene expression. *FEBS Letters*, 589(11), 1249–56.
112. Porat, R. A. M., Teltsch, B., Perelman, A., Dubinsky, Z. V. Y. (2001). Diel buoyancy changes by the cyanobacterium *Aphanizomenon ovalisporum* from a shallow reservoir. *Journal of Plankton Research*, 23(7), 753-63.
113. Prabhakar, N. R., Semenza, G. L. (2012). Adaptive and maladaptive cardiorespiratory responses to continuous and intermittent hypoxia mediated by hypoxia-inducible factors 1 and 2. *Physiological Reviews*, 92(3), 967–1003.
114. Qi, W., Nong, G., Preston, J. F., Ben-Ami, F., Ebert, D. (2009). Comparative metagenomics of *Daphnia* symbionts. *BMC Genomics*, 10, 172.
115. Qian, X., Anzovino, A., Kim, S., Suyama, K., Yao, J., Hulit, J., Agiostratidou, G., Chandiramani, N., McDaid, H. M., Nagi, C., *et al.* (2014). N-cadherin/FGFR promotes metastasis through epithelial-to-mesenchymal transition and stem/progenitor cell-like properties. *Oncogene*, 33, 3411–21.
116. Recamier JC. (1829). Recherches sur le traitement du cancer sur la compression methodique simple ou combinee et sur l'histoire generale de la meme maladie. 2nd ed.

117. Ren, Y., Yang, M., Chen, M., Zhu, Q., Zhou, L., Qin, W., Wang, T. (2017). Microcystin-LR promotes epithelial-mesenchymal transition in colorectal cancer cells through PI3-K/AKT and SMAD2. *Toxicology Letters*, 265, 53-60.
118. Ridley, A. J. (2011). Life at the Leading Edge. *Cell*, 145(7), 1012-22.
119. Lionel Rigottier-Gois, L. (2013). Dysbiosis in inflammatory bowel diseases: the oxygen hypothesis. *The ISME Journal*, 7(7), 1256-61.
120. Rogers, C. D., Saxena, A., Bronner, M. E. (2013) Sip1 mediates an E-cadherin-to-N-cadherin switch during cranial neural crest EMT. *J. Cell Biol.*, 203(5), 835–47.
121. Rossignol, F., Vache, C., Clottes, E. (2002). Natural antisense transcripts of hypoxia-inducible factor 1alpha are detected in different normal and tumour human tissues. *Gene*, 299, 135-40.
122. Routtu, J., Hall, M.D., Albere, B., Beisel, C., Bergeron, R.D., Chaturvedi, A., Choi, J.-H., Colbourne, J., De Meester, L., Stephens, M.T., *et al.* (2014). An SNP-based second-generation genetic map of *Daphnia magna* and its application to QTL analysis of phenotypic traits. *BMC Genomics*, 15(1033).
123. Rowe, R. G., Lin, Y., Shimizu-Hirota, R., Hanada, S., Neilson, E. G., Greenson, J. K., Weiss, S. J. (2011). Hepatocyte-Derived Snail1 Propagates Liver Fibrosis Progression. *Molecular and Cellular Biology*, 31(12), 2392–2403.
124. Rubinstein, M. R., Wang, X., Liu, W., Hao, Y., Cai, G., Han, Y. W. (2013). *Fusobacterium nucleatum* promotes colorectal carcinogenesis by modulating E-cadherin/beta-catenin signaling via its *FadA* adhesin. *Cell Host Microbe*, 14, 195–206.
125. Said, N. A. B. M., Williams, E. D. (2011). Growth factors in induction of epithelial-mesenchymal transition and metastasis. *Cells, Tissues, Organs*, 193(1–2), 85–97.
126. Sarnelle, O., Gustafsson, S., Hansson, L.-A. (2010). Effects of cyanobacteria on fitness components of the herbivore *Daphnia*. *Journal of Plankton Research*, 32(4), 471-77.
127. Sauka-Spengler, T., Bronner-Fraser, M. (2008). A gene regulatory network orchestrates neural crest formation. *Nature Reviews Molecular Cell Biology*, 9(7), 557-68.
128. Semenza, G. L. (2012). Hypoxia-Inducible Factors in Physiology and Medicine. *Cell*, 148(3), 399-408.
129. Semenza, G. L. (2014). Oxygen Sensing, Homeostasis, and Disease. *New England Journal of Medicine*, 365(6), 537–47.
130. Sethi, N., Kang, Y. (2011). Unravelling the complexity of metastasis - molecular understanding and targeted therapies. *Nature Reviews Cancer*, 11(10), 735–48.
131. Shaw, T. J., Martin, P. (2016). Wound repair: a showcase for cell plasticity and migration. *Current Opinion in Cell Biology*, 42, 29–37.
132. Sison-Mangus, M. P., Mushegian, A. a, Ebert, D. (2014). Water fleas require microbiota for survival, growth and reproduction. *ISME*, 9(1), 1–9.

133. Smallhorn, M., Murray, M.J., Saint, R. (2004). The epithelial-mesenchymal transition of the *Drosophila* mesoderm requires the Rho GTP exchange factor Pebble. *Development*, 131(11), 2641-51.
134. Smirnov, N.N. (2017). *Physiology of the Cladocera*, Second Edition. Elsevier Inc., UK, 401p. ISBN:978-0-12-805194-8.
135. Stefanatos R. K. A., Vidal, M. (2011) Tumor invasion and metastasis in *Drosophila*: A bold past, a bright future. *Journal of Genetics and Genomics*, 38(10), 431-38.
136. Steinestel, K., Eder, S., Schrader, A.J., Steinestel, J. (2014). Clinical significance of epithelial-mesenchymal transition. *Clinical and Translational Medicine*, 3(17), 1-12.
137. Takahashi, S., Piao, W., Matsumura, Y., Komatsu, T., Ueno, T. Takuya T., Kamachi, T., Kohno, M., Nagano, T., Hanaoka, K. (2012). Reversible off-on fluorescence probe for hypoxia and imaging of hypoxia-normoxia cycles in live cells. *Journal of the American Chemical Society*, 134(48), 19588-91.
138. Talmadge, J. E., Fidler, I. J. (2010). AACR centennial series: The biology of cancer metastasis: Historical perspective. *Cancer Research*, 70(14), 5649–69.
139. Tam, W. L., Weinberg, R. A. (2013). The epigenetics of epithelial-mesenchymal plasticity in cancer. *Nature Medicine*, 19(11), 1438–49.
140. Tarin, D. (2005). The Fallacy of Epithelial Mesenchymal Transition in Neoplasia. *Cancer research*, 65(14), 5996–6001.
141. Tasiemski, A., Massol, F., Cuvillier-Hot, V., Boidin-Wichlacz, C., Roger, E., Rodet, F., Fournier, I., Thomas, F., Salzet, M. (2015). Reciprocal immune benefit based on complementary production of antibiotics by the leech *Hirudo verbana* and its gut symbiont *Aeromonas veronii*. *Scientific Reports*, 5(1), 17498.
142. Terova, G., Rimoldi, S., Corà, S., Bernardini, G., Gornati, R., Saroglia, M. (2008). Acute and chronic hypoxia affects HIF-1 α mRNA levels in sea bass (*Dicentrarchus labrax*). *Aquaculture*, 279(1), 150–9.
143. Thiery, J. P., Acloque, H., Huang, R. Y. J., Nieto, M. A. (2009). Epithelial-mesenchymal transitions in development and disease. *Cell*, 139(5), 871–90.
144. Tiwari, N., Gheldof, A., Tatari, M., Christofori, G. (2012). EMT as the ultimate survival mechanism of cancer cells. *Seminars in Cancer Biology*, 22(3), 194–207.
145. Uchida, T., Rossignol, F., Matthay, M. A., Mounier, R., Couette, S., Clottes, E., Clerici, C. (2004). Prolonged Hypoxia Differentially Regulates Hypoxia-inducible Factor (HIF)-1 α and HIF-2 α Expression in Lung Epithelial Cells. *Journal of Biological Chemistry*, 279(15), 14871-8.
146. Uchida, H., Maruyama, T., Nishikawa-Uchida, S., Oda, H., Miyazaki, K., Yamasaki, A., Yoshimura, Y. (2012). Studies using an in vitro model show evidence of involvement of epithelial-mesenchymal transition of human endometrial epithelial cells in human embryo implantation. *The Journal of Biological Chemistry*, 287(7), 4441–50.
147. Wächtler, B., Citiulo, F., Jablonowski, N., Förster, S., Dalle, F., Schaller, M., Wilson, D., Hube, B. (2012). *Candida albicans*-Epithelial Interactions: Dissecting the Roles of Active

- Penetration, Induced Endocytosis and Host Factors on the Infection Process. *PLoS ONE*, 7(5), e36952.
148. Wang, P.-J., Chien, M.-S., Wu, F.-J., Chou, H.-N., Lee, S.-J. (2005). Inhibition of embryonic development by microcystin-LR in zebrafish, *Danio rerio*. *Toxicon: Official Journal of the International Society on Toxinology*, 45(3), 303–8.
 149. Wang, P., Zhao, J., Corsi, A. K. (2006). Identification of novel target genes of CeTwist and CeE/DA. *Developmental Biology*, 293(2), 486–98.
 150. Wang, C., Gu, S., Yin, X., Yuan, M., Xiang, Z., Li, Z., Cao, H., Meng, X., Hu, K., Han, X. (2016). The toxic effects of microcystin-LR on mouse lungs and alveolar type II epithelial cells. *Toxicon: Official Journal of the International Society on Toxinology*, 115, 81–8.
 151. Warzecha, C. C., Carstens, R. P. (2012). Complex changes in alternative pre-mRNA splicing play a central role in the epithelial-to-mesenchymal transition (EMT). *Seminars in Cancer Biology*, 22(5-6), 417–27.
 152. Wei, L., Hoole, D., Sun, B. (2014). Identification of apoptosis-related genes and transcription variations in response to microcystin-LR in zebrafish liver. *Toxicology and Industrial Health*, 30(9), 777–84.
 153. Wilhelm, S., Gary R. LeClerc, G. R., Bullerjahn, G. S., McKay, R. M., Saxton, M. A., Twiss, M. R., Bourbonniere, R. A. (2014). Seasonal changes in microbial community structure and activity imply winter production is linked to summer hypoxia in a large lake. *FEMS Microbiology Ecology*, 87(2), 475-85.
 154. Vega, S., Morales, A. V, Ocaña, O. H., Valdés, F., Fabregat, I., Nieto, M. A. (2004). Snail blocks the cell cycle and confers resistance to cell death. *Genes & Development*, 18(10), 1131–43.
 155. Xu, J., Lamouille, S., Derynck, R. (2009). TGF-beta-induced epithelial to mesenchymal transition. *Cell Research*, 19(2), 156–72.
 156. Yang, M.-H., Wu, M.-Z., Chiou, S.-H.; Chen, P.-M., Chang, S.-Y., Liu, C.-J., Teng, S.-C., Wu, K.-J. (2008). Direct regulation of *TWIST* by HIF-1 α promotes metastasis. *Nature Cell Biology*, 10(3), 295-305.
 157. Yang, Q., Li, Z., Cao, J., Zhang, S., Zhang, H., Wu, X., Zhang, Q., Liu, X., Söderhäll, K. (2014). Selection and Assessment of Reference Genes for Quantitative PCR Normalization in Migratory Locust *Locusta migratoria* (Orthoptera: Acrididae). *PLoS ONE*, 9(6), e98164.
 158. Zhang, K., Rodriguez-Aznar, E., Yabuta, N., Owen, R. J., Mingot, J. M., Nojima, H., Nieto, M. A., Longmore, G. D. (2012). Lats2 kinase potentiates Snail1 activity by promoting nuclear retention upon phosphorylation. *The EMBO Journal*, 31(1), 29–43.
 159. Zhou, B. P., Deng, J., Xia, W., Xu, J., Li, Y. M., Gunduz, M., Hung, M.-C. (2004). Dual regulation of Snail by GSK-3beta-mediated phosphorylation in control of epithelial-mesenchymal transition. *Nature Cell Biology*, 6(10), 931–40.
 160. Zhou, Z., Wang, S., Song, C., Hu, Z. (2016). Paeoniflorin prevents hypoxia-induced epithelial -mesenchymal transition in human breast cancer cells. *Oncotargets and therapy*, 9, 2511-18.

Addendum A

Risk analysis

The experiments performed during this master thesis involved the use and exposure to hazardous substances, microorganisms, devices, equipment and high pressure gas bottles.

The Molecular Lab at the Interdisciplinary Research Facility at KULAK (Kortrijk) (IRF-KULAK) belongs to containment Level 1. Lab coat and gloves were standard protective equipment during the molecular work. The lab bench and applied materials were disinfected and cleaned with ethanol (70%) prior to use.

Working with *Daphnia magna* in the breeding facility at the IRF-KULAK did not involve any risks, however a lab coat was worn to prevent contamination.

The use of β -mercaptoethanol (E4), isopropanol (E3), peracetic acid (E3), kit buffers (E1-E4), phenol-chloroform-isoamylalcohol (E4), RNA^{later}® (hazardous to the environment), sodium dodecyl sulfate (E1), EDTA (E1) and ethanol (E3) was done with greatest awareness and precaution. Handling was performed using gloves continuously and a fume hood when needed. When pipetting these products spilling and formation of aerosols was avoided. After use, waste was sorted into the appropriate waste bins.

In this master thesis, the cyanobacteria *Microcystis aeruginosa* was used. These microorganisms produce toxins that are nephrotoxic, neurotoxic, hepatotoxic, dermatotoxic and possibly carcinogenic. Working with these microorganisms involved the use of gloves and lab coat. *Microcystis aeruginosa* may never leave the laboratory or end up in the environment to prevent the formation of algal blooms into water facilities. After use, the ADaM containing *Microcystis aeruginosa* was discarded into the appropriate waste bin and jars were washed with javel and hot water to kill off remaining microorganisms.

Cloning of a PCR fragment was performed in competent *Escherichia coli* bacteria. Handling was always performed in a laminar flow closet using gloves and a lab coat. Laminar flow closet and materials were disinfected with ethanol (70%) and UV radiation. A special Level 2 containment laboratory facility was not required.

The molecular work required the use of several devices (centrifuges, electrophoresis devices, Peltier Thermal Cycler, -20°C freezer, -80°C freezer, fridge, qPCR machine, Qubit™, vortex, microscopes, bead-beater, laminar flow closet, autoclave). All precautions needed for each device were taken and spilling was prevented. The devices were switched off and the log books completed at the end of each use. The placement of high pressure N₂ gas bottles was performed by the lab technicians with appropriate training.

Addendum B

Table Addendum B1: PCR Programs. (A) Reverse transcription PCR program for cDNA synthesis; (B) Primer optimization PCR with different annealing temperatures for the EMT marker genes; (C) qPCR program with primer annealing temperature 61°C for *HIFα* and 58°C for EMT marker genes *ECAD*, *NCAD*, *SNAI1* and *TWIST*; (D) PCR program for amplification of the 16S rRNA gene and (E) preparation of the sequences for Illumina sequencing

(A)

Time (min)	Temperature (°C)
10	25
30	55
5	85
forever	4

(B)

n°	Time (min)	Temperature (°C)
1	5	95
2	0.5	95
3	0.5	54/56/58/60/62
4	1	72
5	back to 2 (35 cycles)	
6	7	72
7	for ever	4

(C)

Step	Time (seconds)	Temperature (°C)	Number of cycles	Analysis Mode
Pre-Incubation	300	95	1	None
Amplification	10	95	45	Quantification
	10	58/61		
	10	72		
Melting	5	95	1	Melting Curves
	60	65		
	forever	97		
Cooling	10	40	NA	None

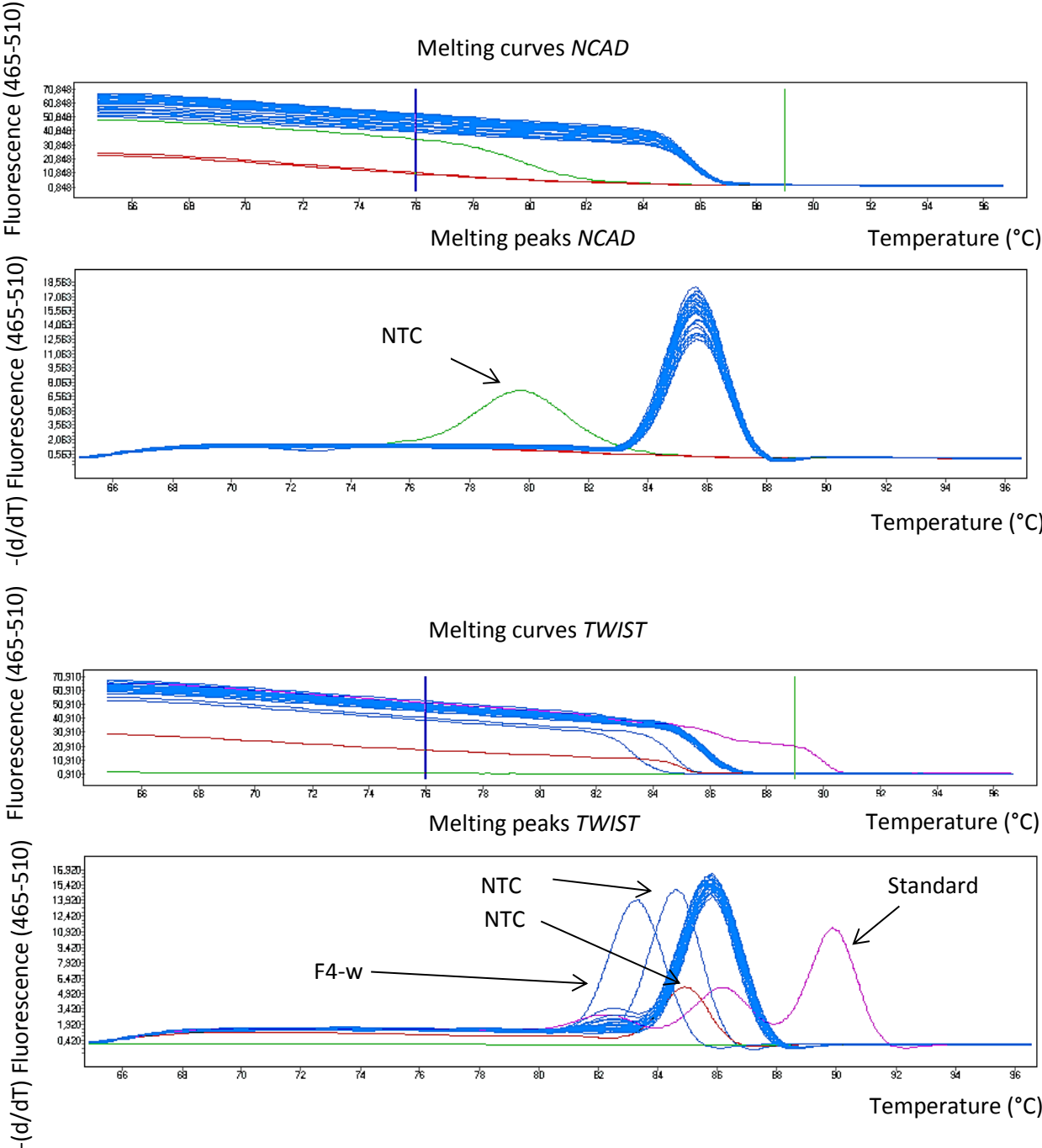
(D)

n°	Time (seconds)	Temperature (°C)
1	180	94
2	30	94
3	45	50
4	90	68
5	back to 2 (30 cycles)	
6	600	68
7	For ever	4

(E)

n°	Time (seconds)	Temperature (°C)
1	180	94
2	30	94
3	30	55
4	60	68
5	back to 2 (30 cycles)	
6	600	68
7	For ever	4

Addendum C



Supplementary Figure 1: Melting peak analysis from the qPCR on (A) *NCAD* and (B) *TWIST* on 3rd LTH exposure. The melting peaks of *NCAD* show an irregular melting peak, possibly a primer dimer. The melting peaks of *TWIST* show very irregular melting peaks, especially the standard melting peak is deviant. NTC peaks might be due to contamination or primer dimers.

AQUATIC BIOLOGY
Etienne Sabbelaan 53
B-8500 KORTRIJK, BELGIUM
tel. + 32 56 24 60 59
fax + 32 56 24 69 99
www.kuleuven-kulak.be

